Computational MRI

From structured low-rank algorithms to model based deep learning

Qing Zou, Sunrita Poddar, Gregory Ongie,
Hemant Aggarwal, Merry Mani,
Mathews Jacob

THE UNIVERSITY OF IOWA

MRI: Versatile tissue contrasts

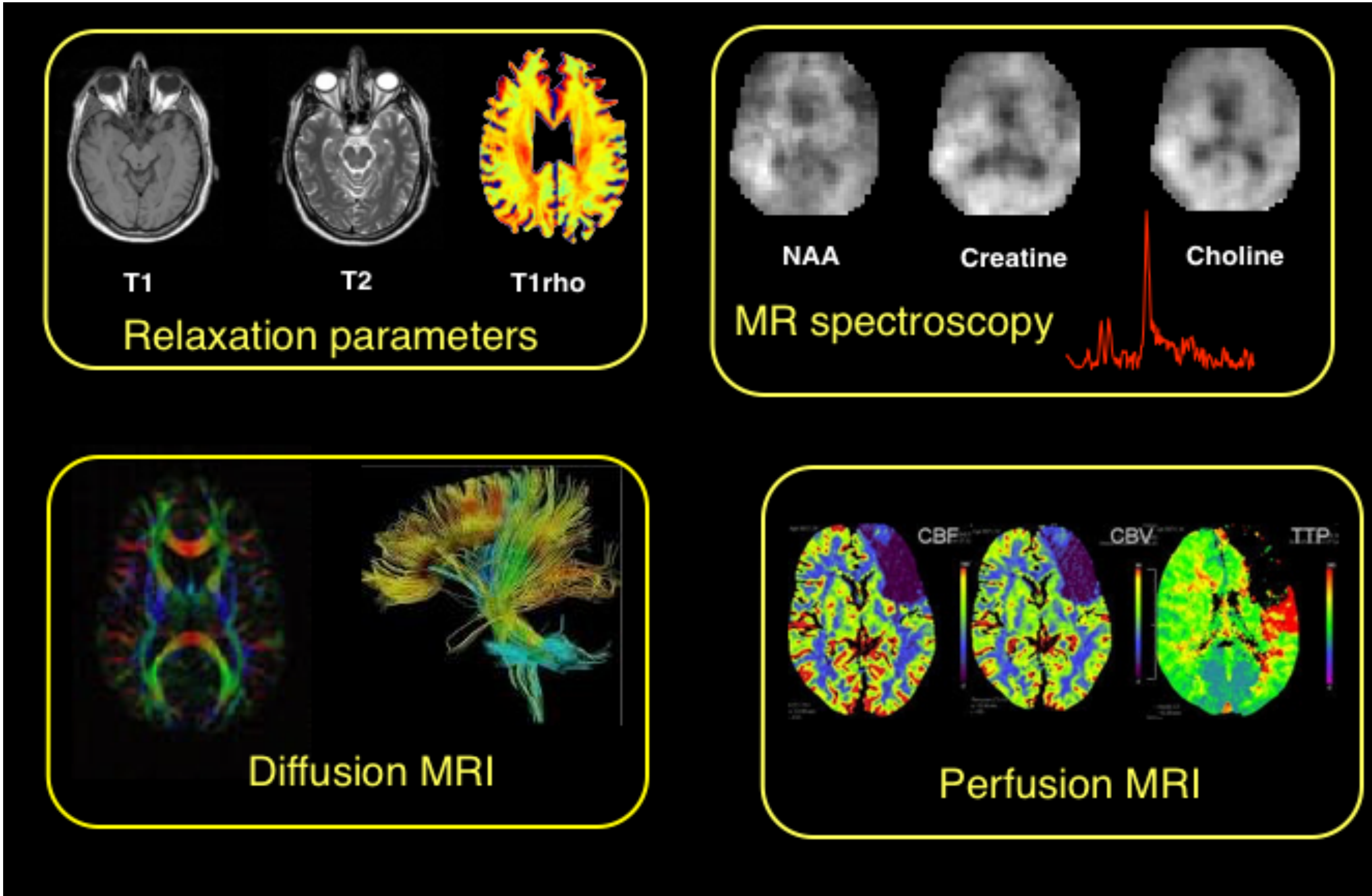

There is nothing nuclear spins will not do for you, as long as you treat them as human beings

Erwin Hahn

Slow acquisition: tradeoffs in static MRI

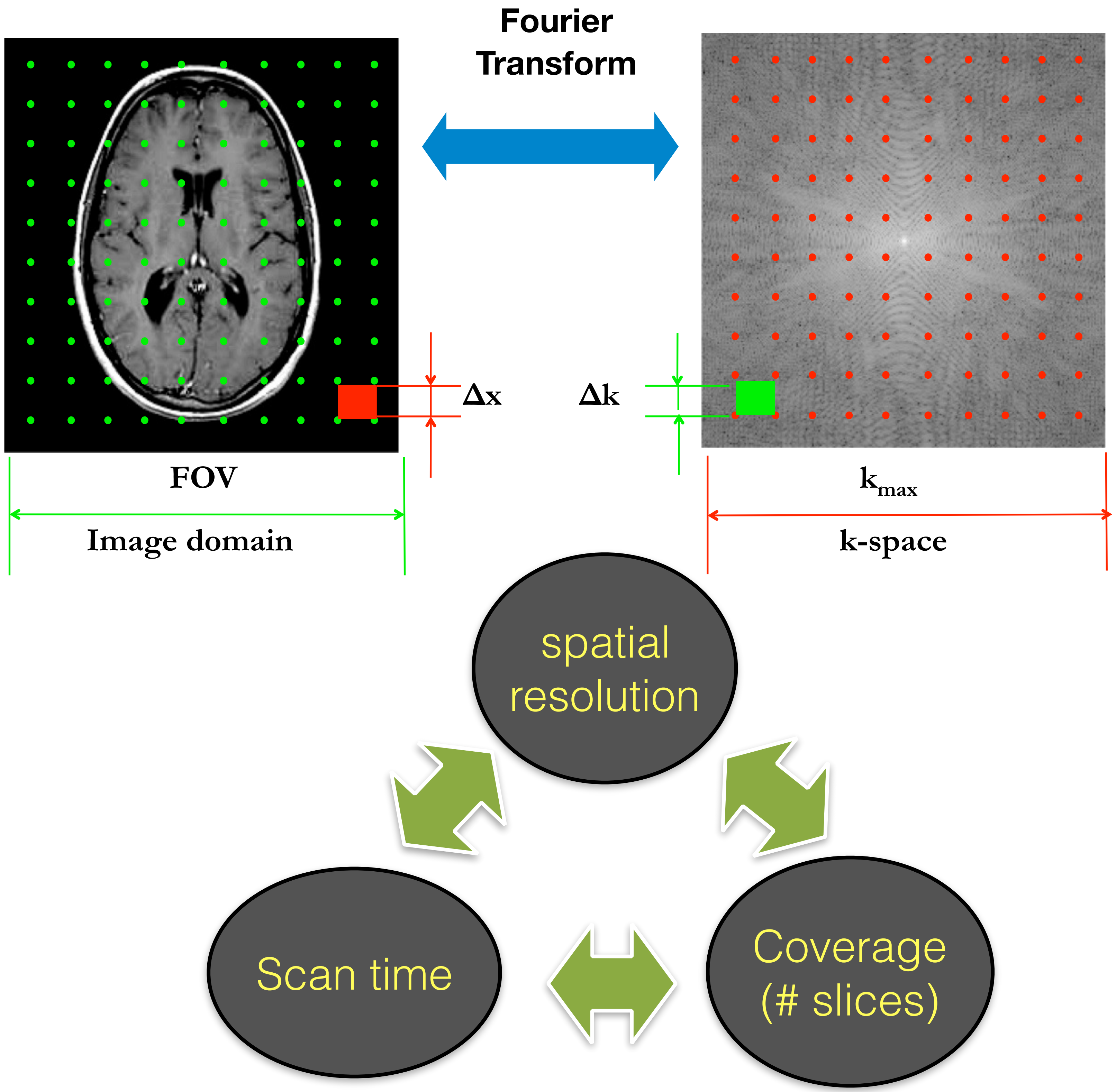

Slow acquisition: tradeoffs in cardiac MRI

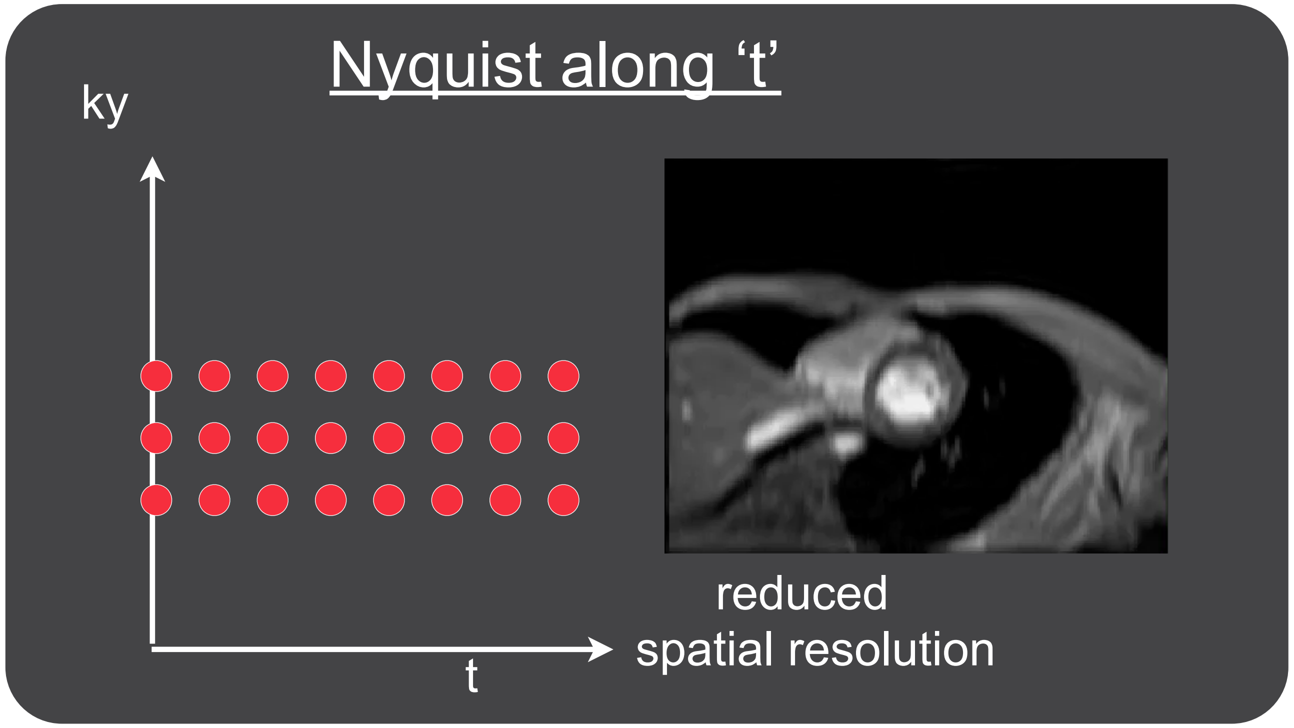

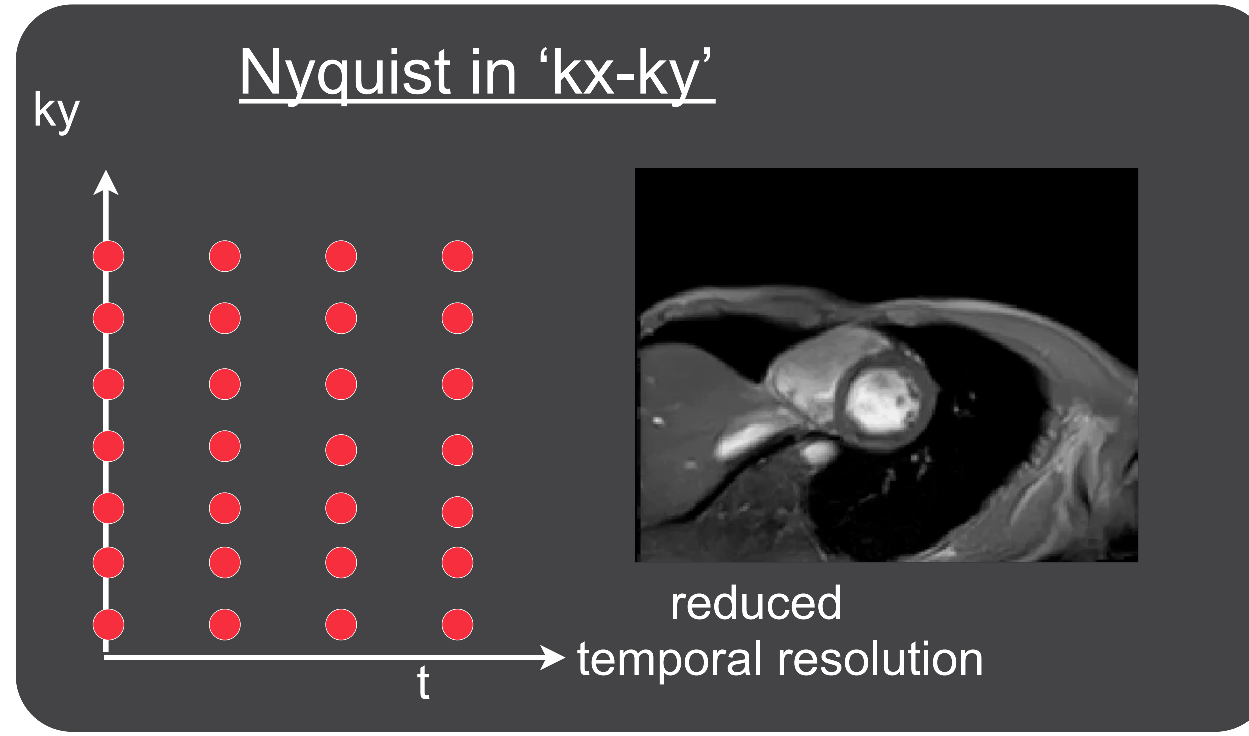

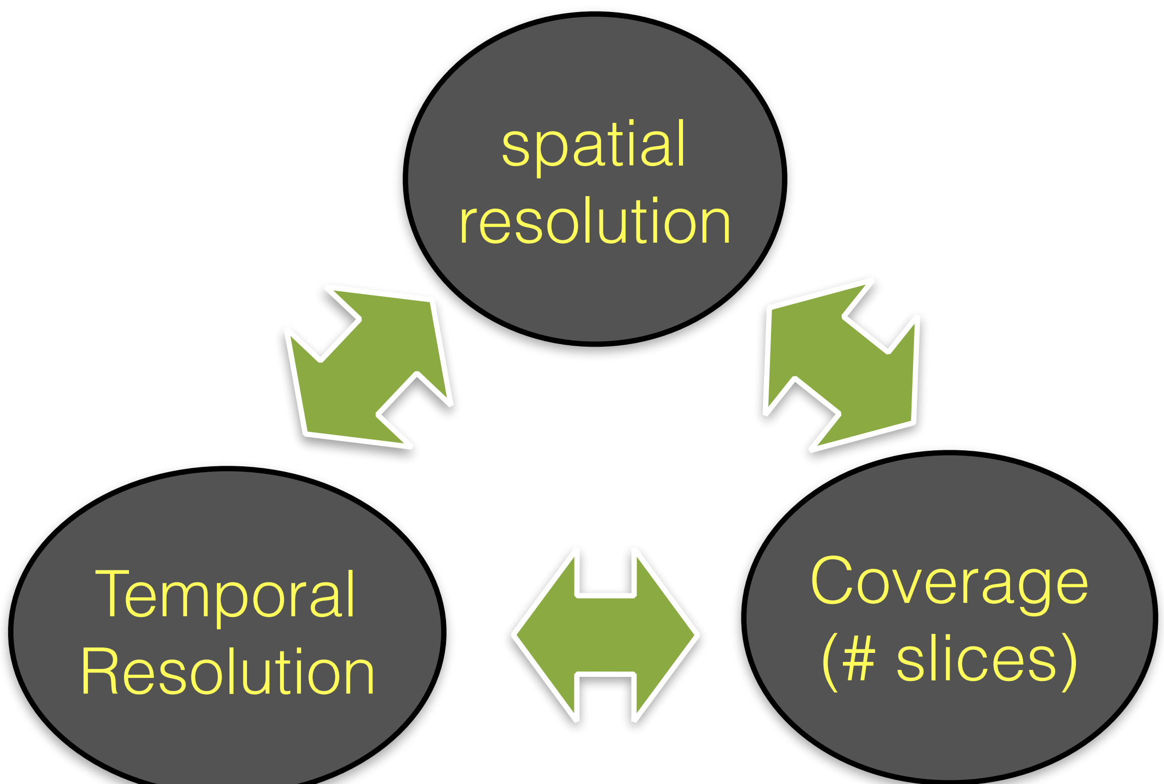

Inconsistencies between excitations

k-space acquired in different time points: inconsistencies

- Patient/physiological motion (cardiac/respiratory pulsation)
- Eddy currents
- Field inhomogeneity artifacts

Inconsistencies between excitations

k-space acquired in different time points: inconsistencies

- Patient/physiological motion (cardiac/respiratory pulsation)
- Eddy currents
- Field inhomogeneity artifacts

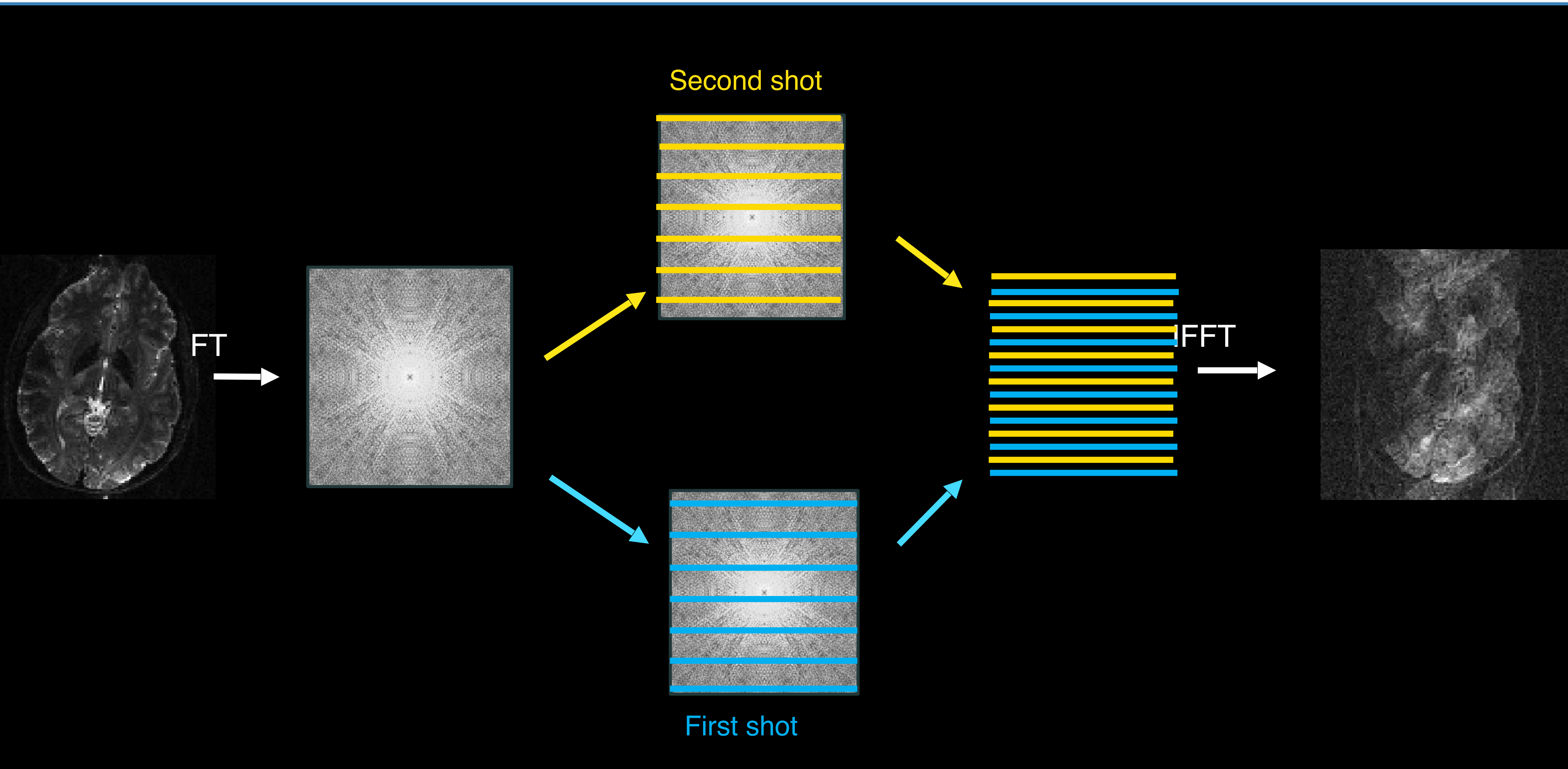

Lift to a high-dimensional space, where solution is simple !!

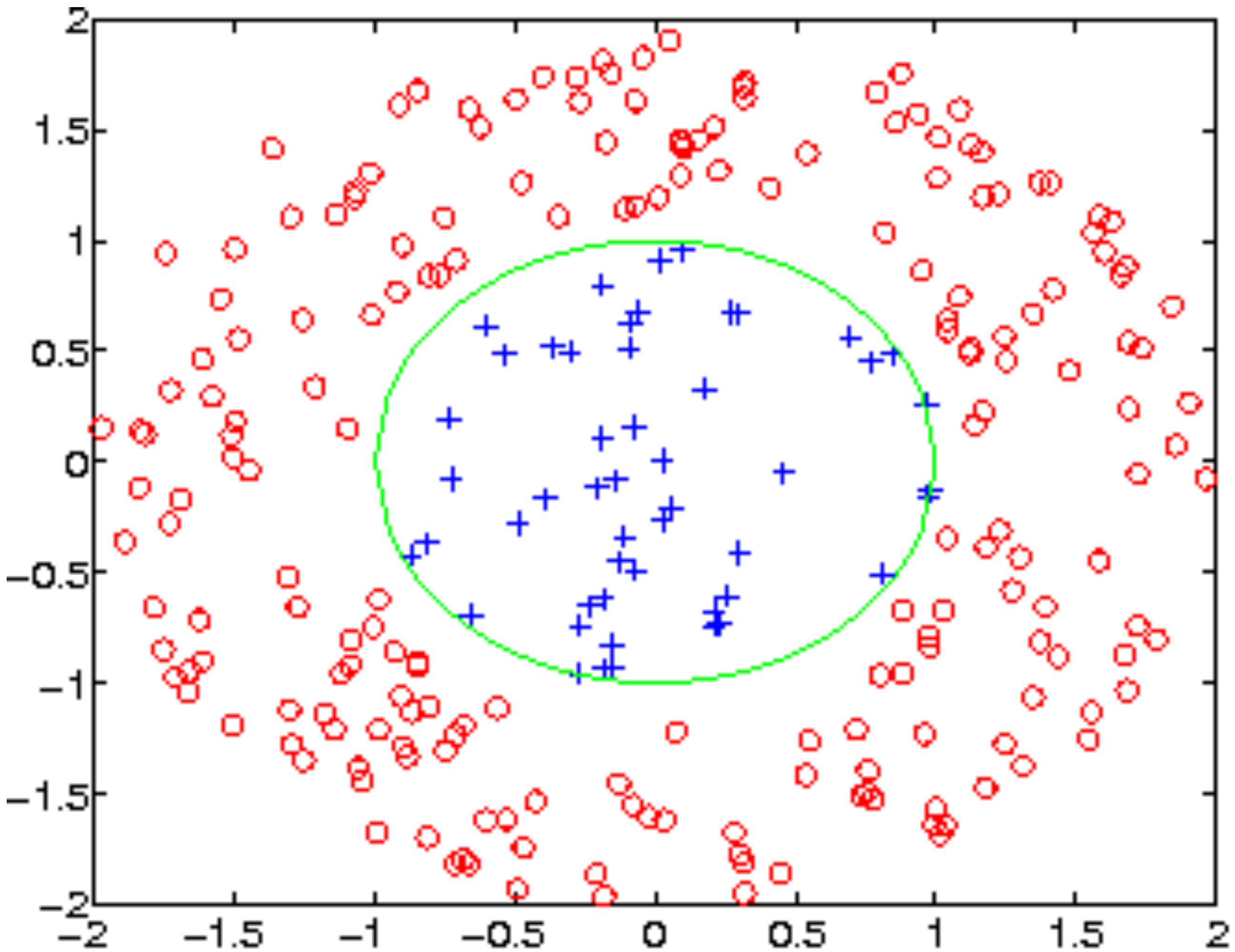

Input Space

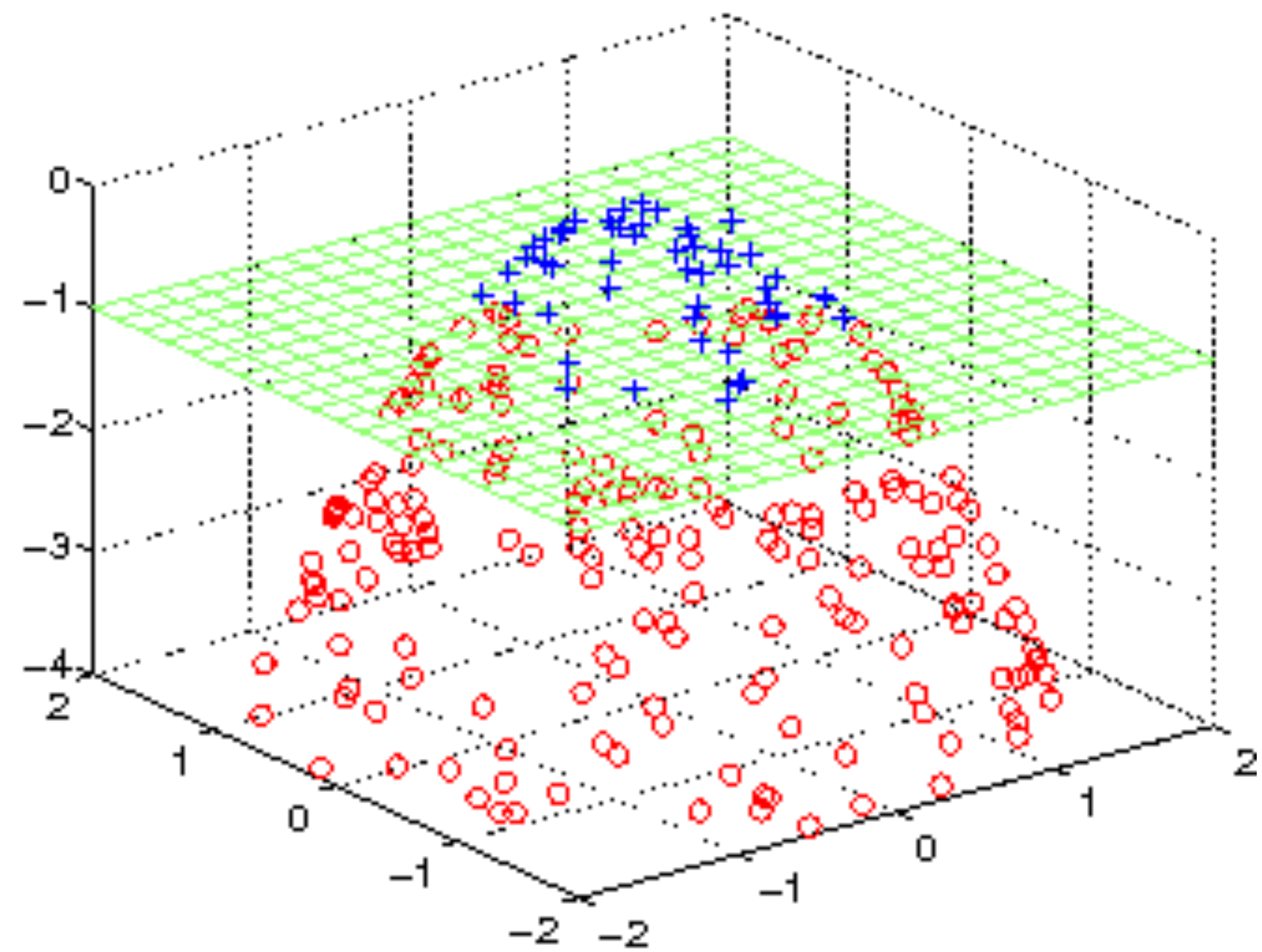

Lifted Space

Learning in lifted spaces

Complexity/type of lifting: shallow vs deep learning

Lift to a high-dimensional space, where solution is simple !!

Linear lifting operations

- Continuous domain compressed sensing
- Auto-calibration: account for inconsistencies in acquisition

Non-linear lifting: data living on surface

- Recovery of data in high dimensional spaces
- Learning functions in high dimensional spaces: links to deep learning

Model based deep learning

- Using learning based models in imaging

Lift to a high-dimensional space, where solution is simple !!

- Uecker et al, Espirit - an eigenvalue approach to autocalibrating PMRI: where SENSE meets GRAPPA,MRM, 2014
- Shin et al, Calibrationless PMRI based on structured low-rank matrix completion,MRM , 2014.
- J.P. Haldar, Low-Rank Modeling of Local-Space Neighborhoods (LORAKS) for Constrained MRI, TMI, 2014.
- G. Ongie, M. Jacob, Super-resolution MRI using finite rate of innovation curves, ISBI, 2015.
- Jin et al. A general framework for compressed sensing and parallel MRI using ALOHA, TCI. 2016.
- Ye et al. Compressive sampling using annihilating filter-based low-rank interpolation, TIT, 2016
- Ongie et al, Off-the-Grid Recovery of Piecewise Constant Images from Few Fourier Samples, SIAM IS, 2016.
- Ongie et al, GIRAF: A Fast Algorithm for Structured Low-Rank Matrix Recovery, IEEE Transactions on Computational Imaging, Dec 2017, pp. 535 - 550.
- Ongie et al, Convex recovery of continuous domain piecewise constant images, TSP, 2018
- Mani et al, Multishot sensitivity encoded diffusion data recovery using structured low rank matrix completion (MUSSELS), Magnetic Resonance in Medicine, Volume 78, Issue 2,2017 pp 494–507.
- Lobos et al, Navigator-free EPI ghost correction with structured low-rank matrix models: new theory and methods,TMI, 2018.
- Poddar et al, Manifold recovery using kernel low-rank regularization: application to dynamic imaging, TCI, 2018.
- S. Poddar, M.Jacob, Recovery of Noisy Points on Band-limited Surfaces:, ICASSP 2018

Linear lifting: general idea

1-D Example:

$\hat{\mathbf{f}}$

Linear lifting: general idea

1-D Example:

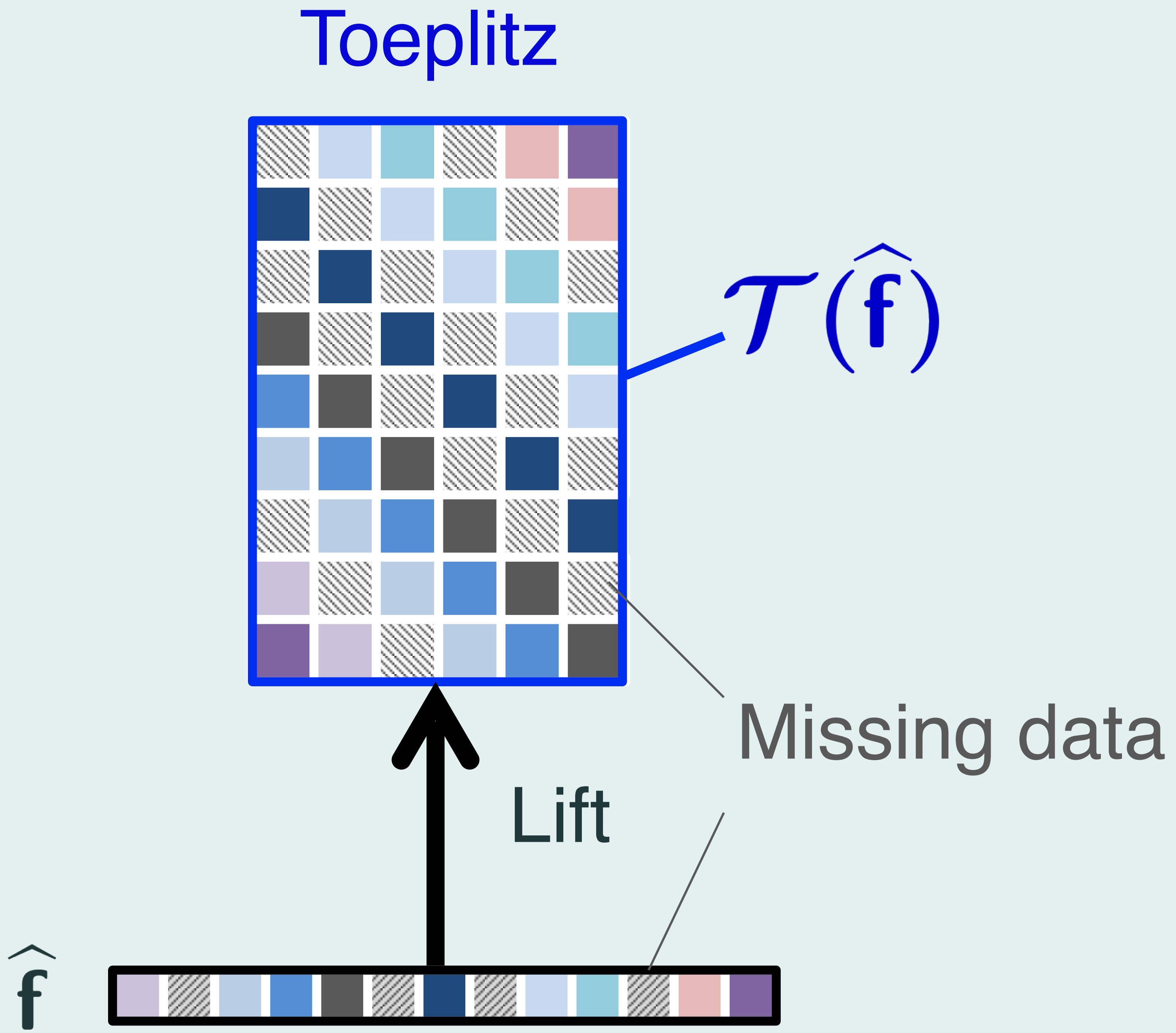

Structured matrix is often low-rank

$$\min_{\widehat{\mathbf{f}}} \quad \mathrm{rank}[\mathcal{T}(\widehat{\mathbf{f}})] \quad \textbf{s.t.} \quad \widehat{\mathbf{f}}[\mathbf{k}] = \widehat{\mathbf{b}}[\mathbf{k}], \mathbf{k} \in \mathbf{\Gamma}$$

1-D Example:

Toeplitz

Complete matrix

$\mathcal{T}(\widehat{\mathbf{f}})$

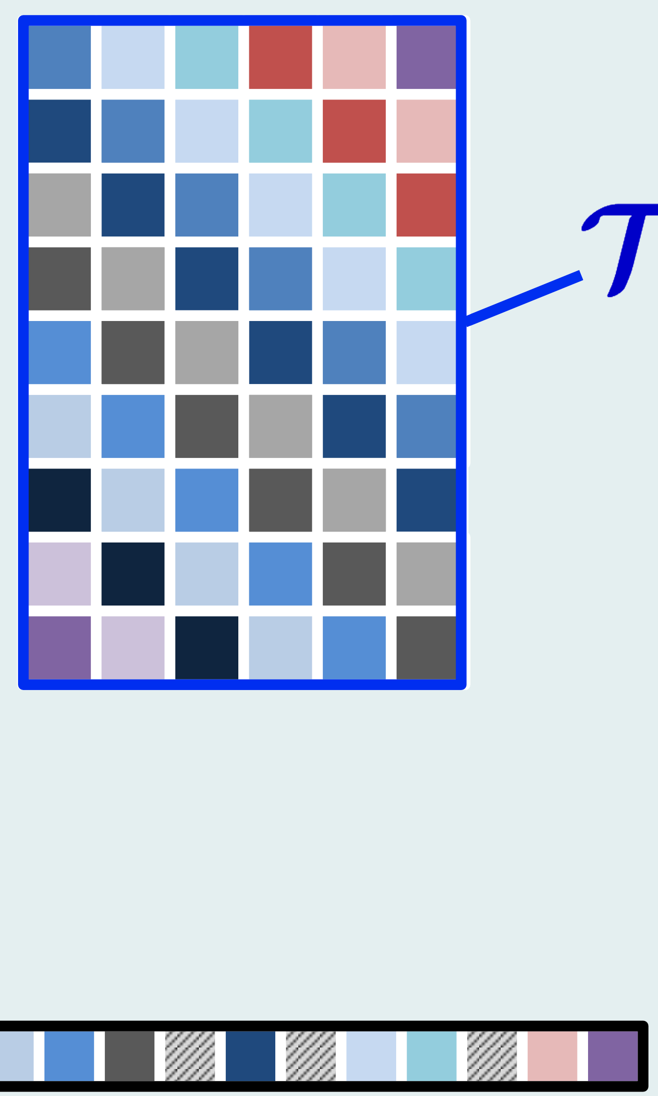

$\widehat{\mathbf{f}}$

Structured low-rank matrix completion: general idea

$$\min_{\widehat{\mathbf{f}}} \quad \mathrm{rank}[\mathcal{T}(\widehat{\mathbf{f}})] \quad \textbf{s.t.} \quad \widehat{\mathbf{f}}[\mathbf{k}] = \widehat{\mathbf{b}}[\mathbf{k}], \mathbf{k} \in \boldsymbol{\Gamma}$$

1-D Example:

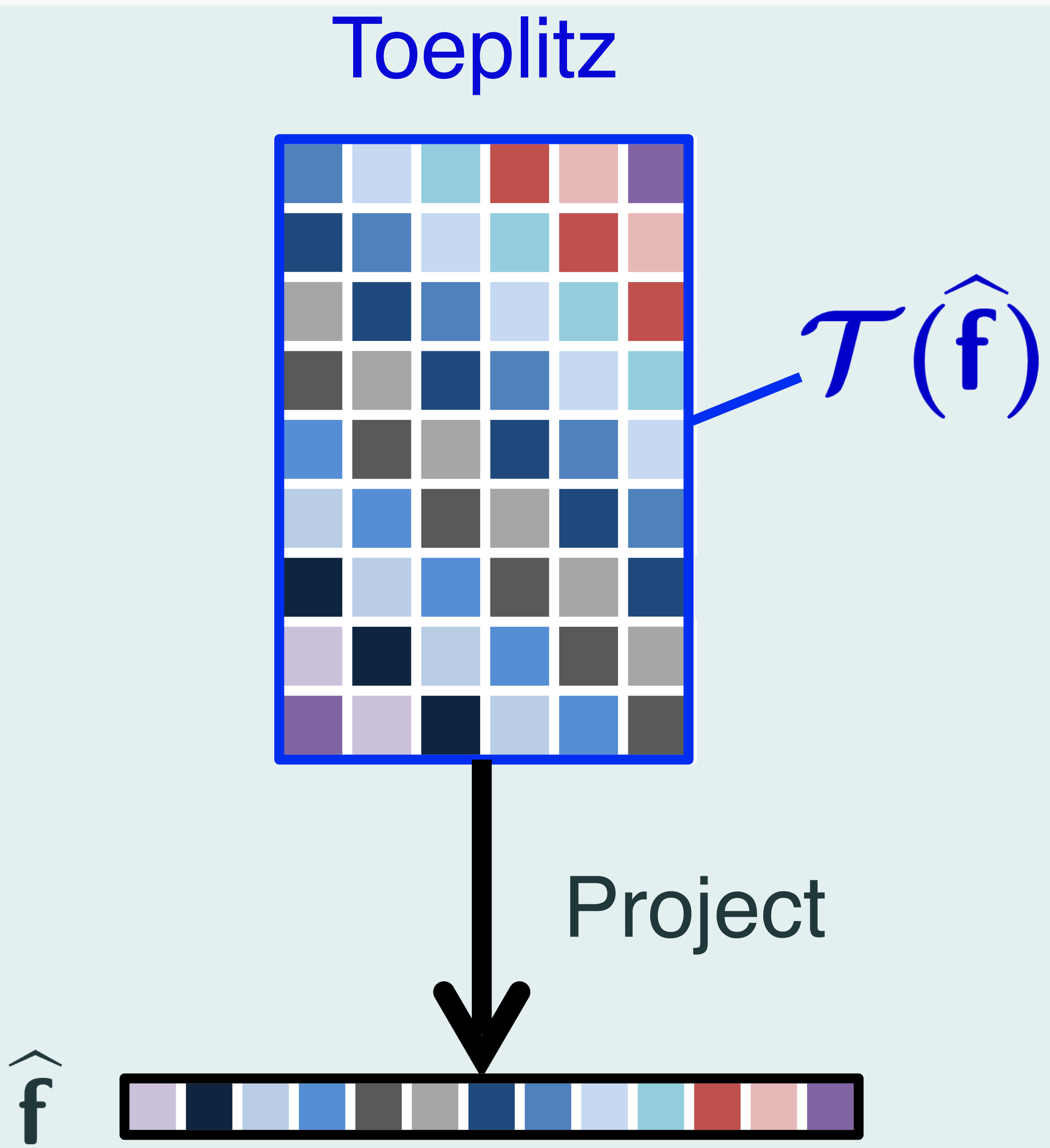

Recovery as a structured low-rank matrix completion

$$\min_{\widehat{\mathbf{f}}} \quad \mathrm{rank}[\mathcal{T}(\widehat{\mathbf{f}})] \quad \textbf{s.t.} \quad \widehat{\mathbf{f}}[\mathbf{k}] = \widehat{\mathbf{b}}[\mathbf{k}], \mathbf{k} \in \boldsymbol{\Gamma}$$

NP-Hard!

Recovery as a structured low-rank matrix completion

$$\min_{\widehat{\mathbf{f}}} \quad \mathrm{rank}[\mathcal{T}(\widehat{\mathbf{f}})] \;\; \textbf{s.t.} \;\; \widehat{\mathbf{f}}[\mathbf{k}] = \widehat{\mathbf{b}}[\mathbf{k}], \mathbf{k} \in \mathbf{\Gamma}$$

Convex Relaxation

$$\min_{\widehat{\mathbf{f}}} \quad \|\mathcal{T}(\widehat{\mathbf{f}})\|_* \;\; \textbf{s.t.} \;\; \widehat{\mathbf{f}}[\mathbf{k}] = \widehat{\mathbf{b}}[\mathbf{k}], \mathbf{k} \in \mathbf{\Gamma}$$

Nuclear norm – sum of singular values

[Ongie & Jacob, ICIP 16](#)
[Ongie, Biswas & Jacob,TSP,2018](#)

Lifting: potential for high computational complexity

1-D Example:

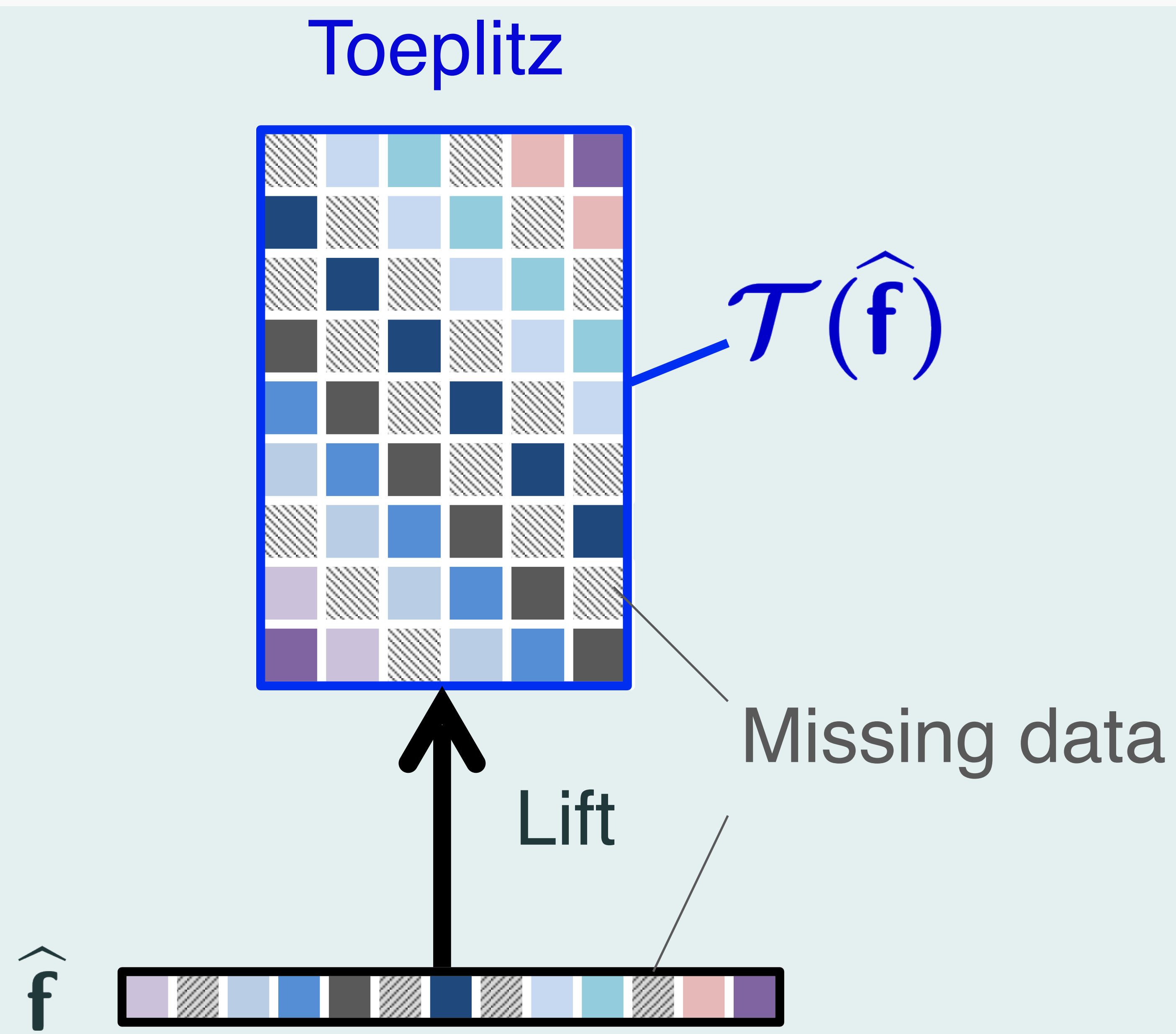

Exploit convolutional structure of the matrix

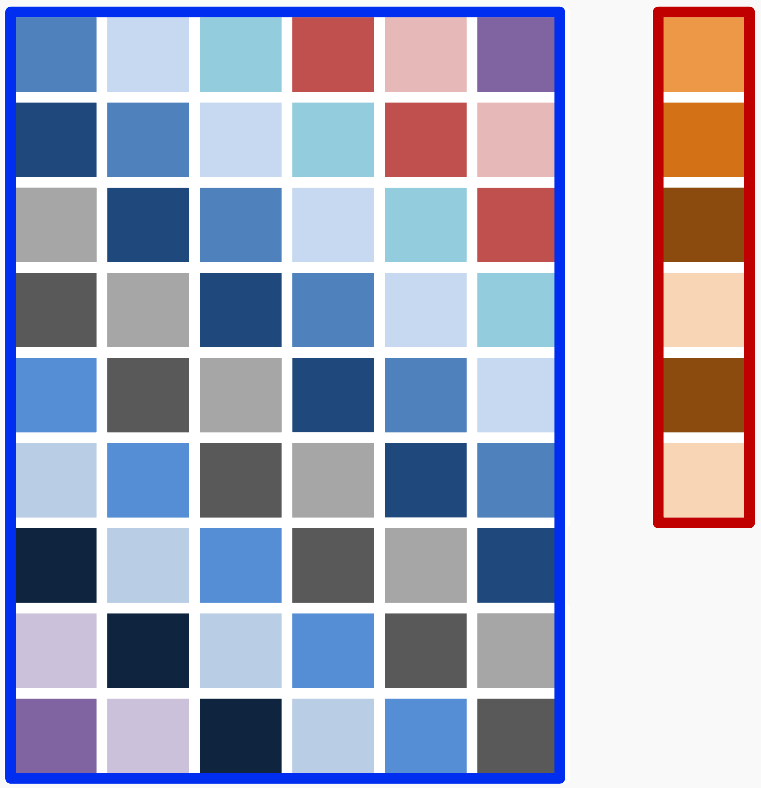

$$\mathcal{T}(\hat{\mathbf{f}})\;\mathbf{c} \approx \hat{\mathbf{f}} * \mathbf{c}$$

Fast evaluation using FFT

Direct computation of small Gram matrix: avoid storage

[Ongie & Jacob, IEEE TCI 17](#)
[Software available at https://research.engineering.uiowa.edu/cbig/software](https://research.engineering.uiowa.edu/cbig/software)

GSLR: fast algorithms with similar complexity as TV

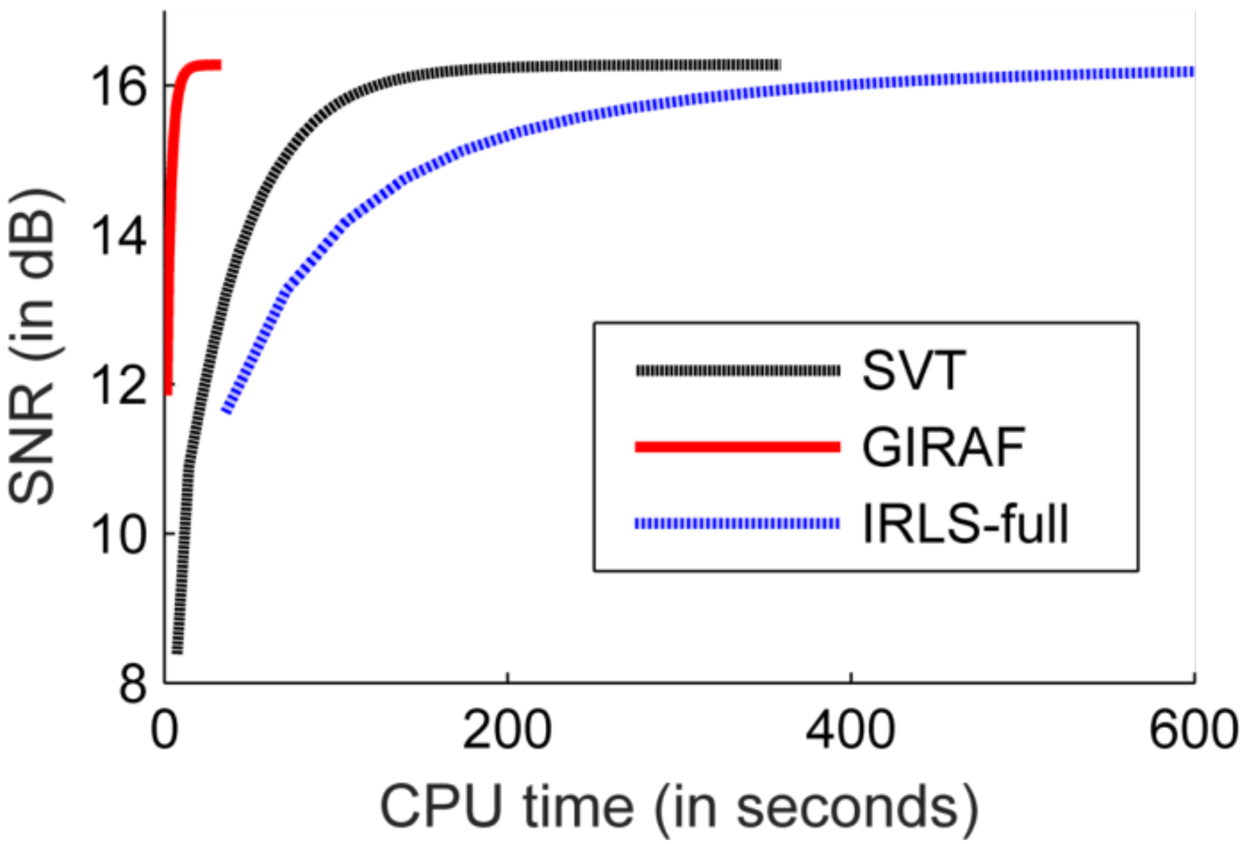

	15×15 filter		31×31 filter	
Algorithm	# iter	total	# iter	total
SVT	7	110s	11	790 s
GIRAF	6	20s	7	44 s

Table: iterations/CPU time to reach convergence tolerance of NMSE < 10^{-4}.

[Ongie & Jacob, IEEE TCI 17](#)
[Software available at https://research.engineering.uiowa.edu/cbig/software](https://research.engineering.uiowa.edu/cbig/software)

Lift to a high-dimensional space where solution is simple !!

Linear lifting operations

- Continuous domain compressed sensing
- Recovery of exponential signals: EPI correction & parameter mapping
- Auto-calibration: account for inconsistencies in acquisition

Non-linear lifting

- Recovery of data in high dimensional spaces
- Learning functions in high dimensional spaces: links to deep learning

Model based deep learning

- Using learning based models in imaging

Continuous domain CS: piecewise constant signals

Edges specified by zero set of a BL function

2-D PWC function

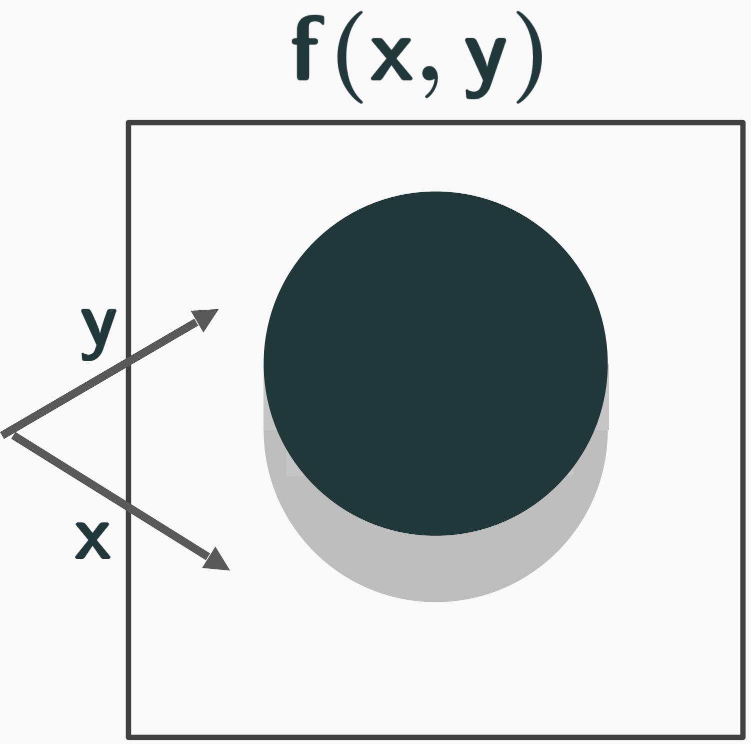

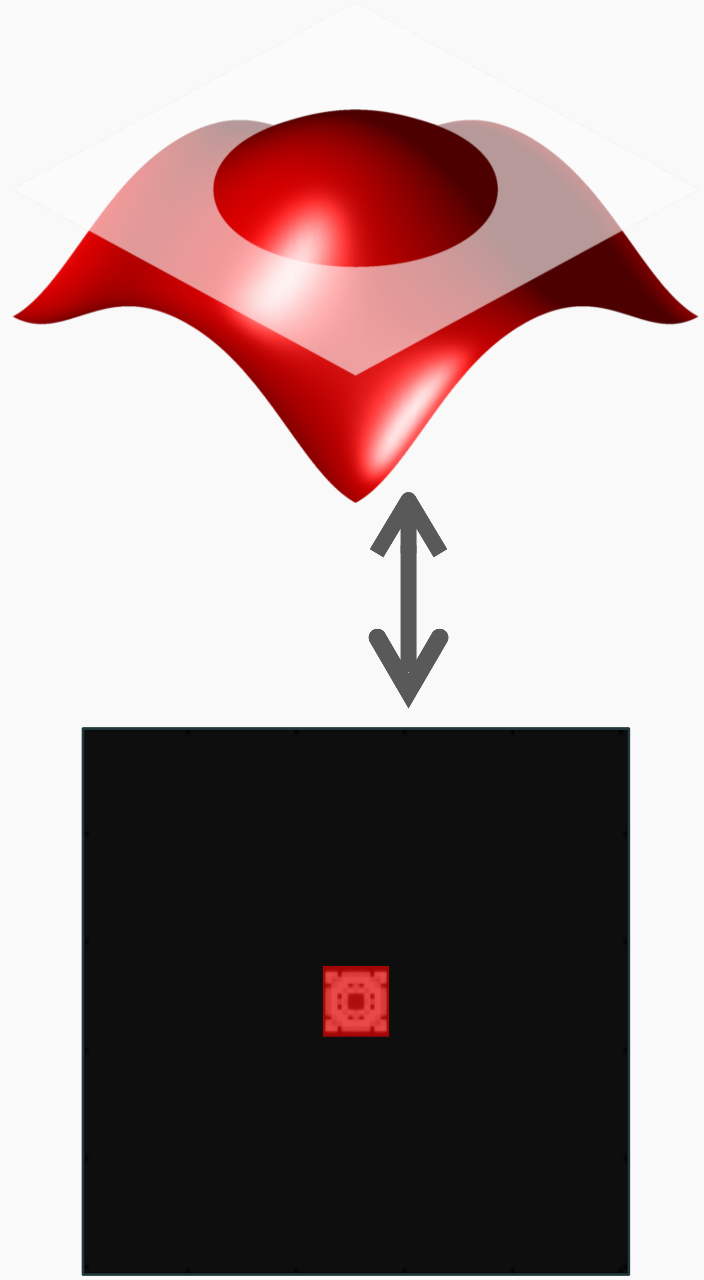

BL curves can represent complex shapes

Multiple curves
& intersections

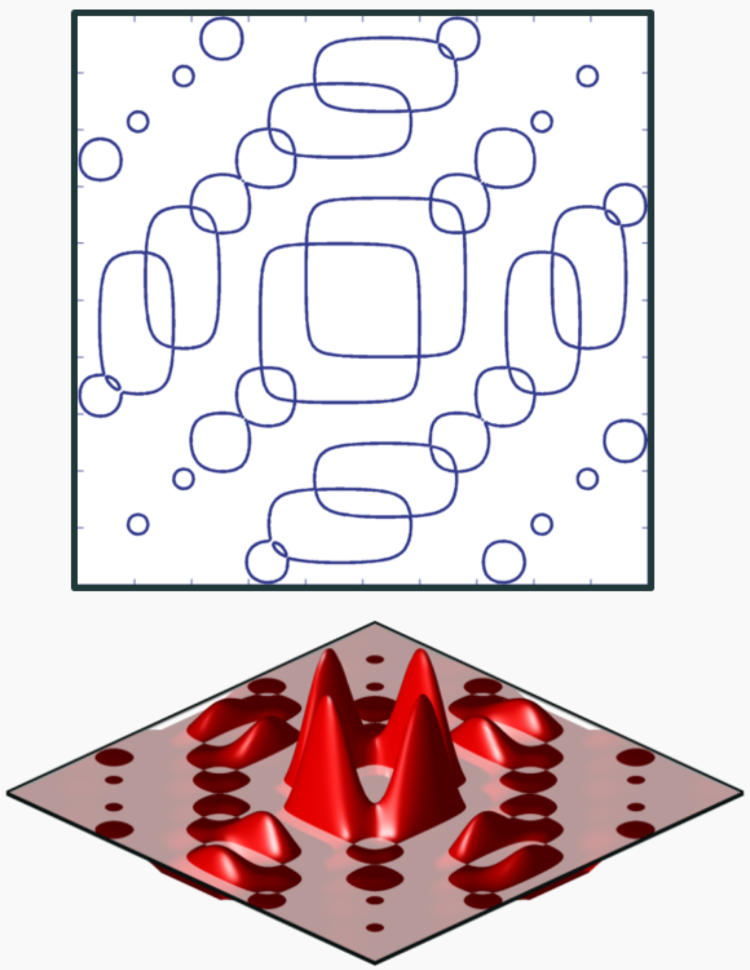

13x13 coefficients

Non-smooth
points

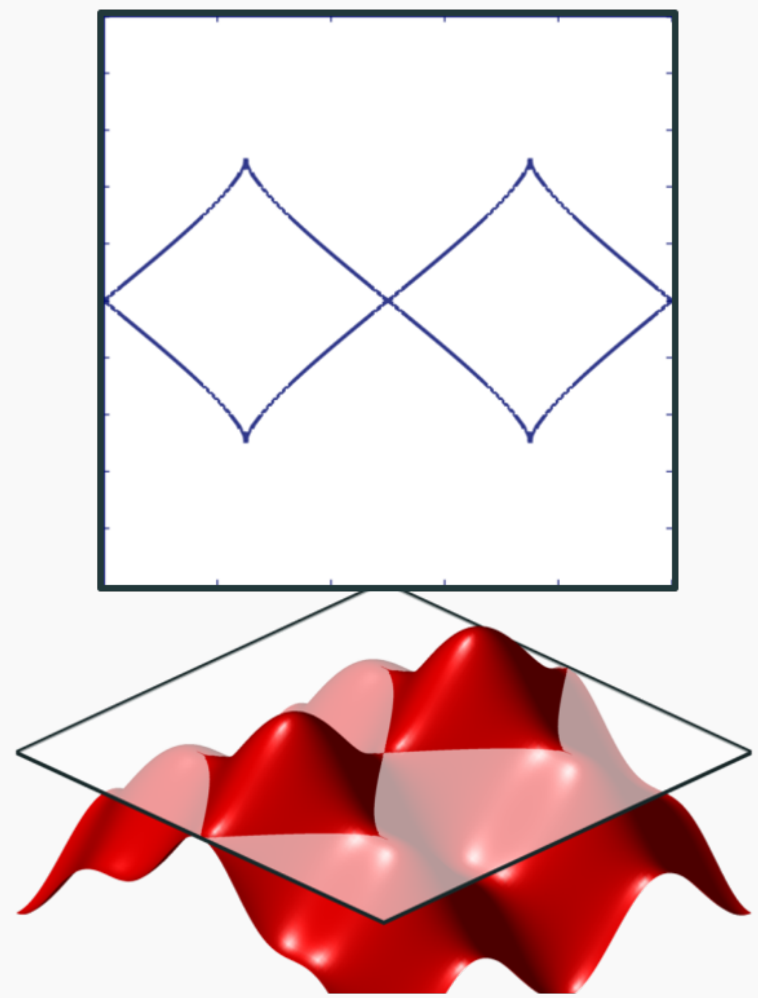

7x9 coefficients

Approximate
arbitrary curves

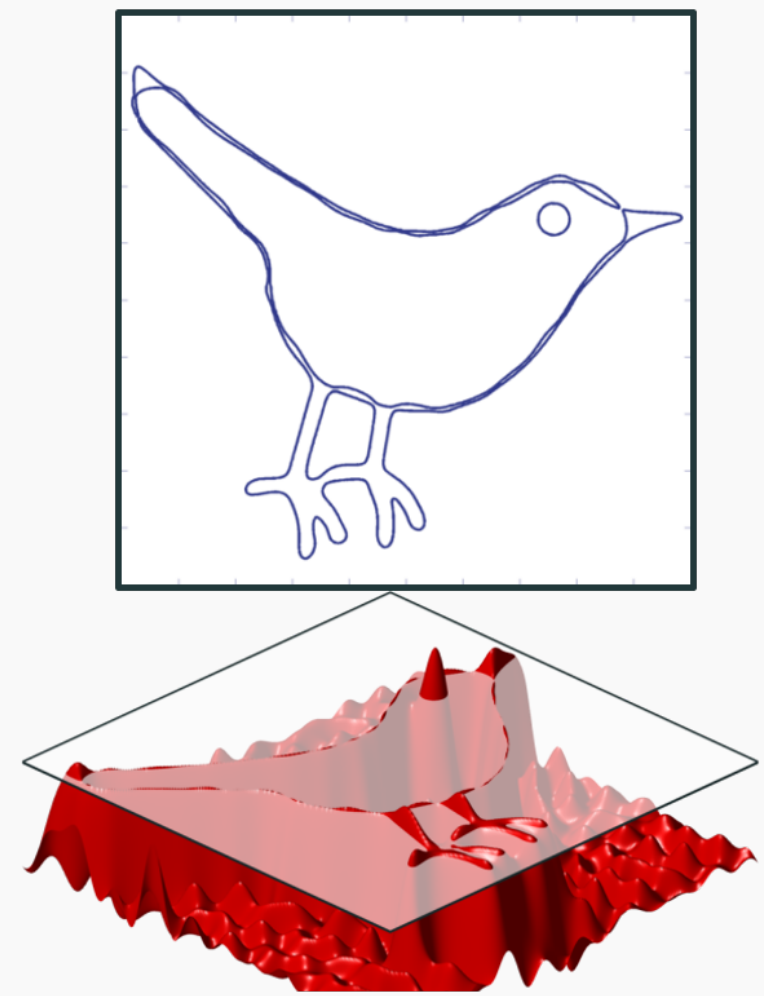

25x25 coefficients

Annihilation relations & structured low-rank matrix

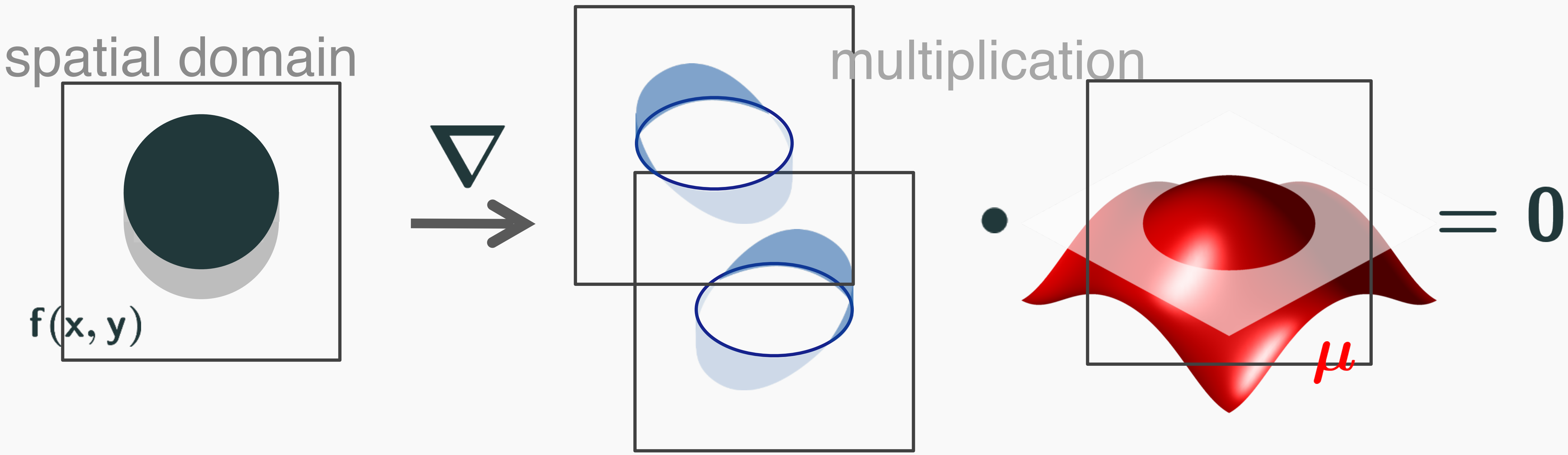

Annihilation relations & structured low-rank matrix

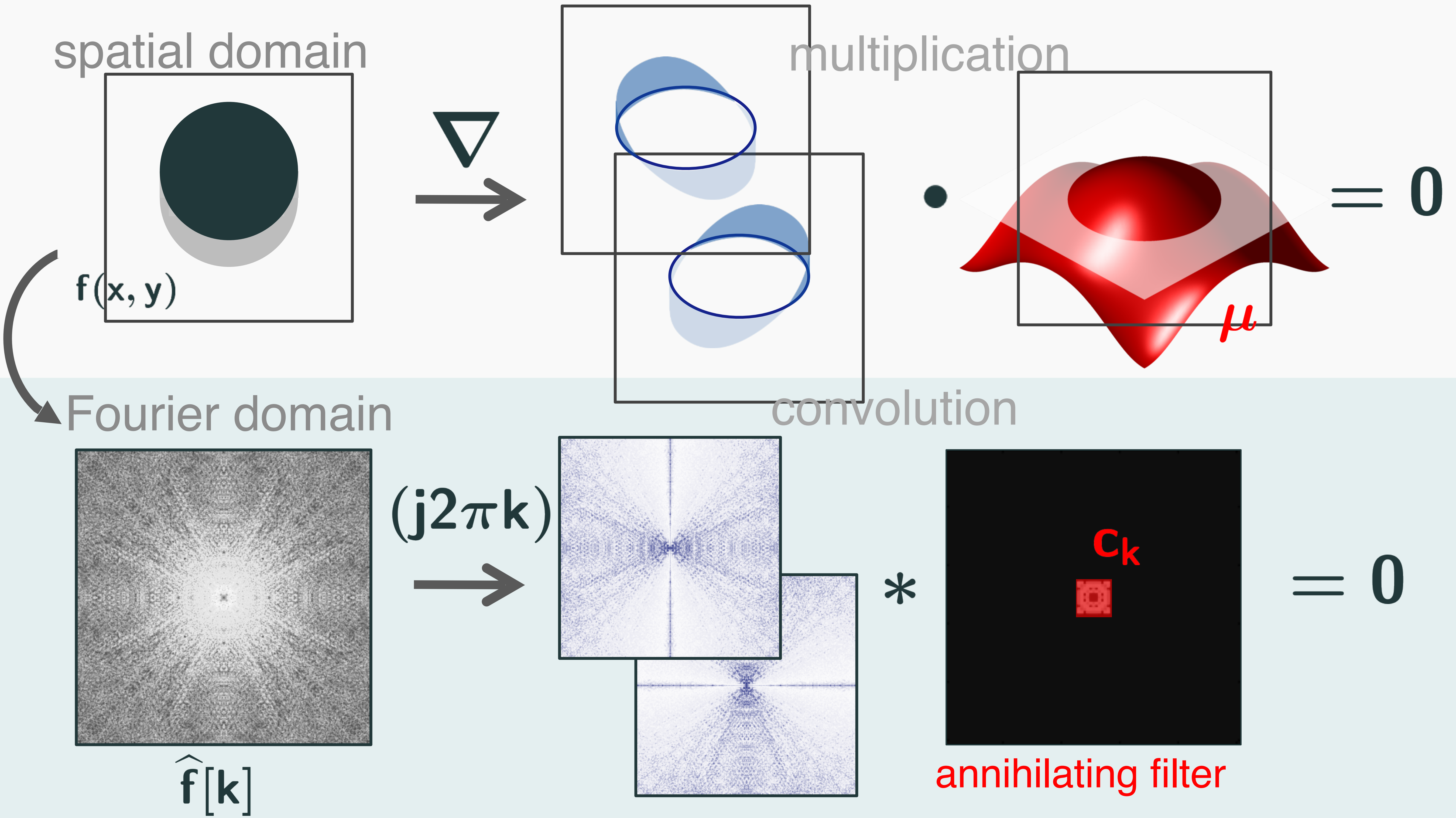

Annihilation relation: $\sum_{\mathbf{k}} \widehat{\nabla \mathbf{f}}[\ell - \mathbf{k}]\,\mathbf{c_k} = 0$

Matrix representation of annihilation

$$\mathcal{T}(\widehat{f})\,\boldsymbol{c} = \mathbf{0}$$

2-D convolution matrix
(block Toeplitz)

vector of filter coefficients

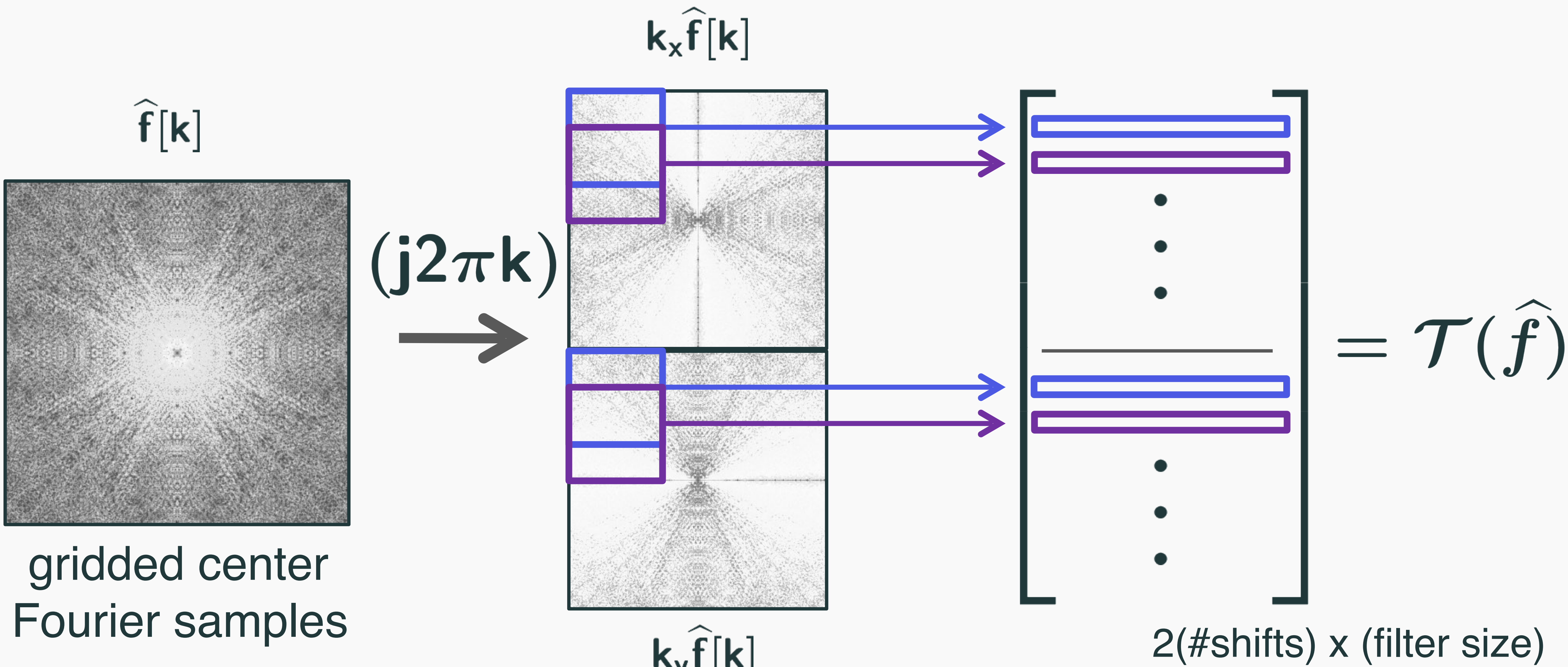

Basis of algorithms: Annihilation matrix is low-rank

$$\mathcal{T}(\widehat{f})\boldsymbol{c} = \mathbf{0}$$

Example:
Shepp-Logan

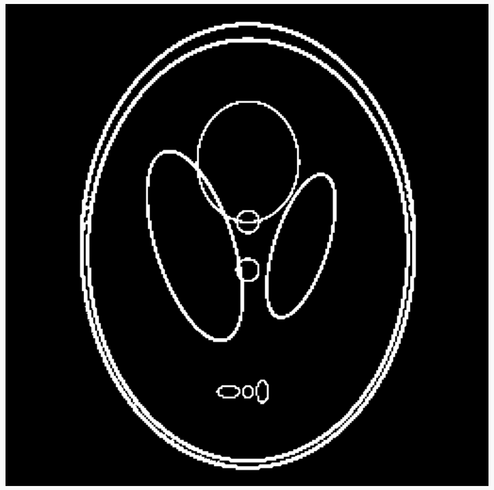

Fourier domain

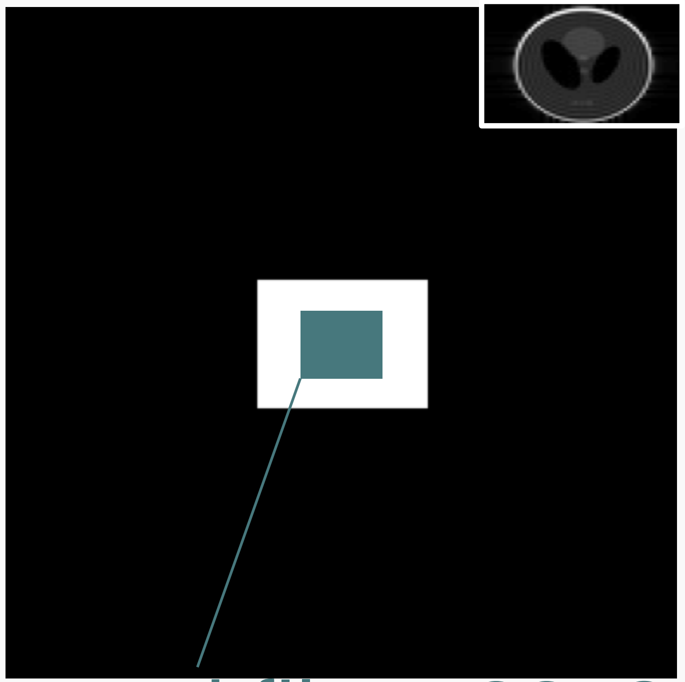

Assumed filter: 33x25

Samples: 65x49

$$\sigma(\mathcal{T}(\widehat{f}))$$

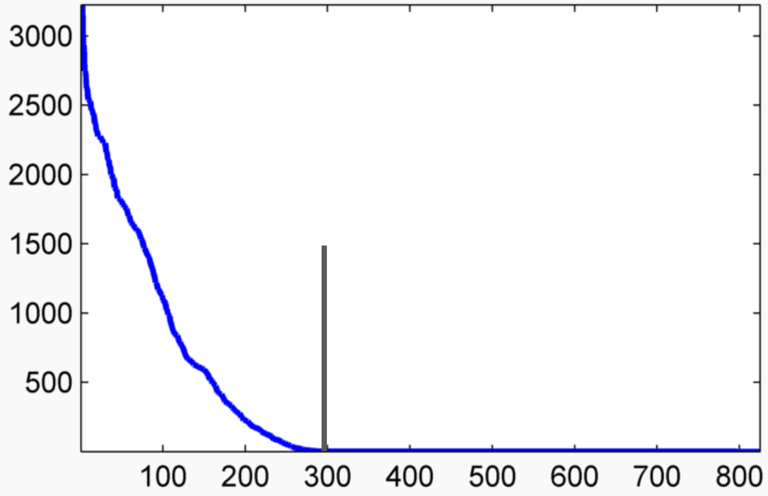

Rank $\approx$ 300

Annihilation matrix is low-rank: Basis of algorithms

Prop: If the level-set function is bandlimited to Λ and the assumed filter support $\Lambda' \supset \Lambda$ then

$$\mathrm{rank}[\mathcal{T}(\widehat{\mathbf{f}})] \leq |\Lambda'| - (\#\text{shifts } \Lambda \text{ in } \Lambda')$$

Fourier domain

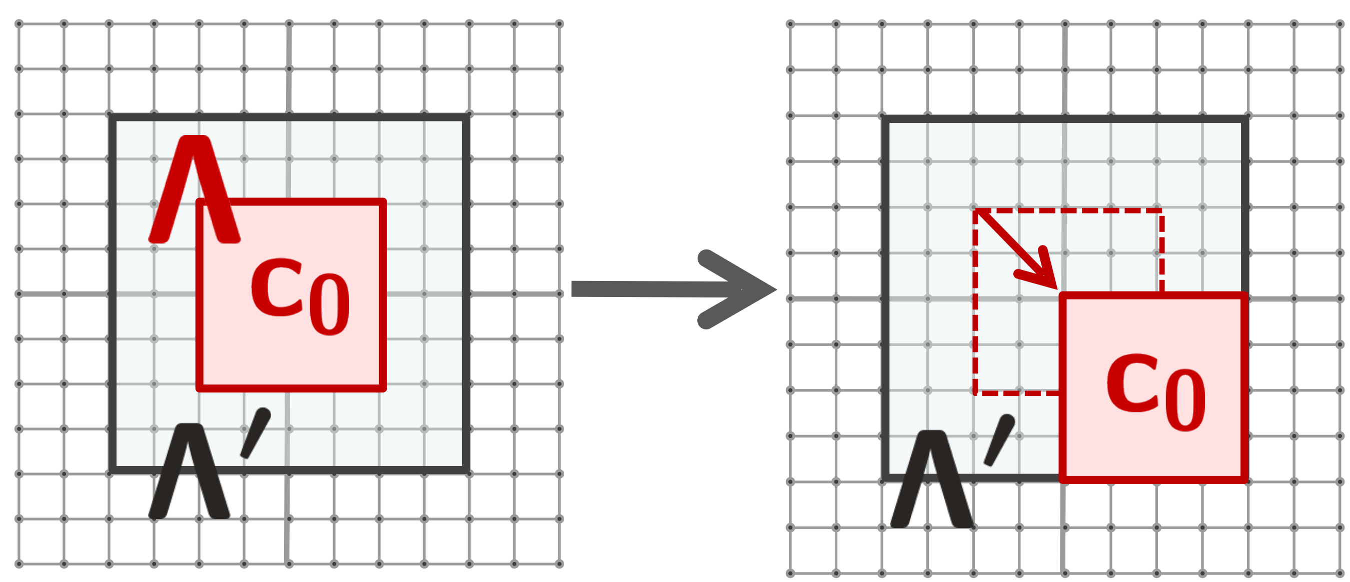

Spatial domain $\mu(\mathbf{x},\mathbf{y}) \longrightarrow e^{j2\pi(\mathbf{kx}+\mathbf{ly})}\mu(\mathbf{x},\mathbf{y})$

Recovery as a structured low-rank matrix completion

$$\min_{\widehat{\mathbf{f}}} \quad \mathrm{rank}[\mathcal{T}(\widehat{\mathbf{f}})] \;\; \textbf{s.t.} \;\; \widehat{\mathbf{f}}[\mathbf{k}] = \widehat{\mathbf{b}}[\mathbf{k}], \mathbf{k} \in \boldsymbol{\Gamma}$$

Convex Relaxation

$$\min_{\widehat{\mathbf{f}}} \quad \|\mathcal{T}(\widehat{\mathbf{f}})\|_* \;\; \textbf{s.t.} \;\; \widehat{\mathbf{f}}[\mathbf{k}] = \widehat{\mathbf{b}}[\mathbf{k}], \mathbf{k} \in \boldsymbol{\Gamma}$$

Nuclear norm – sum of singular values

[Ongie & Jacob, ICIP 16](#)

[Ongie, Biswas & Jacob,TSP,2018](#)

Performance guarantee

Assume that f is sampled uniformly at m locations random on a Fourier domain grid Γ. Then, f can be recovered from the samples using SLR if

$$\mathsf{m} > \rho_1 \, \mathsf{c_s} \, \mathsf{r} \, \log^4 |\Gamma|$$

$$\boldsymbol{\rho_1} = \text{incoherence measure of edge-set}$$

$$\mathbf{r} = \text{rank of } \mathcal{T}(\widehat{\mathbf{f}})$$

$$\mathbf{c_s} = \text{ratio of grid size to filter size}$$

Ongie & Jacob, ICIP 16
Ongie, Biswas & Jacob,TSP,2018

Phase transition plot

Randomly generated synthetic PWC images

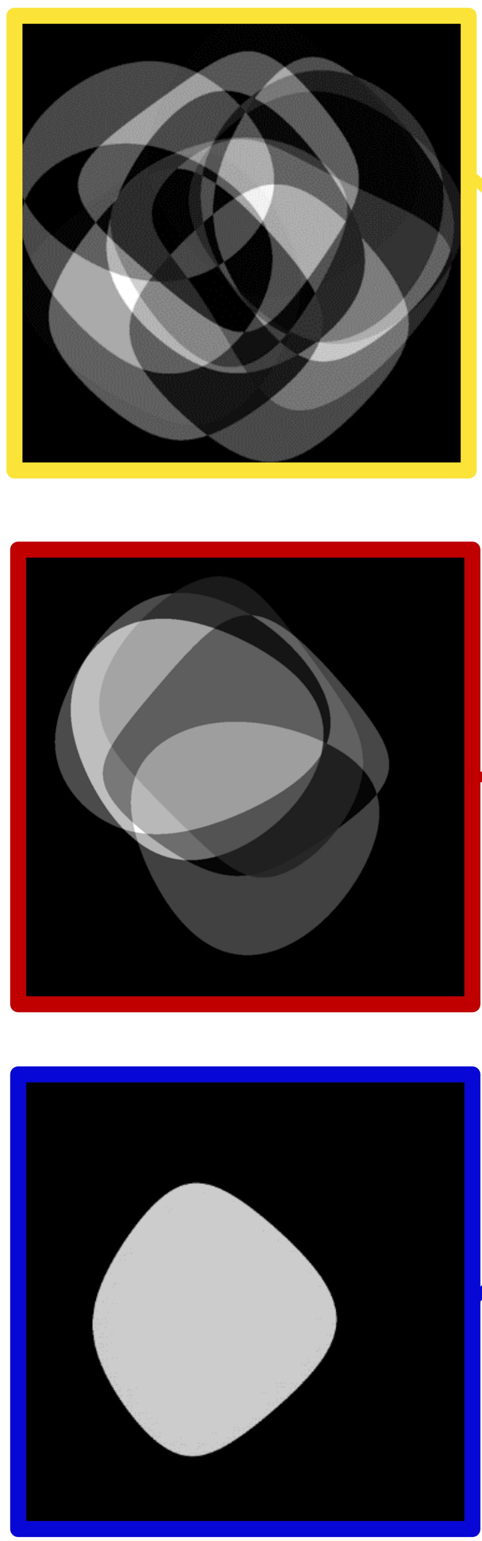

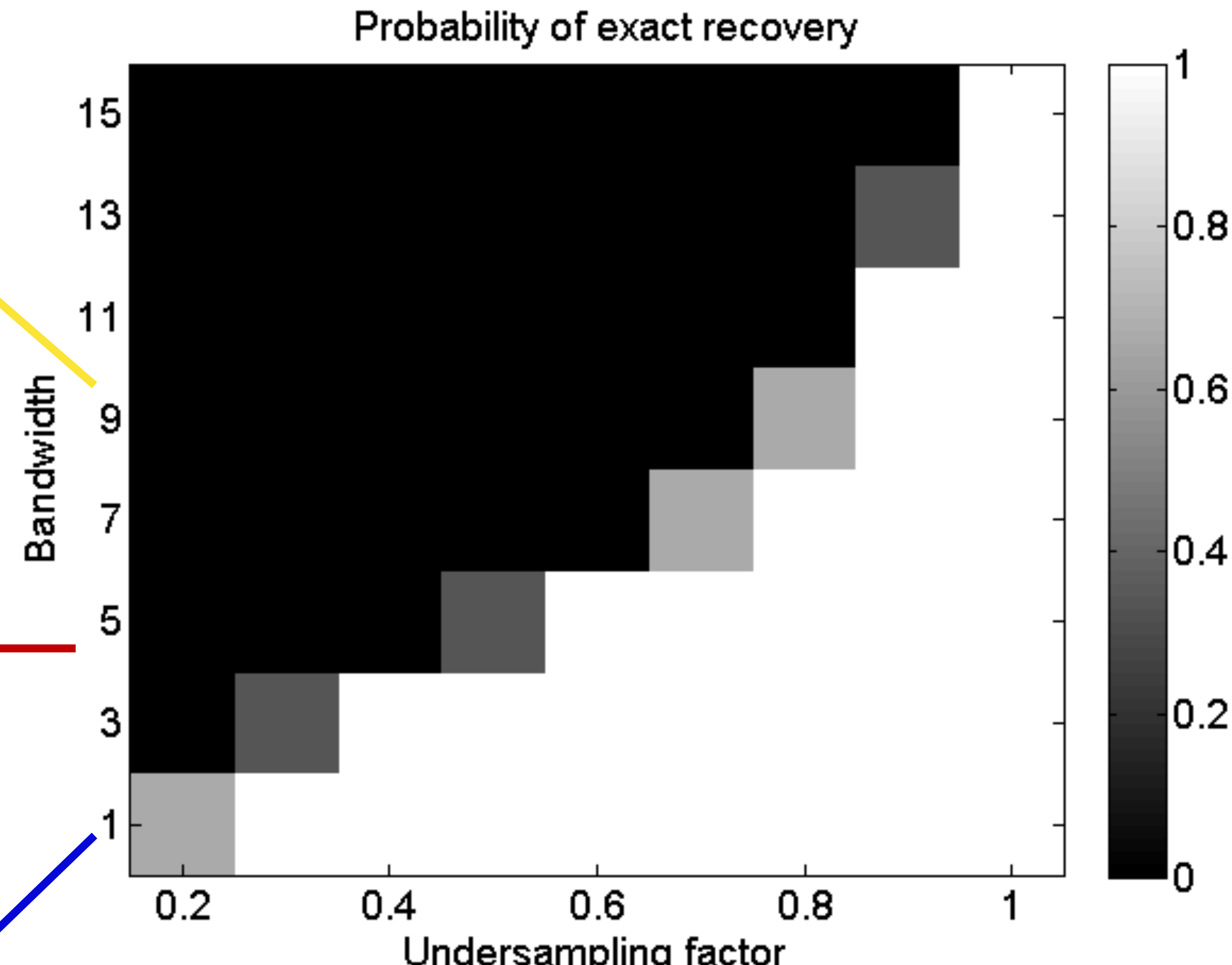

- 10 trials
- Uniform random Fourier samples
- 64x64 Fourier sampling window

Ongie & Jacob, ICIP 16
Ongie, Biswas & Jacob,TSP,2018

Fully sampled TV (SNR=17.8dB) GIRAF (SNR=19.0)

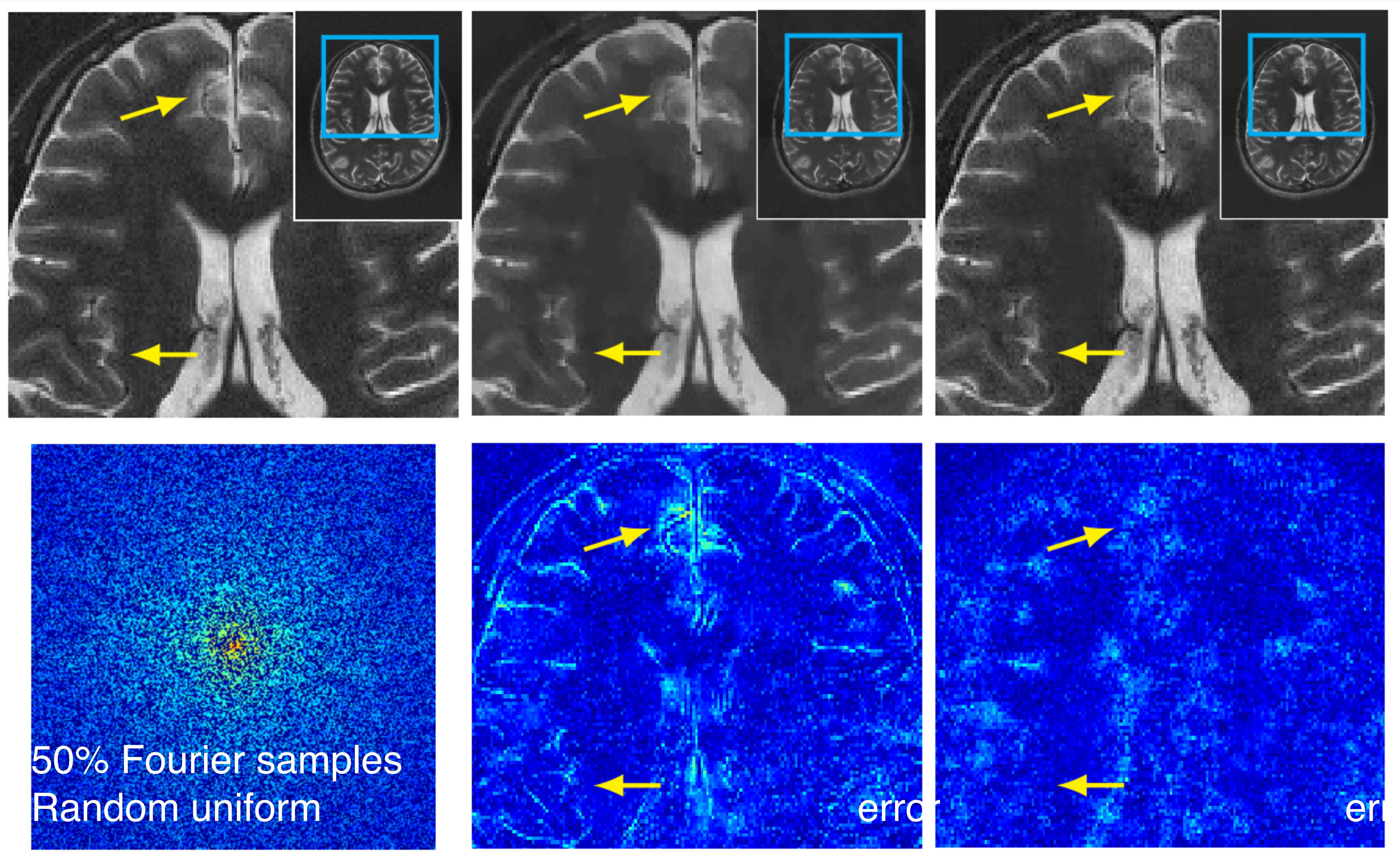

Ongie, Biswas & Jacob, IEEE TSP, 2017

Generalized SLR: PWC + PWL image representation

$$\underbrace{\{\rho_1, \rho_2\}}_{\boldsymbol{\rho}} = \arg\min_{\boldsymbol{\rho}} \|\mathcal{A}(\rho_1 + \rho_2) - \mathbf{b}\|^2 + \|\mathcal{H}_1(\boldsymbol{\rho}_1)\|_* + \|\mathcal{H}_2(\boldsymbol{\rho}_2)\|_*$$

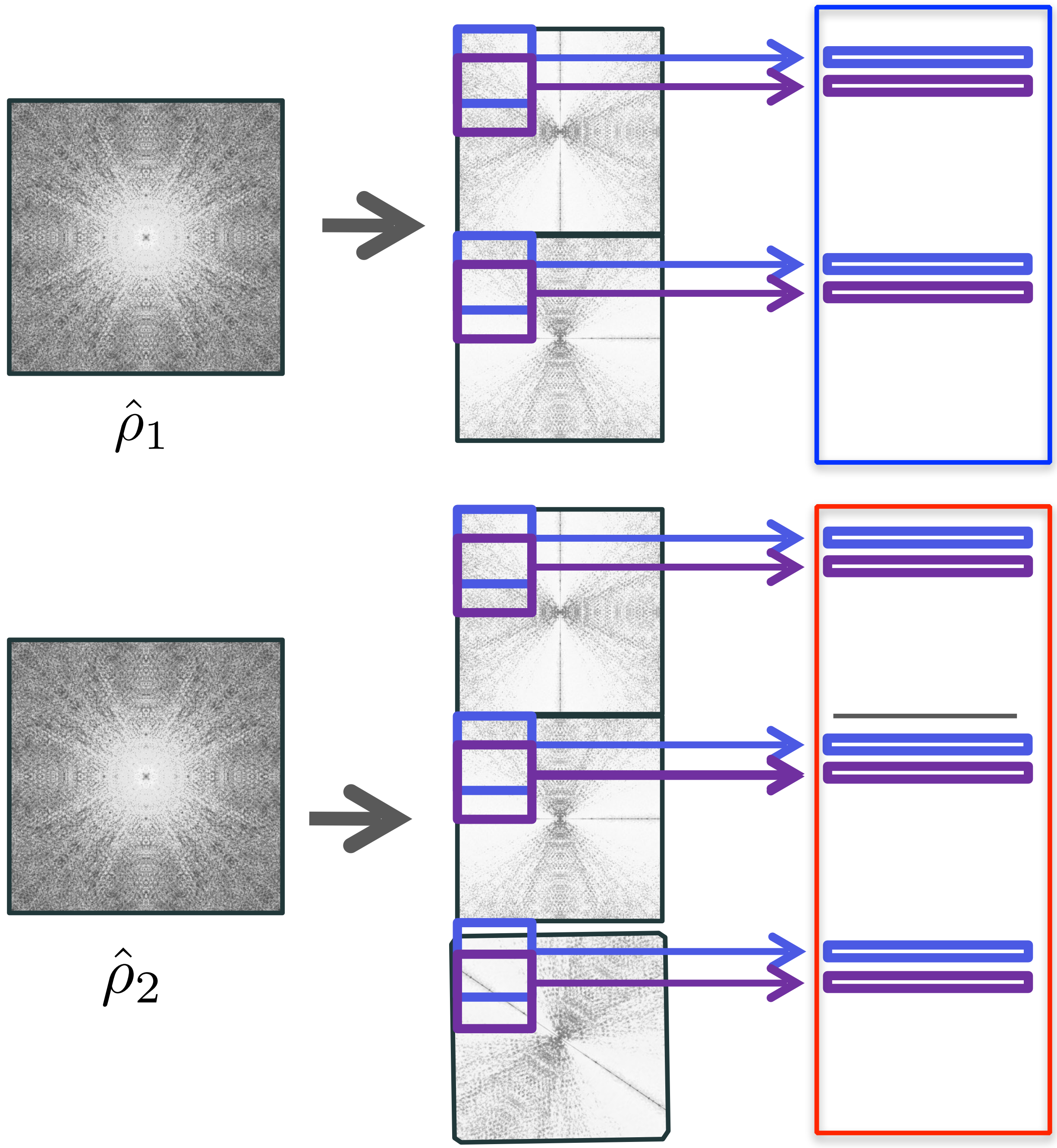

Hu, Liu & Jacob,TMI, 2019

GSLR: results

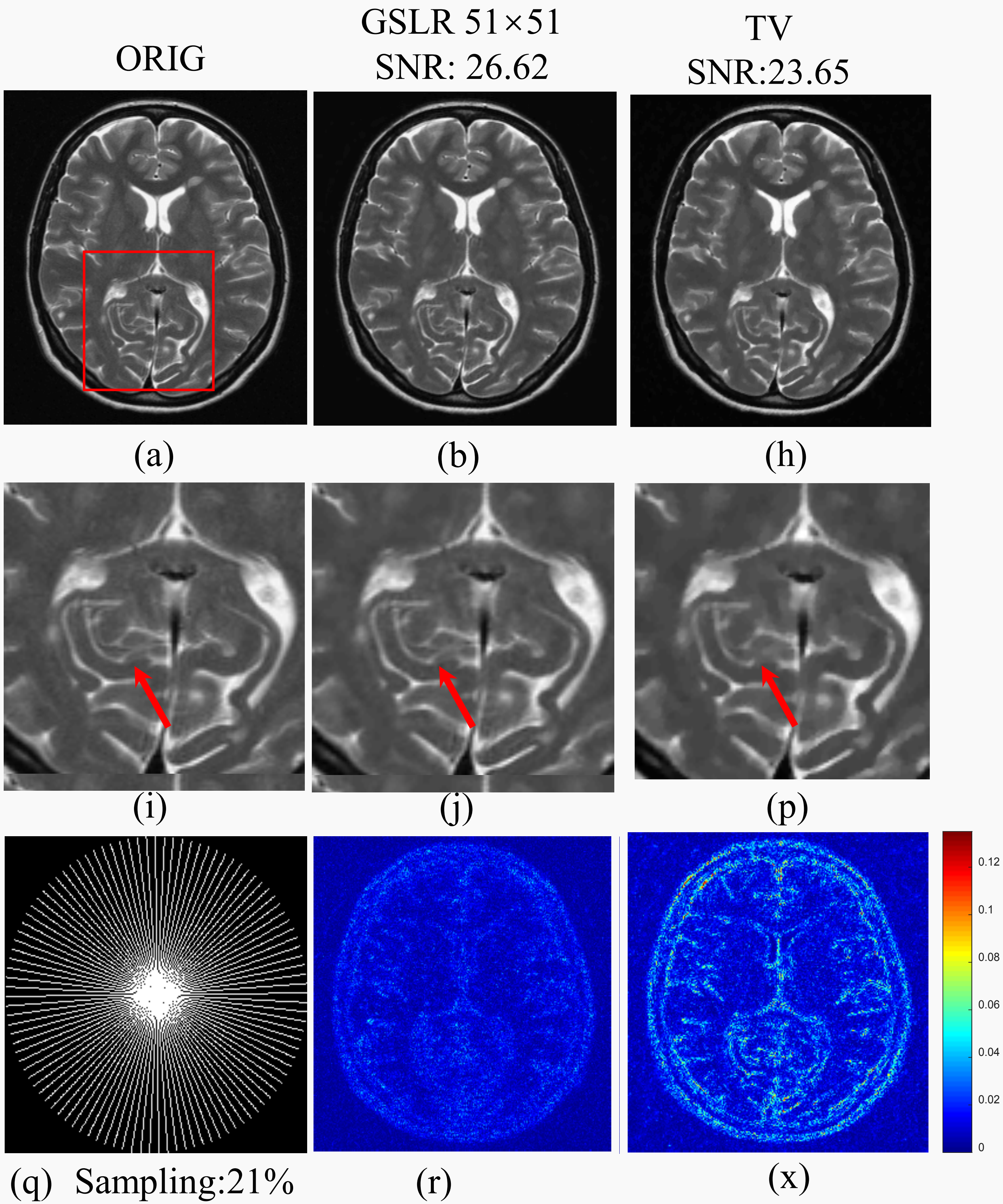

Results

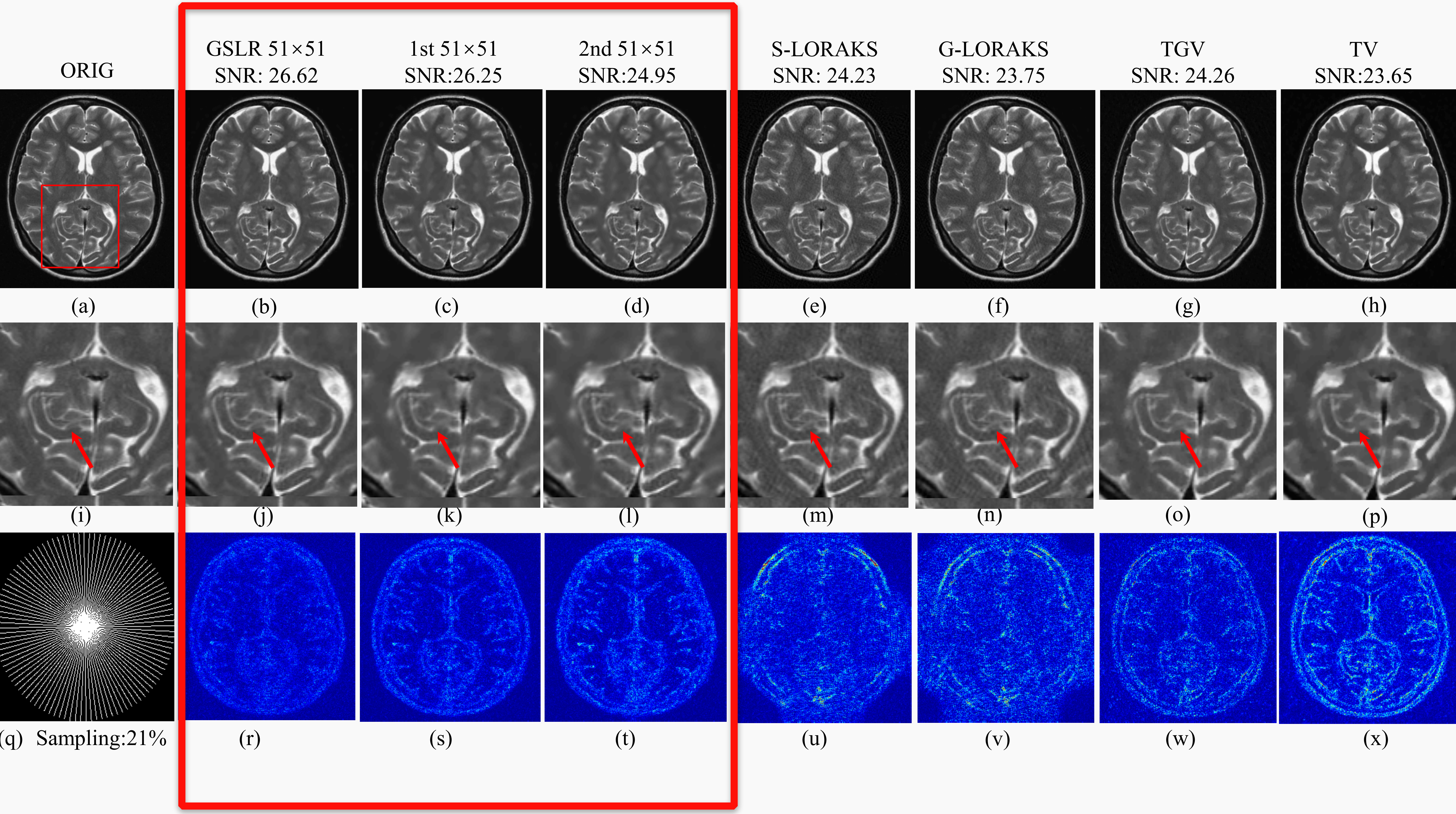

Hu, Liu & Jacob,TMI, in press

Lift to a high-dimensional space where solution is simple !!

Linear lifting operations

- Continuous domain compressed sensing
- Auto-calibration: account for inconsistencies in acquisition

Non-linear lifting

- Recovery of data in high dimensional spaces
- Learning functions in high dimensional spaces: links to deep learning

Model based deep learning

- Using learning based models in imaging

Auto-calibration in diffusion MRI

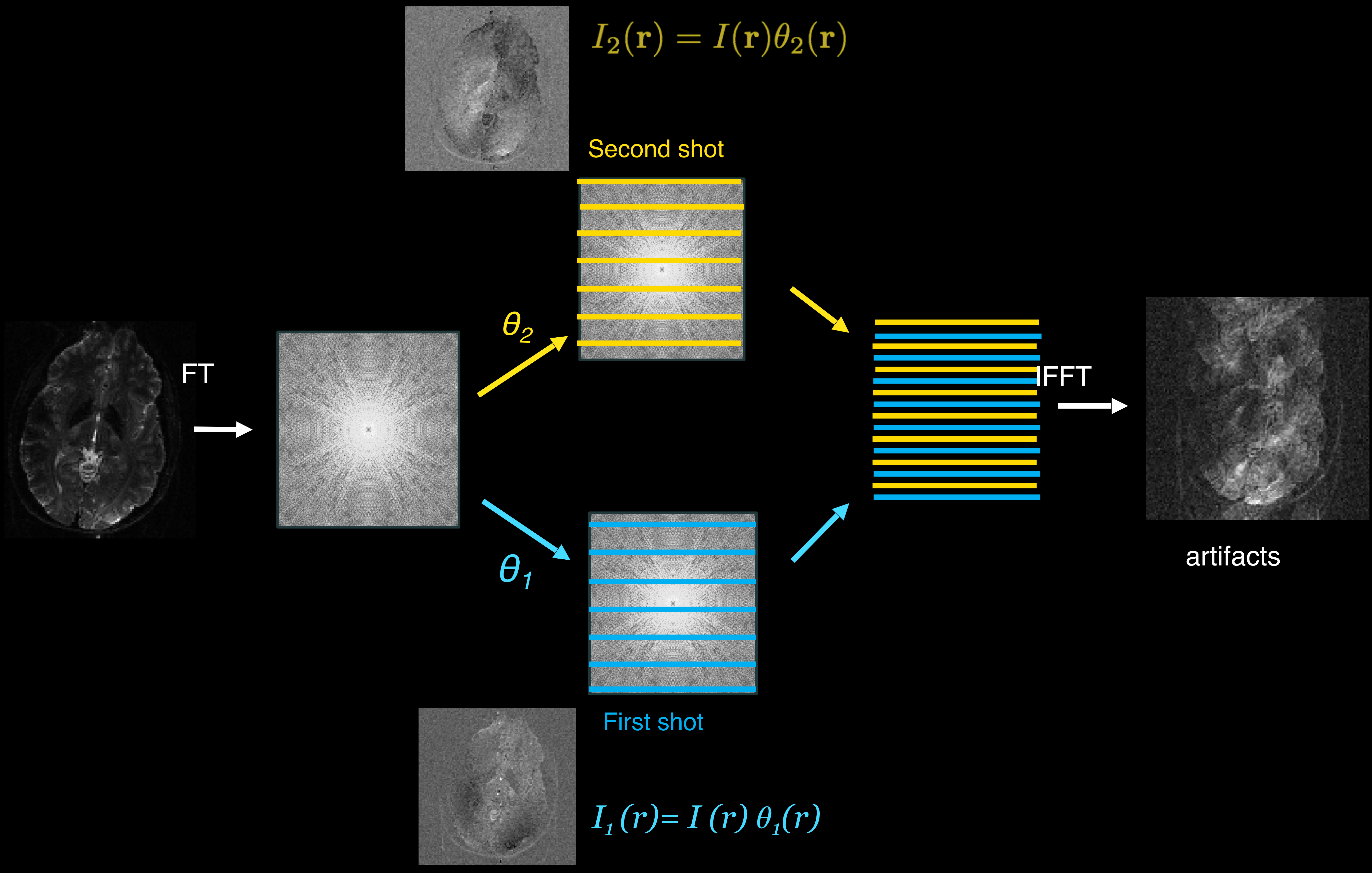

Linear prediction/annihilation of multichannel data

Image domain annihilation relation

$$\rho_1 \cdot s_2 - \rho_2 \cdot s_1 = 0$$

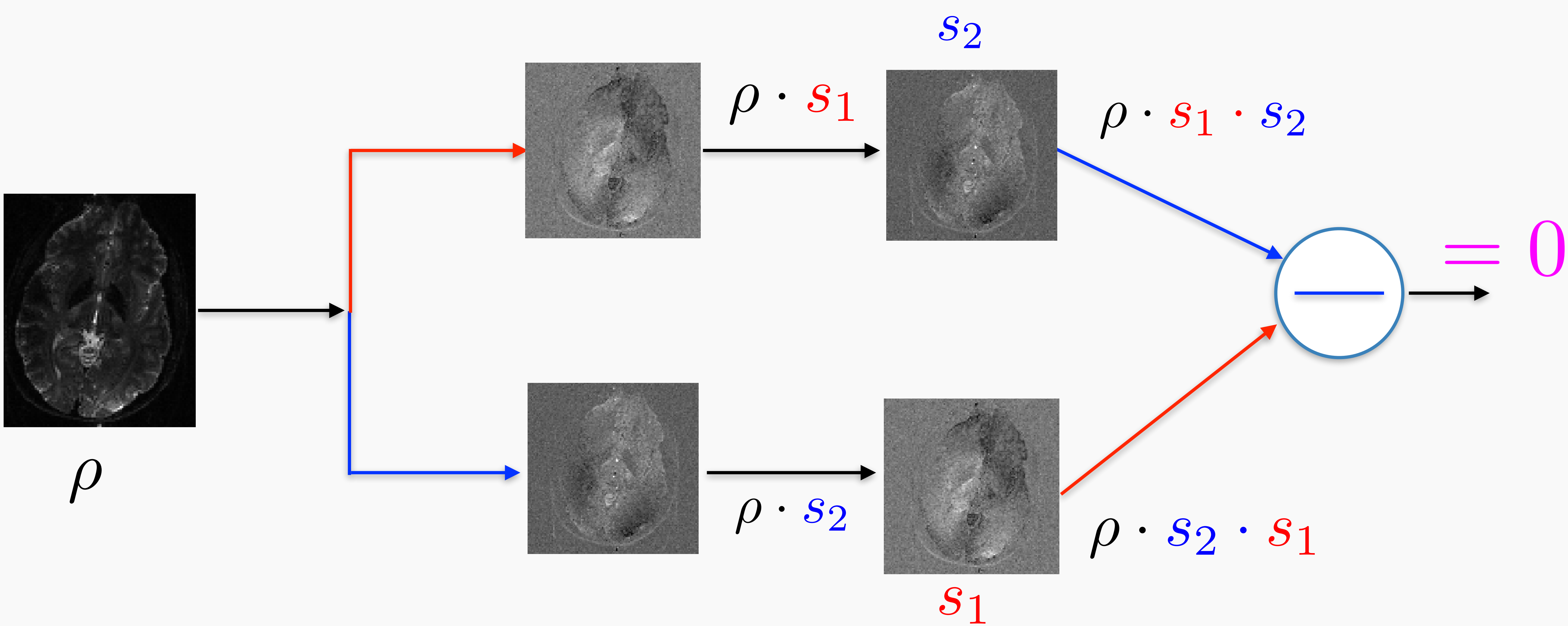

Morrison, Jacob & Do, ISBI 2007

Multichannel annihilation relations

Fourier domain convolution relation

$$\hat{\rho}_1 * \hat{s}_2 - \hat{\rho}_2 * \hat{s}_1 = 0$$

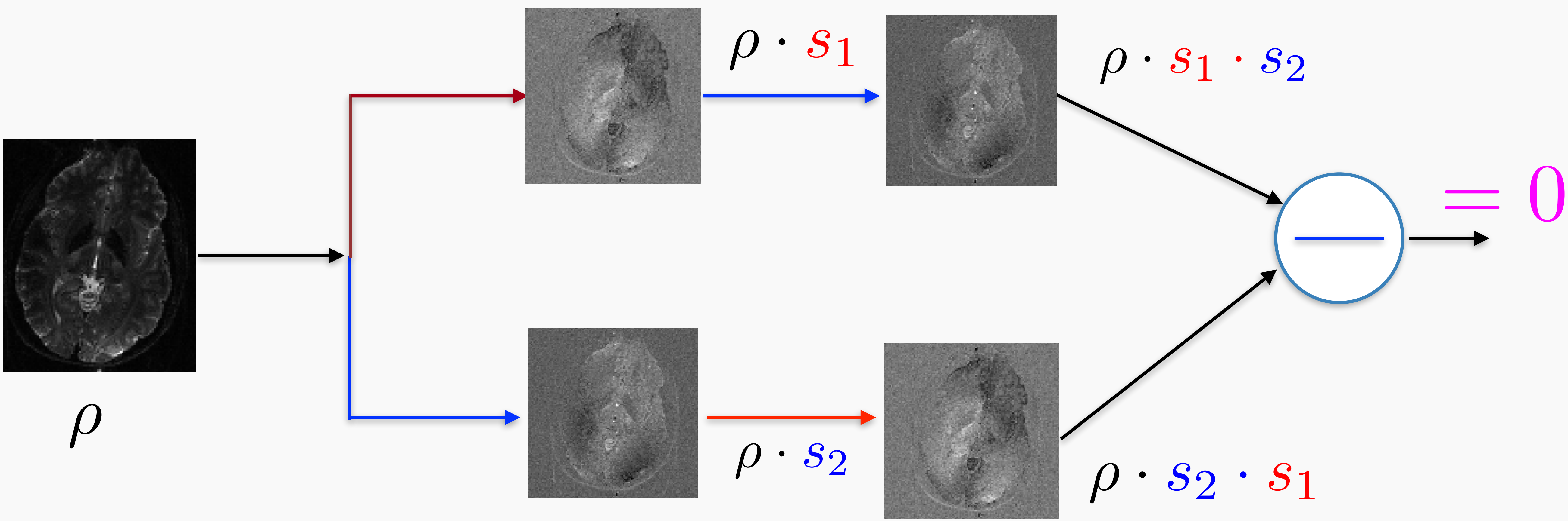

Shin et al, MRM, 2014, Uecker et al, MRM 2014

Multichannel annihilation relations

Convolution: multiplication with Toeplitz matrix

$$\mathcal{T}\left(\hat{\rho}_1\right)\hat{s}_2 - \mathcal{T}\left(\hat{\rho}_2\right)\hat{s}_1 = 0$$

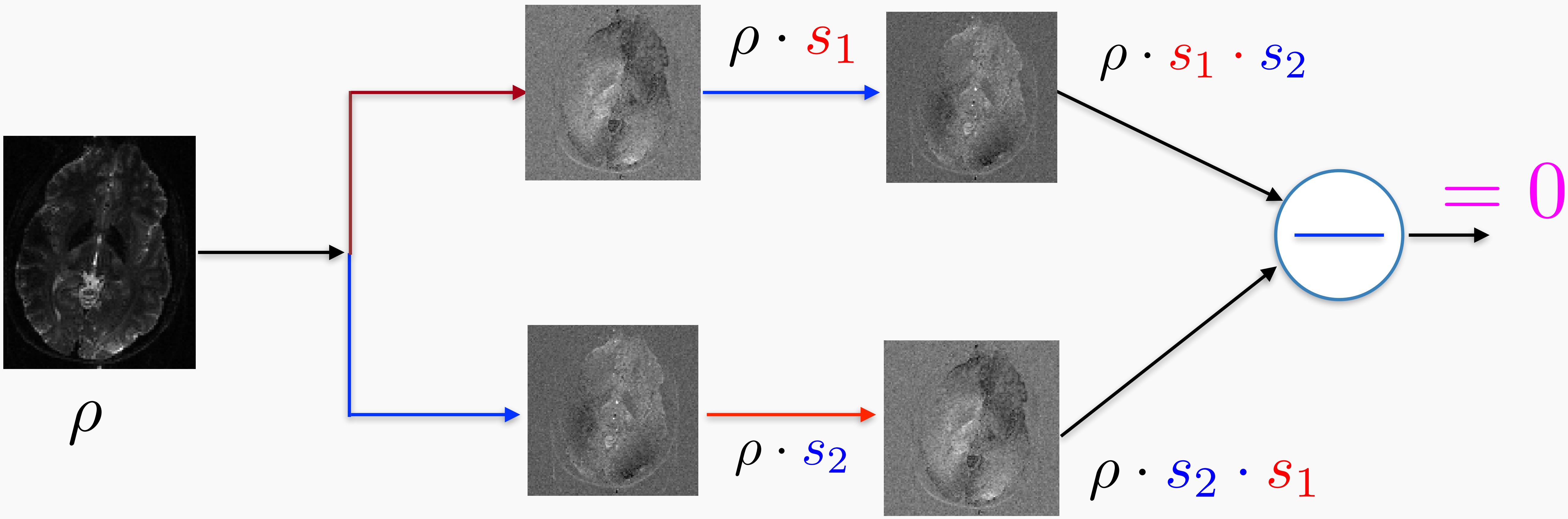

Shin et al, MRM, 2014, Uecker et al, MRM 2014

Multichannel annihilation relations

Matrix form

$$\underbrace{\left[\mathcal{T}\left(\hat{\rho}_1\right)\mathcal{T}\left(\hat{\rho}_2\right)\right]}_{\mathcal{H}(\boldsymbol{\rho})}\begin{bmatrix}\hat{s}_2\\-\hat{s}_1\end{bmatrix}=0$$

Blind recovery from under sampled multi-multi-channel data

$$\underbrace{\{\rho_1,\rho_2\}}_{\boldsymbol{\rho}}=\arg\min_{\boldsymbol{\rho}}\|\mathcal{A}(\boldsymbol{\rho})-\mathbf{b}\|^2+\|\mathcal{H}(\boldsymbol{\rho})\|_*$$

Shin et al, MRM, 2014, Uecker et al, MRM 2014

Mani et al, MUSSELS, MRM 2017, MRM 2018

Recovery using structured low-rank optimization

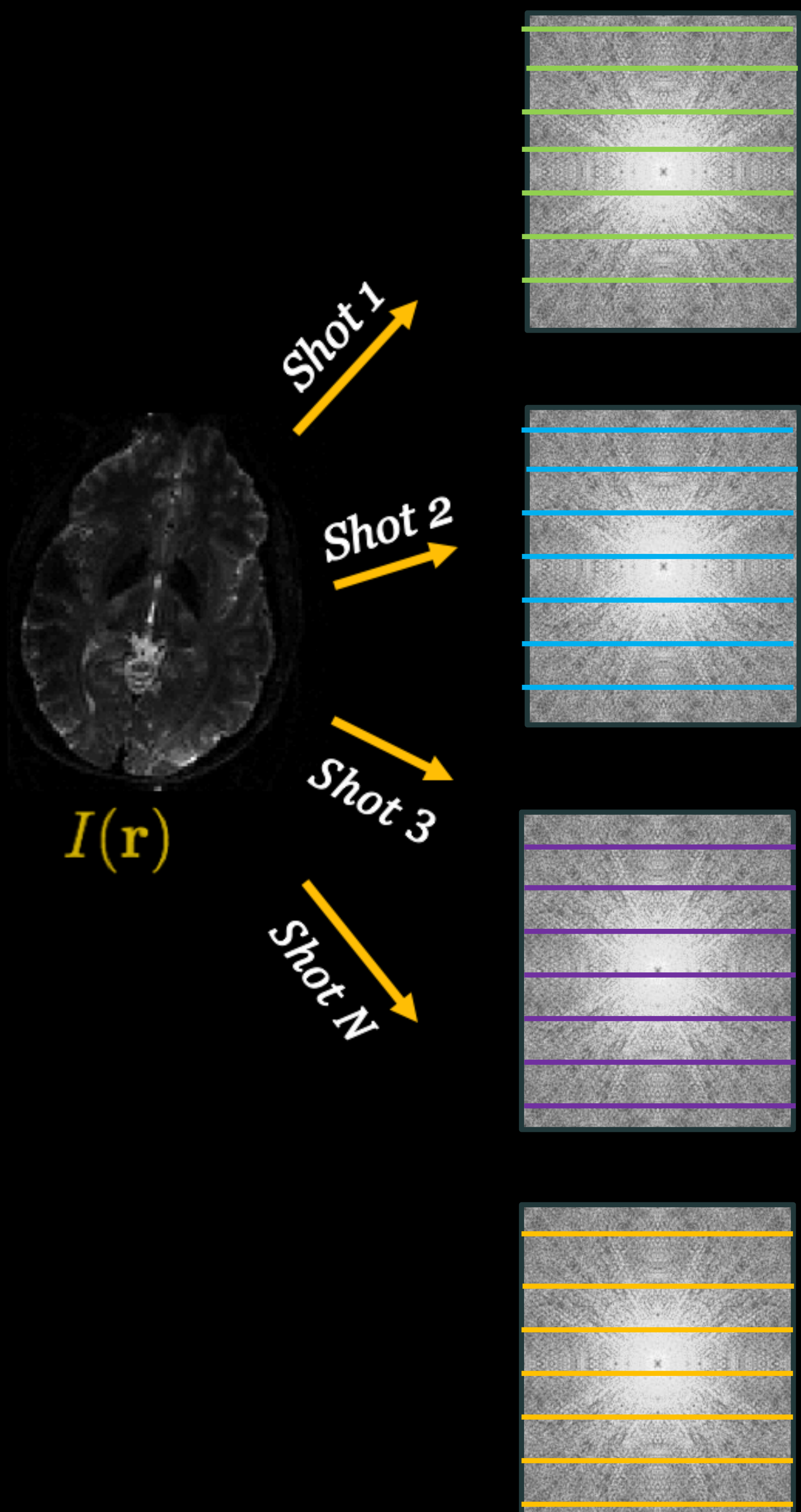

$$\arg\min_{\boldsymbol{\rho}} \|\mathcal{A}(\boldsymbol{\rho}) - \mathbf{b}\|^2 + \|\mathcal{H}(\boldsymbol{\rho})\|_*$$

MUSSELS

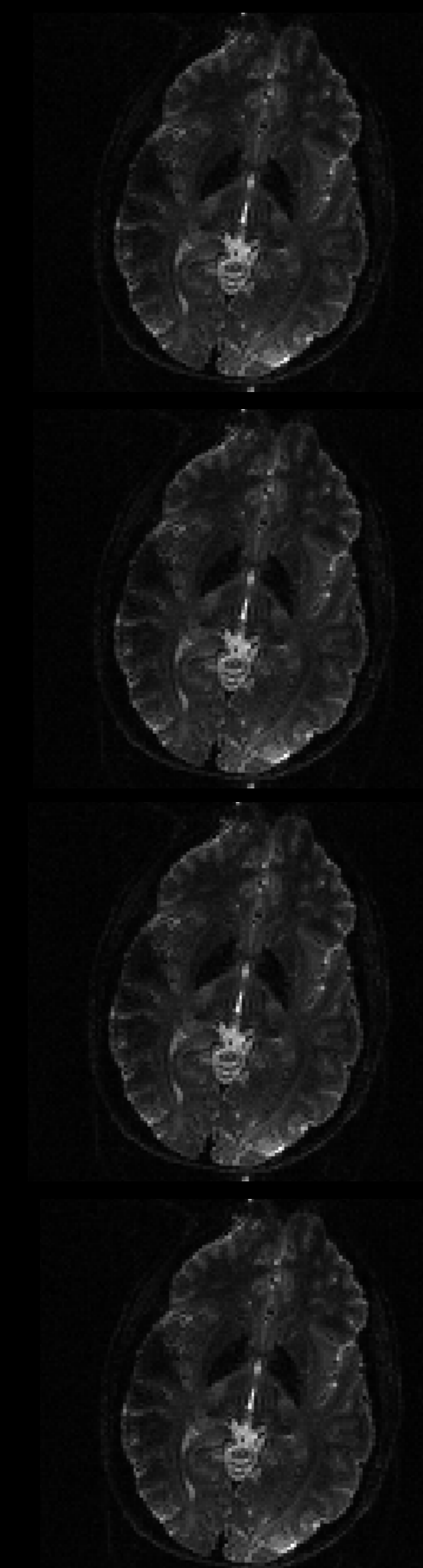

High resolution diffusion MRI on 3T

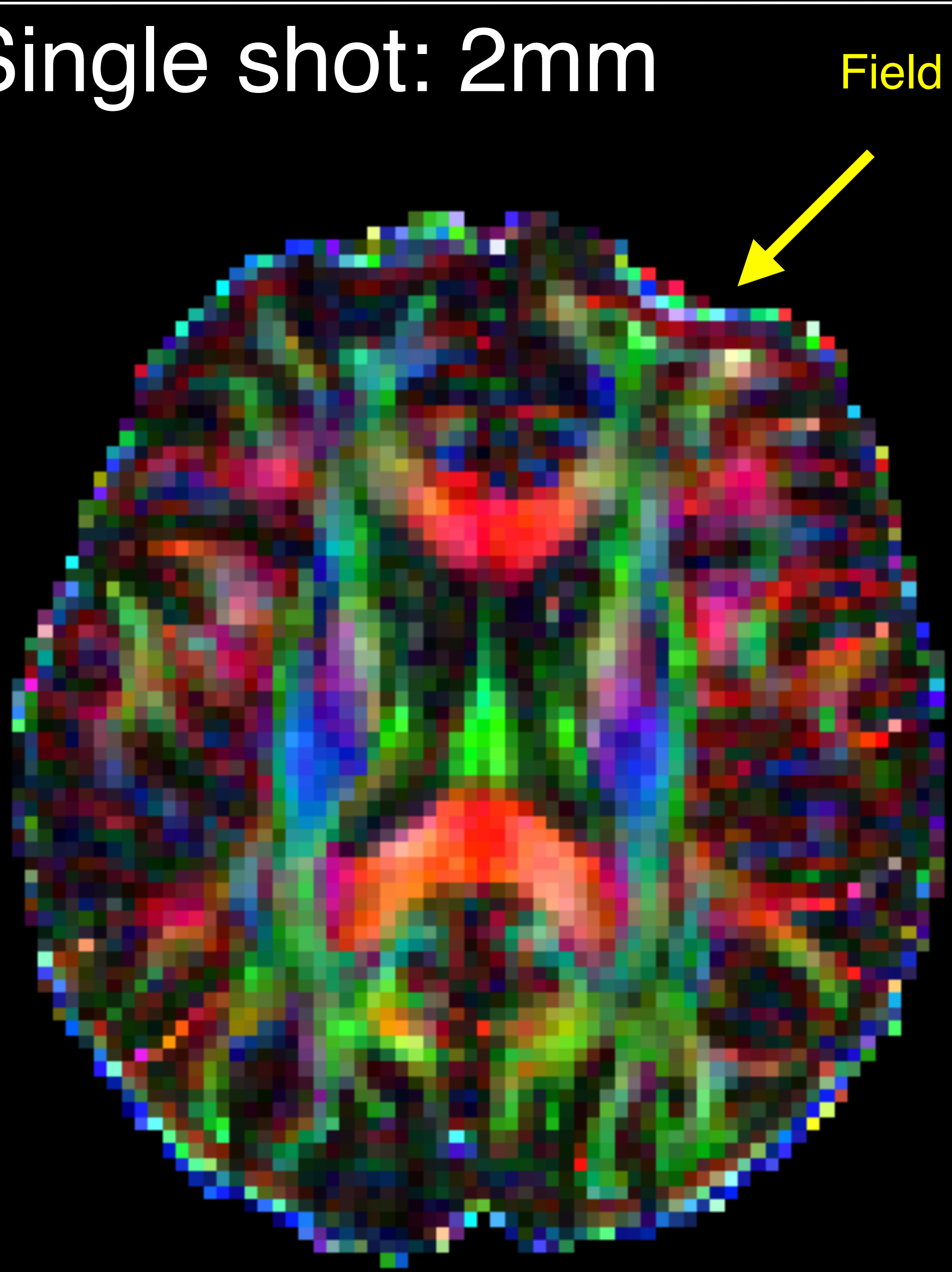

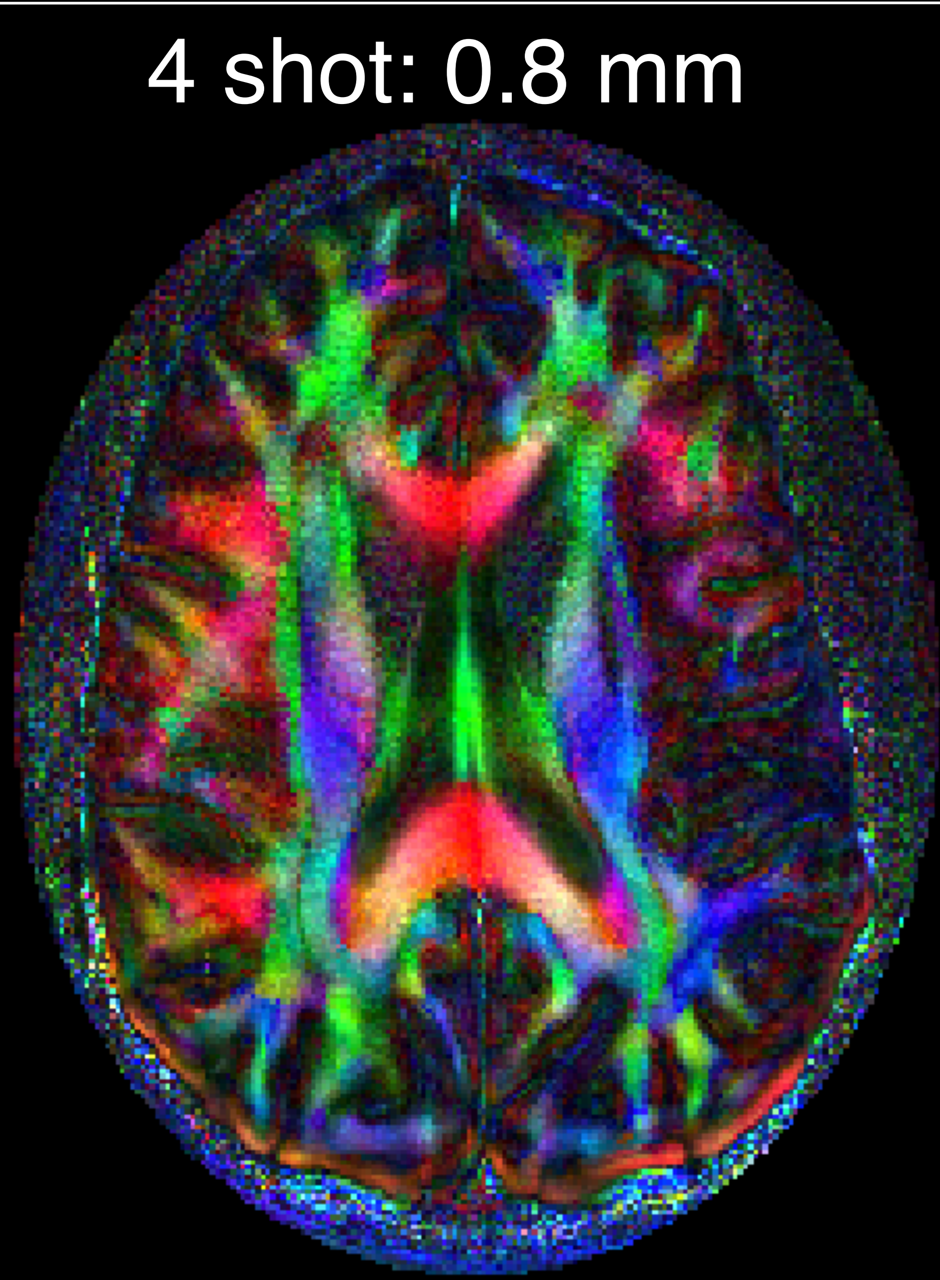

Red: Fibers oriented left-right
Green: Fibers oriented anterior-posterior
Blue: Fibers oriented inferior-superior

High resolution diffusion MRI on 3T

THE UNIVERSITY OF IOWA

ed left-right
anterior-posterio
nferior-superior

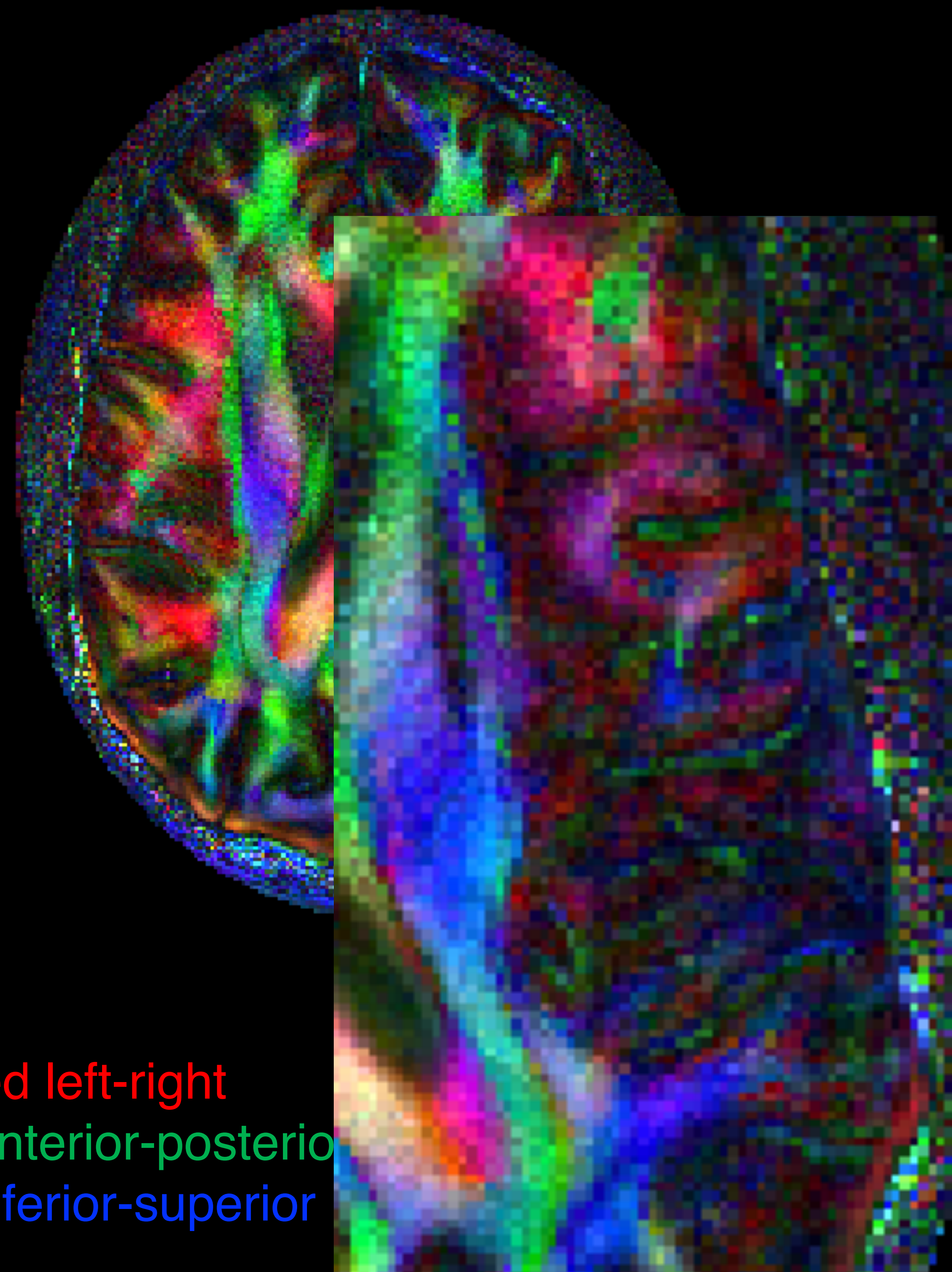

Lift to a high-dimensional space where solution is simple !!

Linear lifting operations

- Continuous domain compressed sensing
- Auto-calibration: account for inconsistencies in acquisition

Non-linear lifting

- Recovery of data in high dimensional spaces
- Learning functions in high dimensional spaces: links to deep learning

Model based deep learning

- Using learning based models in imaging

Non-linear SLR: Union of Surfaces Model

Many subjects cannot tolerate breath-held MRI

- Free breathing & ungated cardiac MRI data

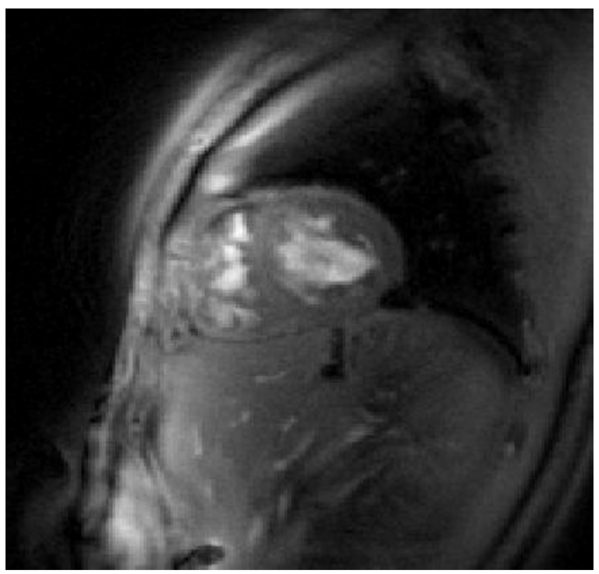
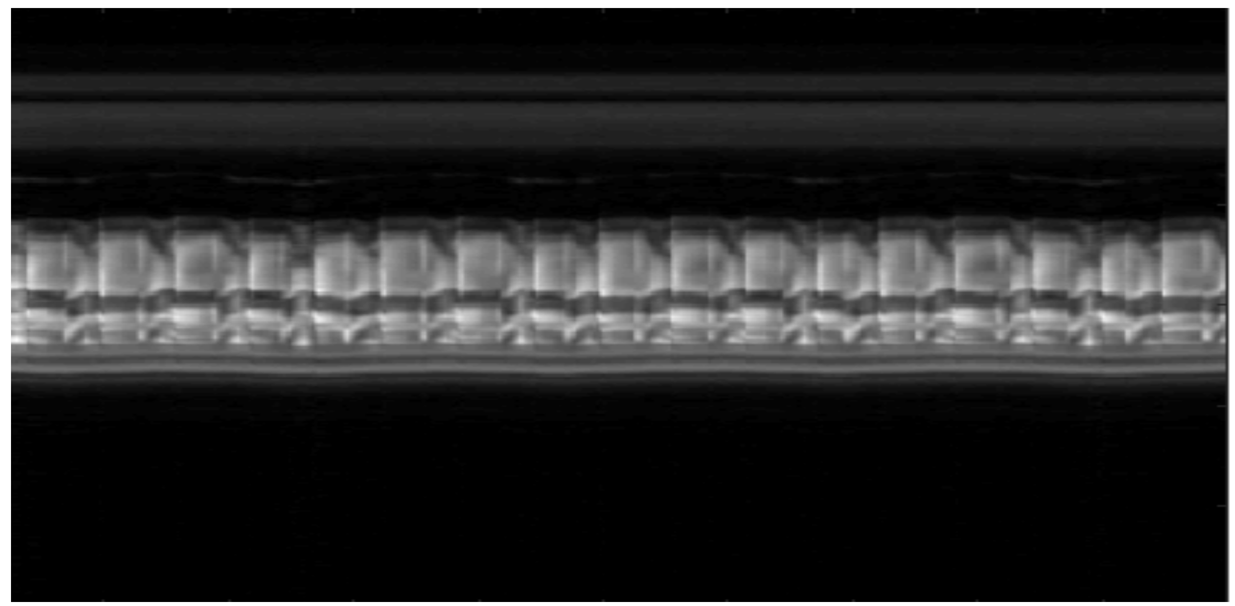

Challenges

- MRI is slow: every frame is undersampled by x50 or more

Model images as points on a smooth surface

Union of Surfaces model

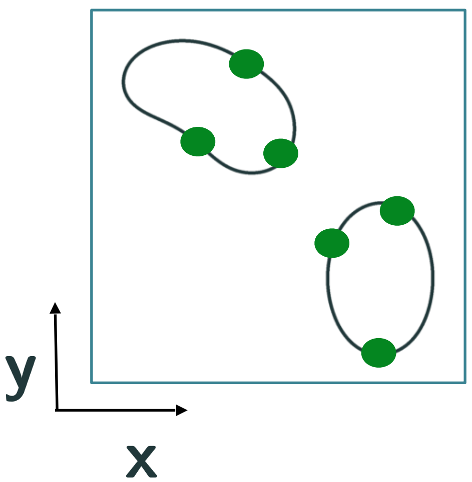

$$\{\mathbf{r} \in \mathbf{R}^n | \psi(\mathbf{r}) = 0\}$$

Level set

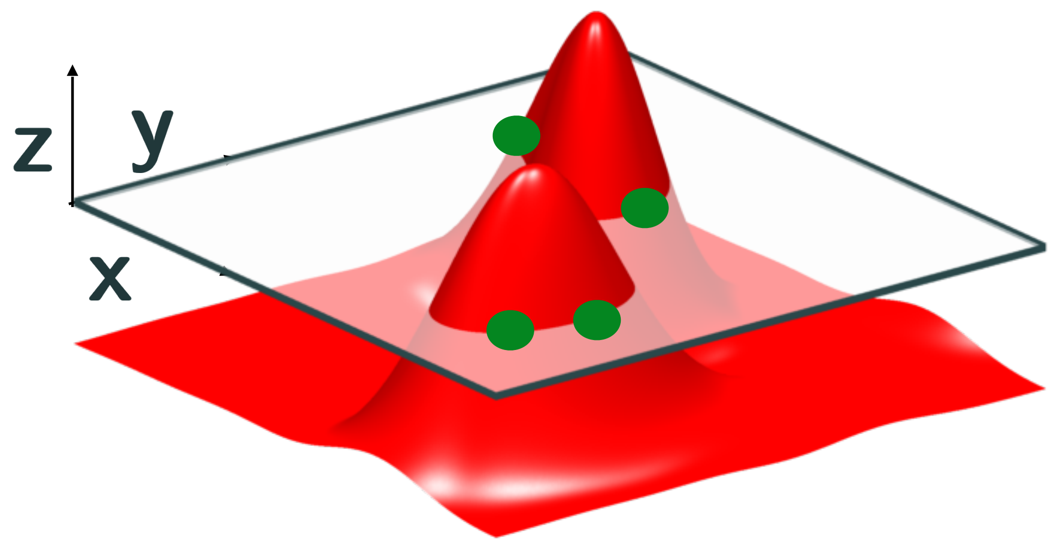

$$\psi(\mathbf{r}) = \sum_{\mathbf{k} \in \Lambda} \mathbf{c_k} e^{j\ 2\pi \mathbf{k}^T \mathbf{r}}$$

Lowpass function

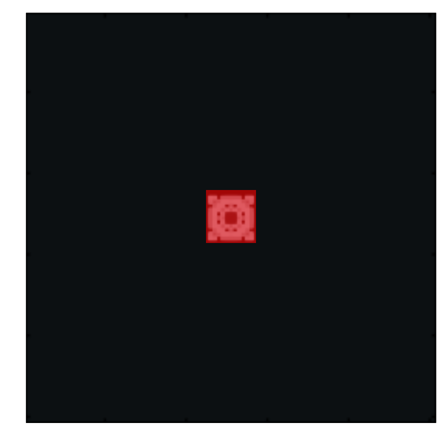

$\mathbf{c_k}$

Fourier coefficients

Non-linear generalization of Union of Subspaces model

Poddar & Jacob, ICASSP, 2018, TCI in press,
https://arxiv.org/abs/1810.11575

Annihilation conditions

Any point on the curve: Low pass function is zero

$$\sum_{\mathbf{k}\in\mathbf{\Lambda}} \mathbf{c_k} e^{j\ 2\pi \mathbf{k}^T \mathbf{x}_i} = \mathbf{0}$$

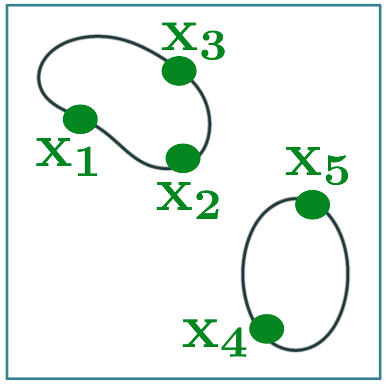

$$\{\mathbf{r} \in \mathbf{R}^n | \psi(\mathbf{r}) = \mathbf{0}\}$$

Annihilation conditions

Any point on the curve: Low pass function is zero

$$\sum_{\mathbf{k}\in\boldsymbol{\Lambda}} \mathbf{c}_{\mathbf{k}} e^{j\ 2\pi\mathbf{k}^T\mathbf{x}_i} = \mathbf{0}$$

$$\mathbf{c}^T \underbrace{\begin{bmatrix} e^{j2\pi\mathbf{k}_1^T\mathbf{x}_i} \\ e^{j2\pi\mathbf{k}_2^T\mathbf{x}_i} \\ \cdots \\ e^{j2\pi\mathbf{k}_{|\Lambda|}^T\mathbf{x}_i} \end{bmatrix}}_{\phi(\mathbf{x}_i)} = \mathbf{0}$$

High dimensional feature vector

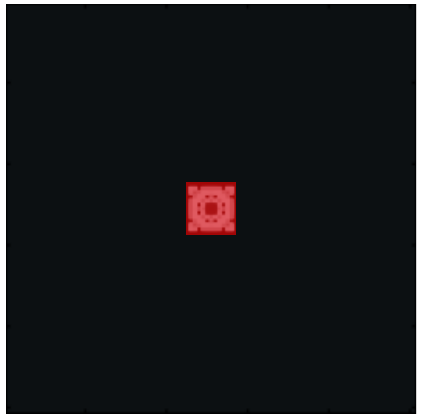

$\mathbf{c}_{\mathbf{k}}$

Fourier coefficients

Feature matrix is low-rank

Any point on the curve: $\psi(\mathbf{x}_i) = 0$

$$\sum_{\mathbf{k}\in\mathbf{\Lambda}} \mathbf{c_k} e^{j\ 2\pi\mathbf{k}^T\mathbf{x}_i} = 0$$

$$\downarrow$$

$$\mathbf{c}^T \underbrace{\left[\phi(\mathbf{x_1})\ \phi(\mathbf{x_2})\ \ldots\ \phi(\mathbf{x}_N)\right]}_{\mathbf{\Phi(X)}} = \mathbf{0}$$

Feature matrix

Rank of feature matrix is at most N-1

Poddar & Jacob, ICASSP, 2018, TCI in press,
https://arxiv.org/abs/1810.11575

When is curve recovery well-posed ?

Rank of feature matrix is rank is N-1

$$\underbrace{\begin{bmatrix} \boldsymbol{\phi(\mathbf{x_1})} & \boldsymbol{\phi(\mathbf{x_2})} & \ldots & \boldsymbol{\phi(\mathbf{x}_N)} \end{bmatrix}}_{\boldsymbol{\Phi(\mathbf{X})}}$$

1.How many points are needed to recover the curve ?

2. How should the points be distributed guarantee recovery ?

Result: High probability recovery in 2D and beyond

Let $\{\mathbf{x}_1, \cdots, \mathbf{x}_N\}$ are independent random samples from the zero level set of $\psi(\mathbf{x})$ whose bandwidth is given by Λ. The curve can be recovered with probability 1, if

$$N \geq |\Lambda| - 1.$$

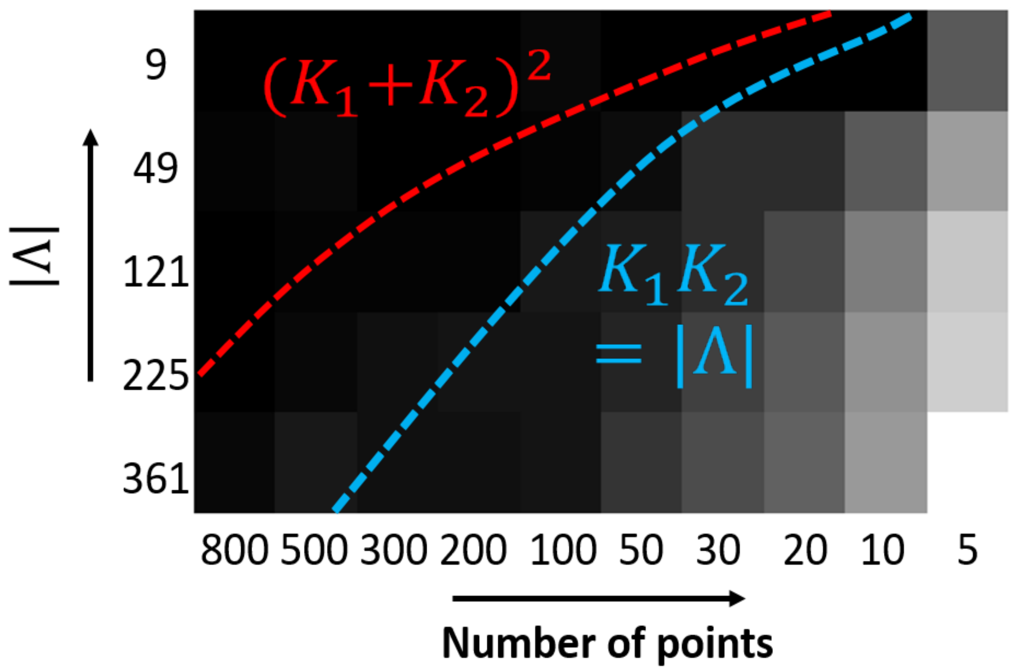

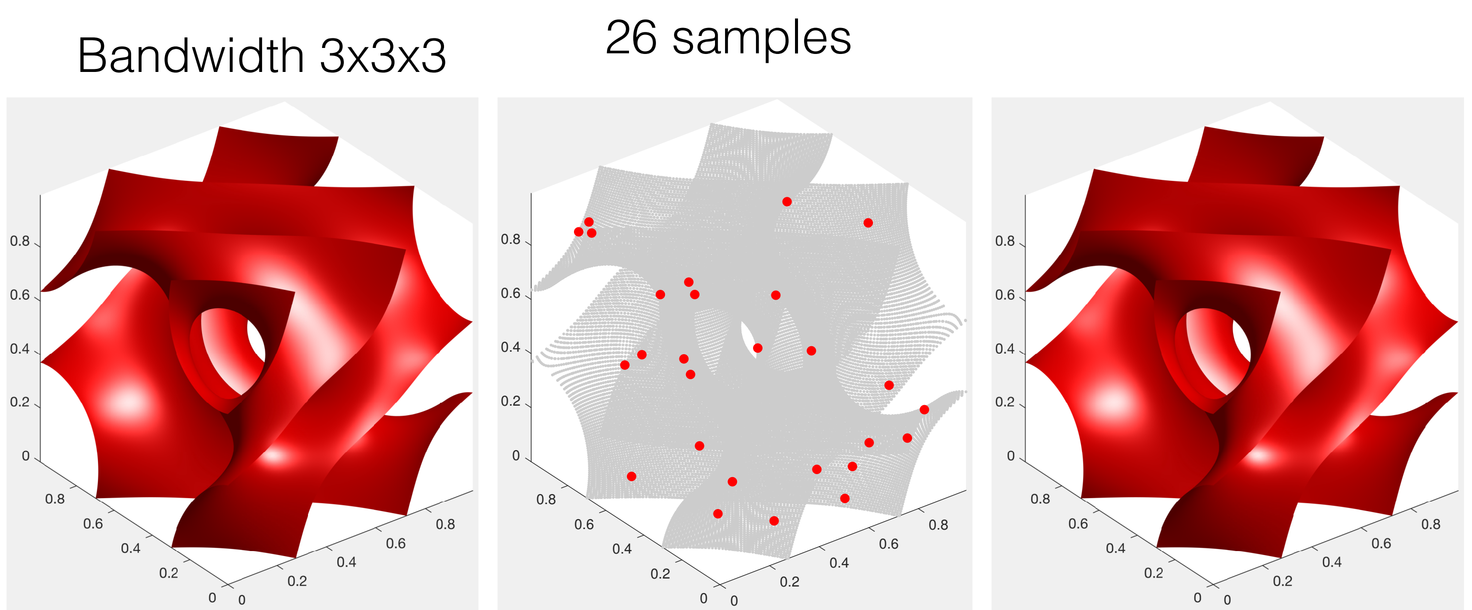

(a) True surface (b) Sampling points (c) Recovered surface

From Union of Surfaces to Union of Subspaces

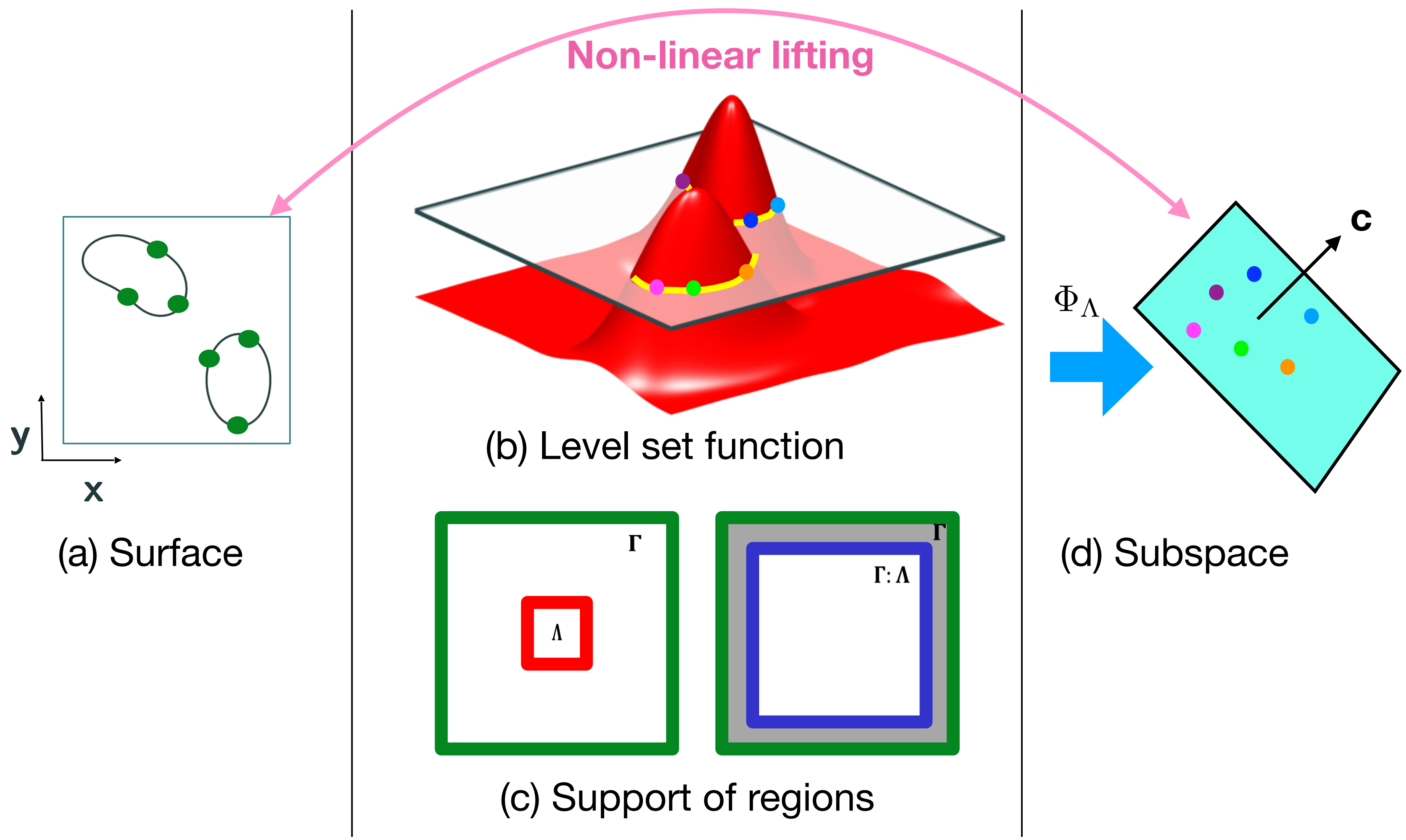

Nonlinear lifting

Poddar & Jacob, ICASSP, 2018, TCI in press,
https://arxiv.org/abs/1810.11575

Feature matrix is low-rank

Fourier support is fully known

$$\mathbf{c}^T \underbrace{\left[\boldsymbol{\phi}(\mathbf{x}_1)\ \boldsymbol{\phi}(\mathbf{x}_2)\ \ldots\ \boldsymbol{\phi}(\mathbf{x}_N)\right]}_{\boldsymbol{\Phi}(\mathbf{X})} = \mathbf{0}$$

Rank of feature matrix is rank is N-1

Overestimated Fourier support

$$\text{rank}\left(\boldsymbol{\Phi}(\mathbf{X})\right) = |\boldsymbol{\Gamma}| - |\boldsymbol{\Gamma} : \boldsymbol{\Lambda}|$$

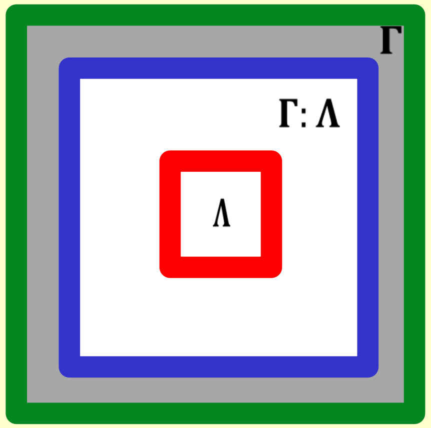

Poddar & Jacob, ICASSP, 2018, TCI in press,
https://arxiv.org/abs/1810.11575

Use low-rank property to denoise/recover points ?

Problem: Recover points $\{\mathbf{x}_i\}$ from corrupted measurements:

$$\mathbf{b}_i = \mathcal{A}(\mathbf{x}_i) + \eta_i$$

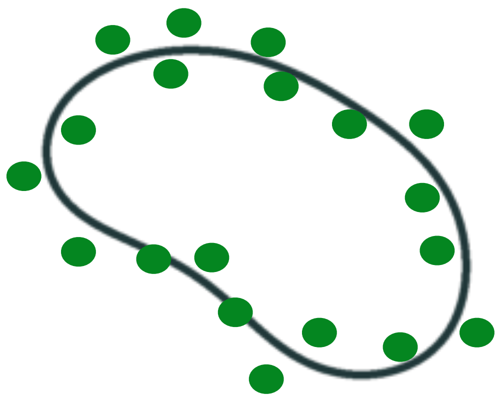

Low-rank minimization

$$\min_{\mathbf{X}} \|\boldsymbol{\mathcal{A}}(\mathbf{X}) - \mathbf{b}\|^2 + \boldsymbol{\lambda}\|\boldsymbol{\Phi}(\mathbf{X})\|_*$$

Iterative reweighed least-squares algorithm

$$\min_{\mathbf{X}} \|\mathcal{A}(\mathbf{X}) - \mathbf{b}\|^2 + \lambda \|\Phi(\mathbf{X})\|_*$$

$$\Big\Downarrow \text{ IRLS}$$

$$\mathbf{X}^{(n)} = \arg\min_{\mathbf{X}} \|\mathcal{A}(\mathbf{X}) - \mathbf{b}\|^2 + \lambda \; \mathrm{trace}[\mathcal{K}(\mathbf{X})\mathbf{Q}^{(n-1)}]$$

$$\mathbf{Q}^{(n)} = [\mathcal{K}(\mathbf{X}^{(n)}) + \gamma^{(n)}\mathbf{I}]^{-\frac{1}{2}}$$

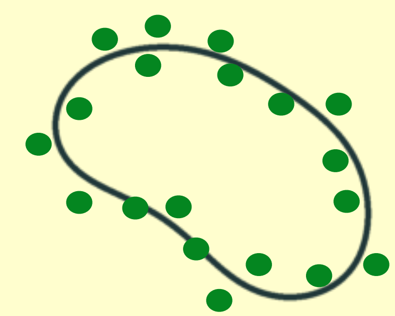

$$\Big\Downarrow \text{ Gradient linearization}$$

$$\mathbf{X}^{(n)} = \arg\min_{\mathbf{X}} \|\mathcal{A}(\mathbf{X}) - \mathbf{b}\|^2 + \lambda \; \mathrm{trace}(\mathbf{X}^T \mathbf{L}^{(n-1)} \mathbf{X})$$

where $\mathbf{L}^{(n-1)} = f(\mathcal{K}(\mathbf{X}^{(n-1)}), \mathbf{Q}^{(n-1)})$

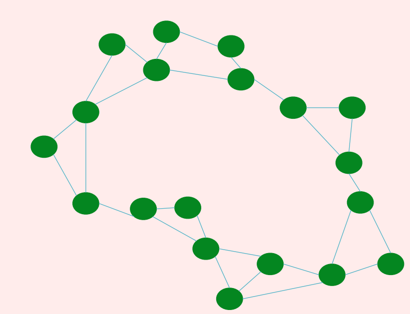

Laplacian of graph

Graph smoothness regularization

IRLS denoising: illustration

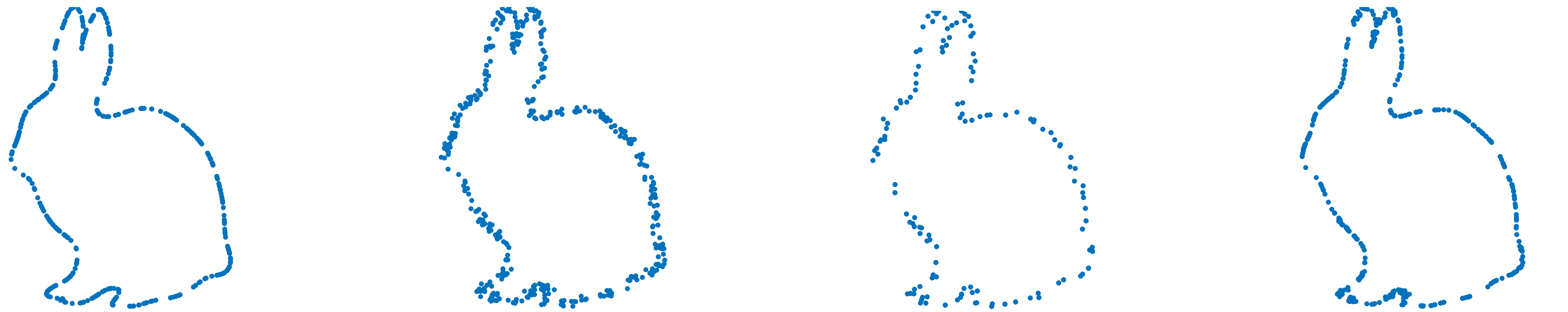

(a) Original #1 (b) Noisy #1, SNR = 31.85 dB (c) GLR, SNR = 32.09 dB (d) KLR, SNR = 35.21 dB

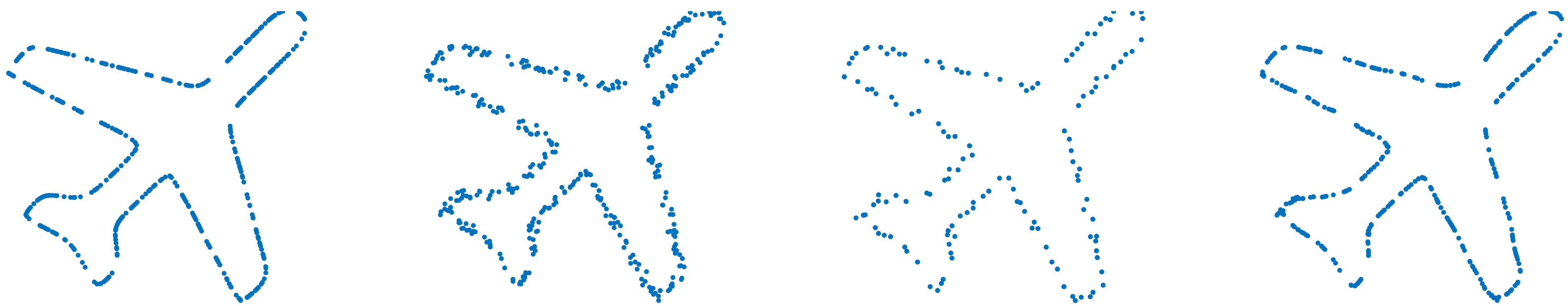

(e) Original #2 (f) Noisy #2, SNR = 29.94 dB (g) GLR, SNR = 30.01 dB (h) KLR, SNR = 33.01 dB

(i) Original #3 (j) Noisy #3, SNR= 28.33 dB (k) GLR, SNR = 28.95 dB (l) KLR, SNR = 31.84 dB

Main idea: recovery using kernel low-rank

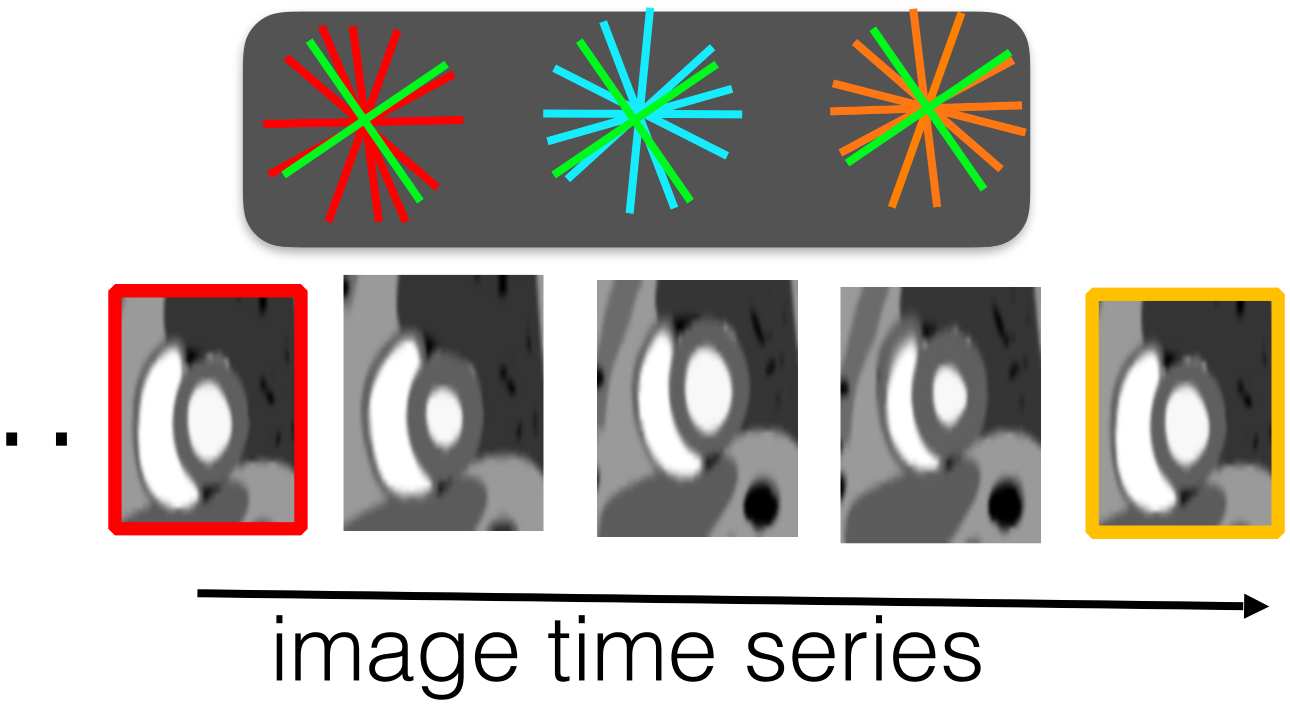

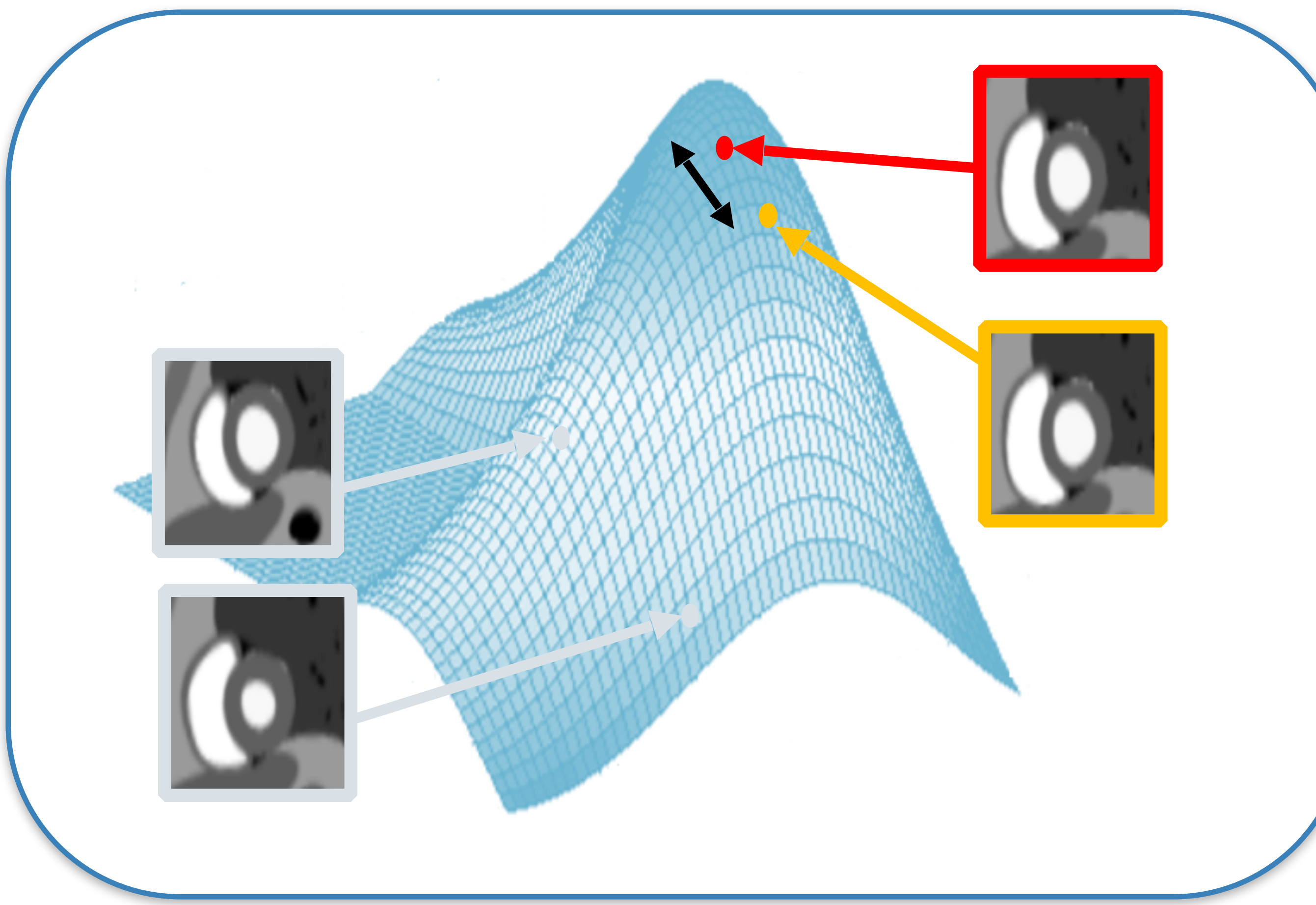

Algebraic Variety Models for High-Rank Matrix Completion

Greg Ongie [1] Rebecca Willett [2] Robert D. Nowak [2] Laura Balzano [1]

Main idea

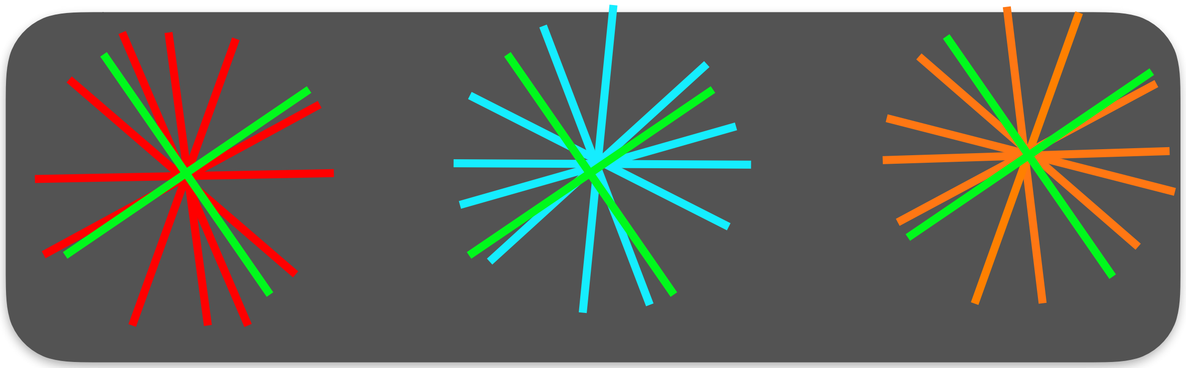

$$\min_{\mathbf{X}} \|\boldsymbol{\mathcal{A}}(\mathbf{X}) - \mathbf{b}\|^2 + \boldsymbol{\lambda}\|\boldsymbol{\Phi}(\mathbf{X})\|_*$$

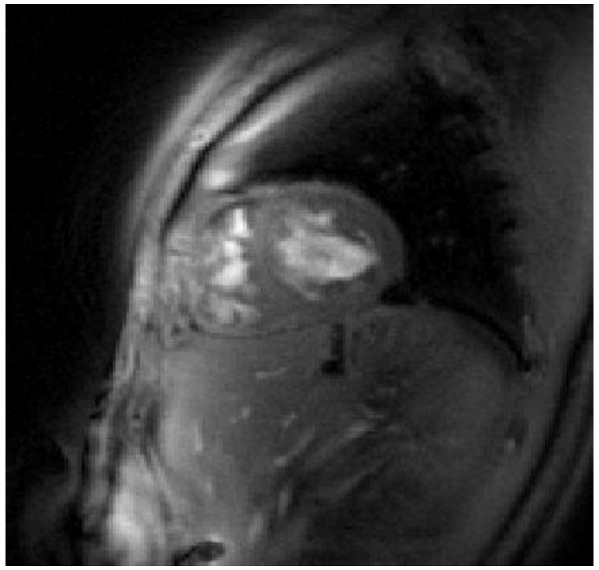

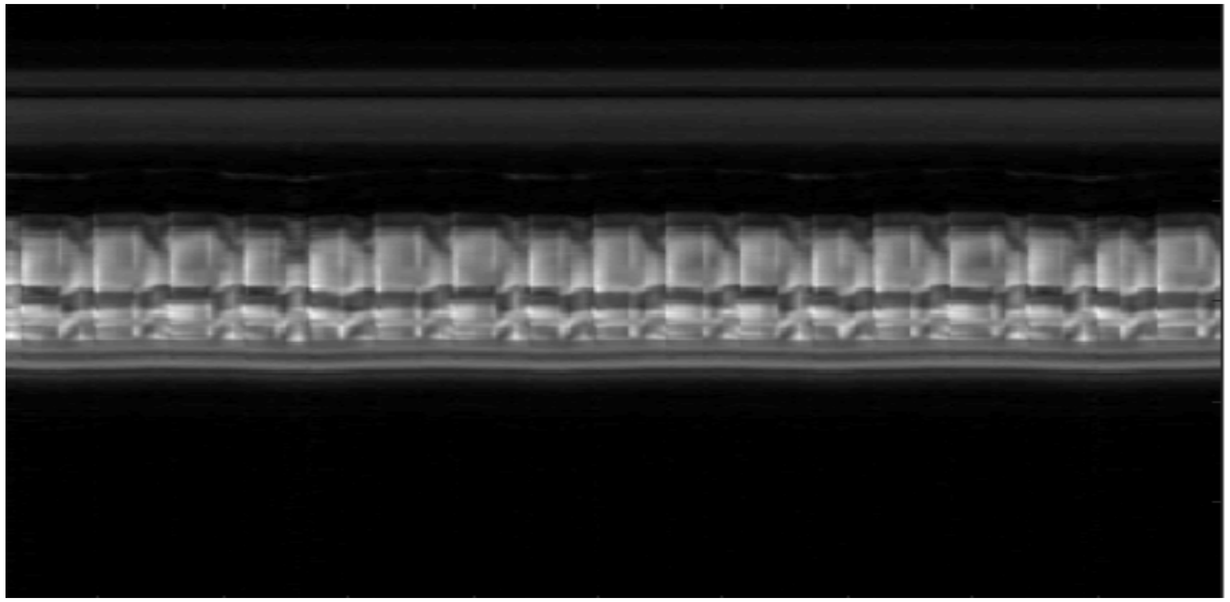

Results: normal subject

Slice 1

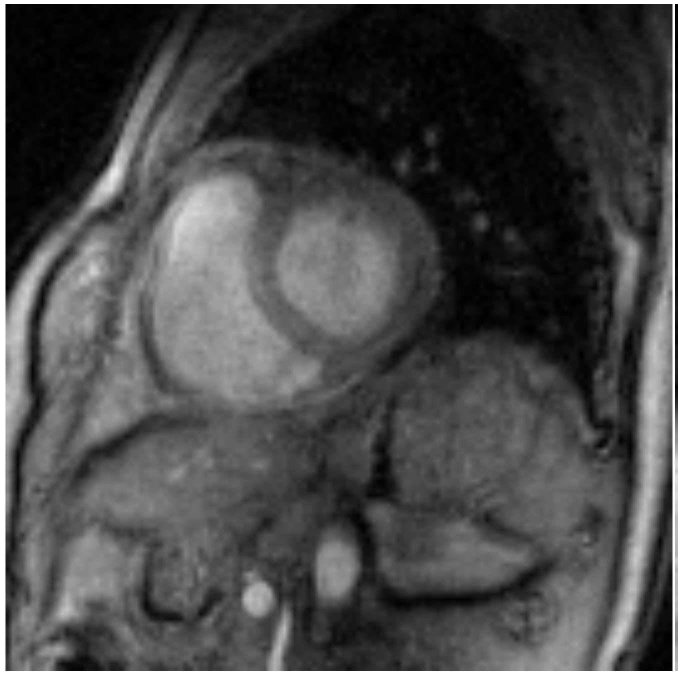

Slice 2

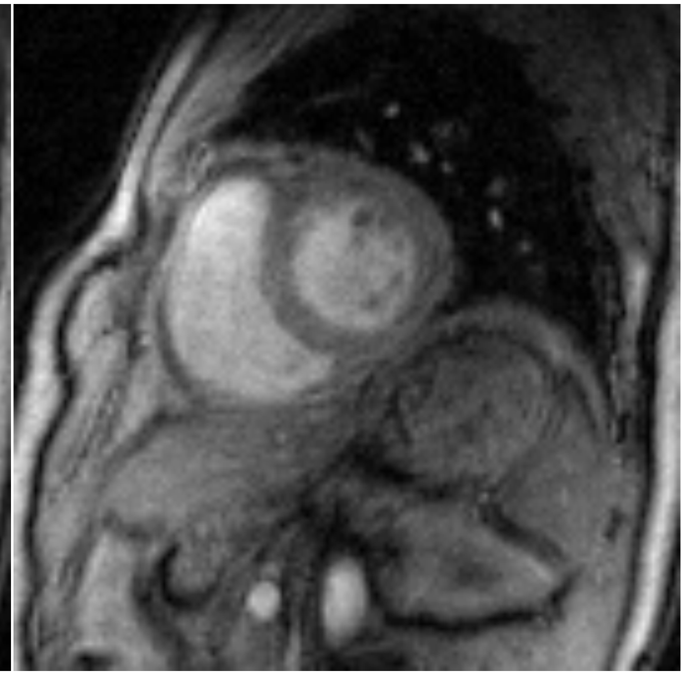

Slice 3

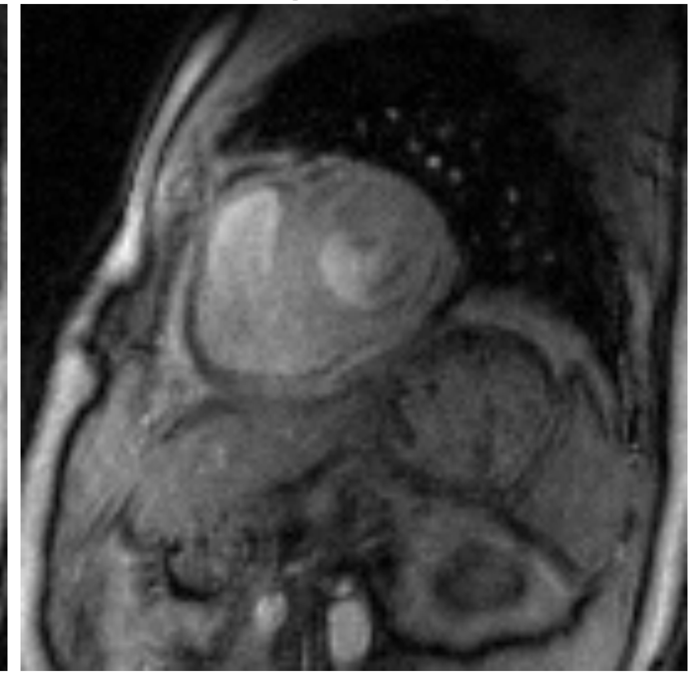

Slice 4

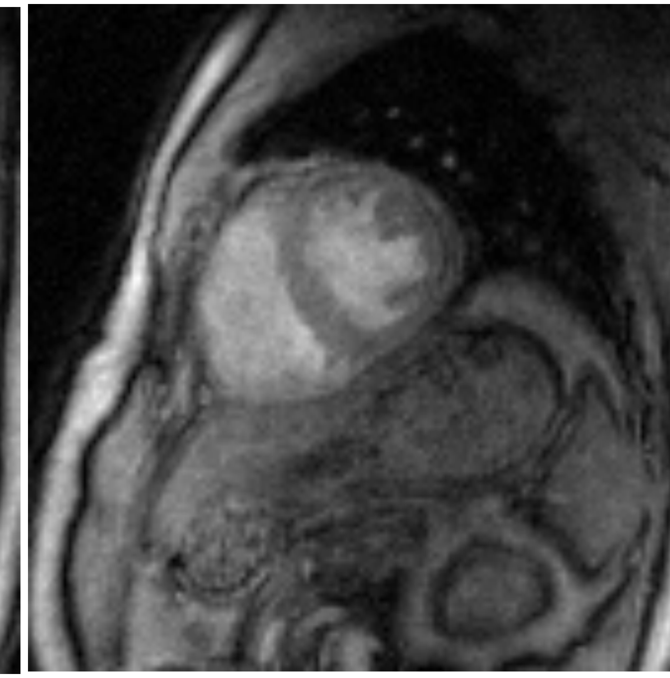

Slice 5

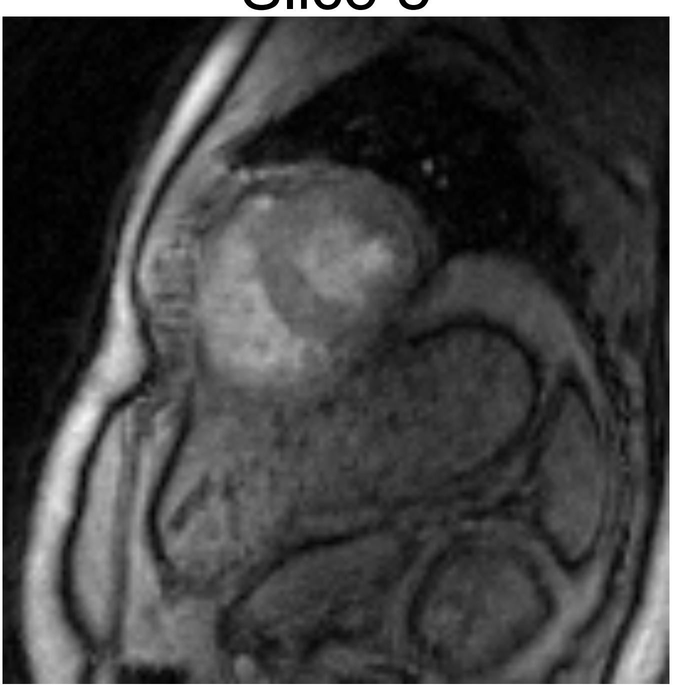

Slice 6

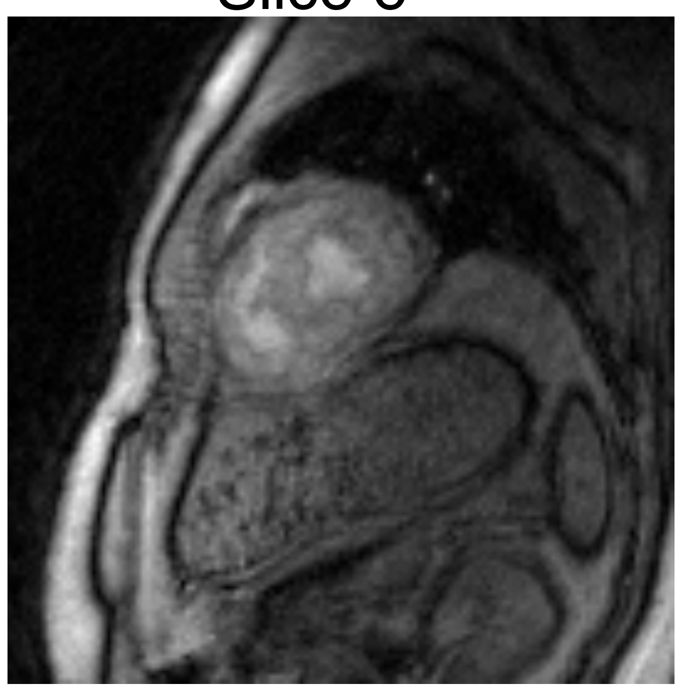

Slice 7

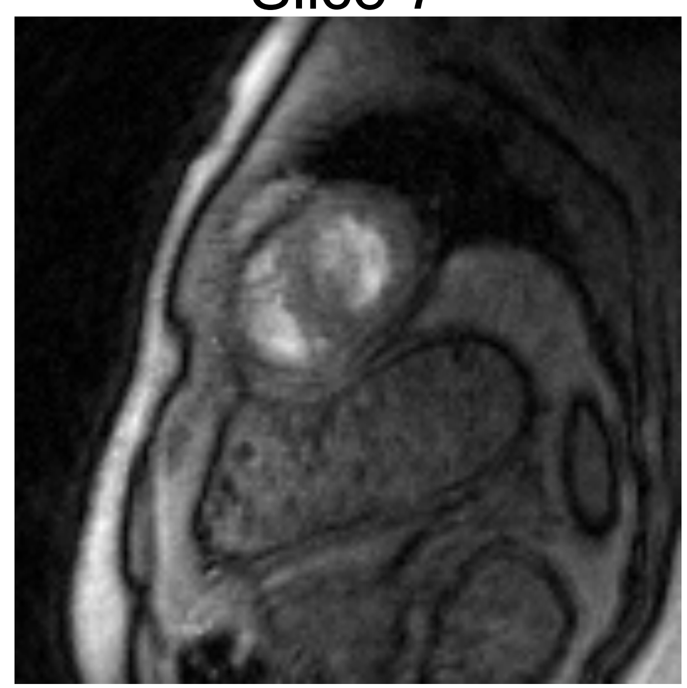

Slice 8

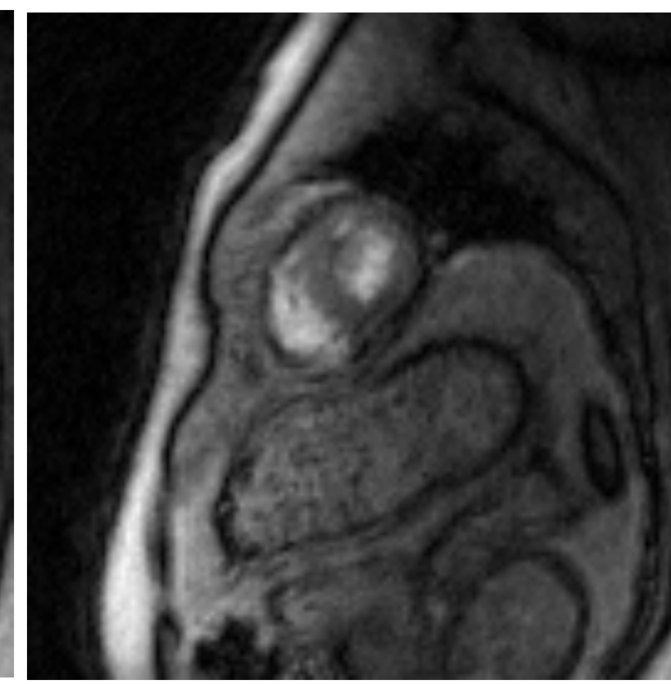

Comparable to Breath-held CINE

Breath-held frames

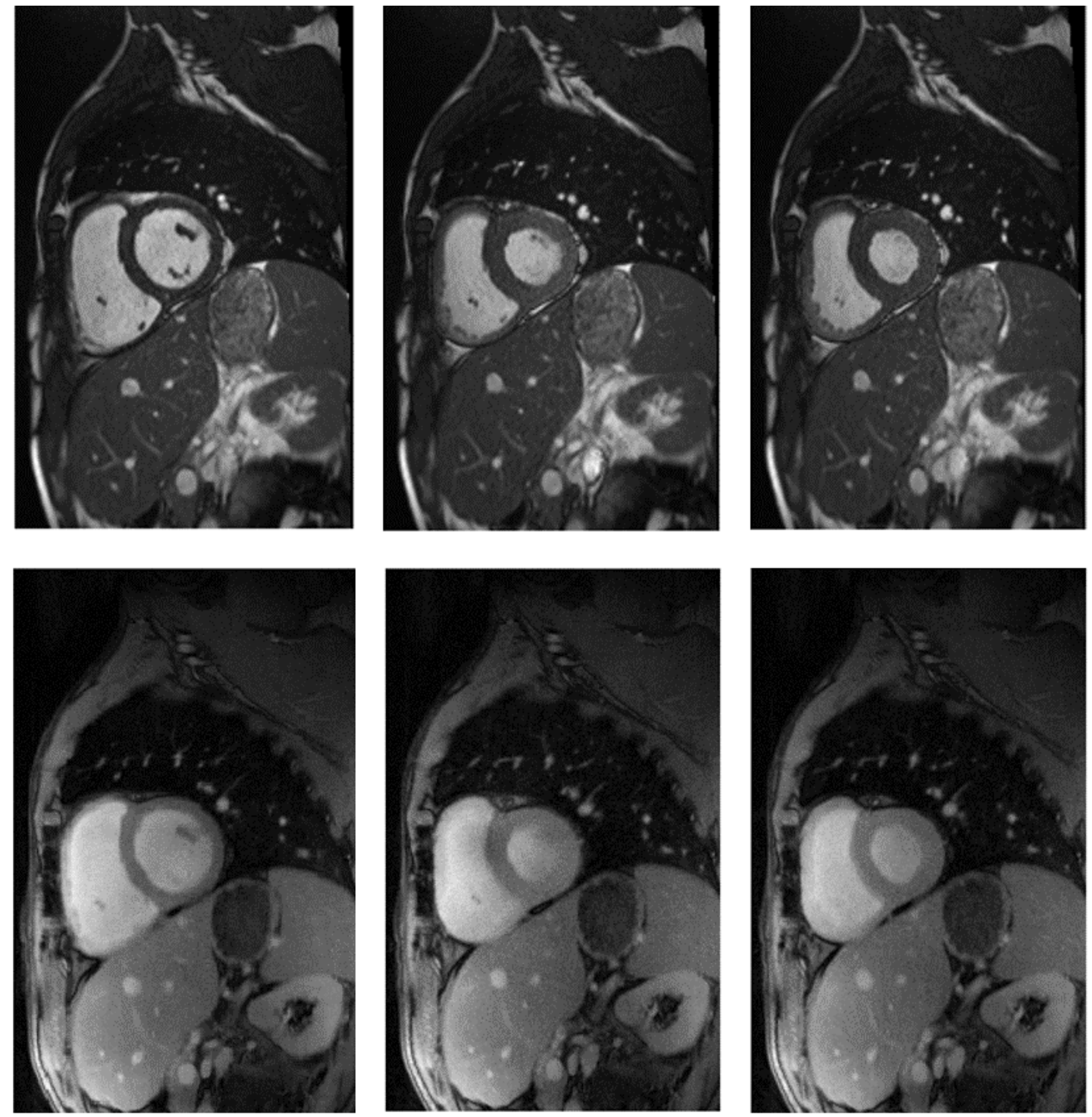

SSFP acquisition

Free-breathing frames

Gradient echo Acquisition

Temporal profiles

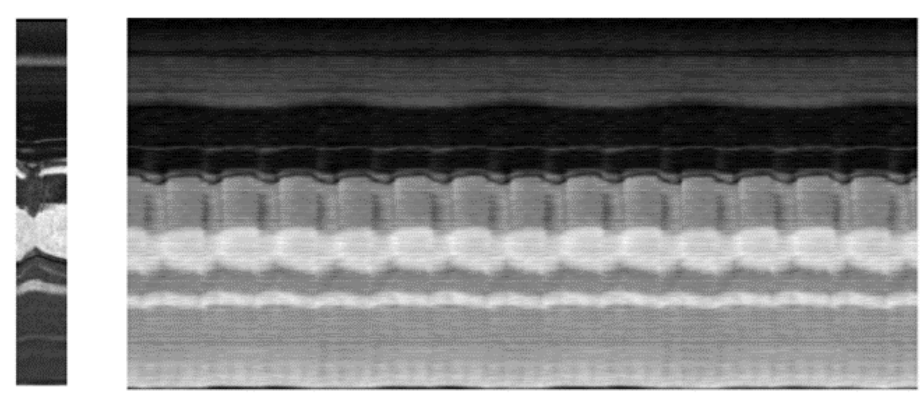

Left: Breath-held, Right: Free-breathing

STORM

TMI 2016, TCI 2019, TMI 2019

Comparable to Breath-held CINE

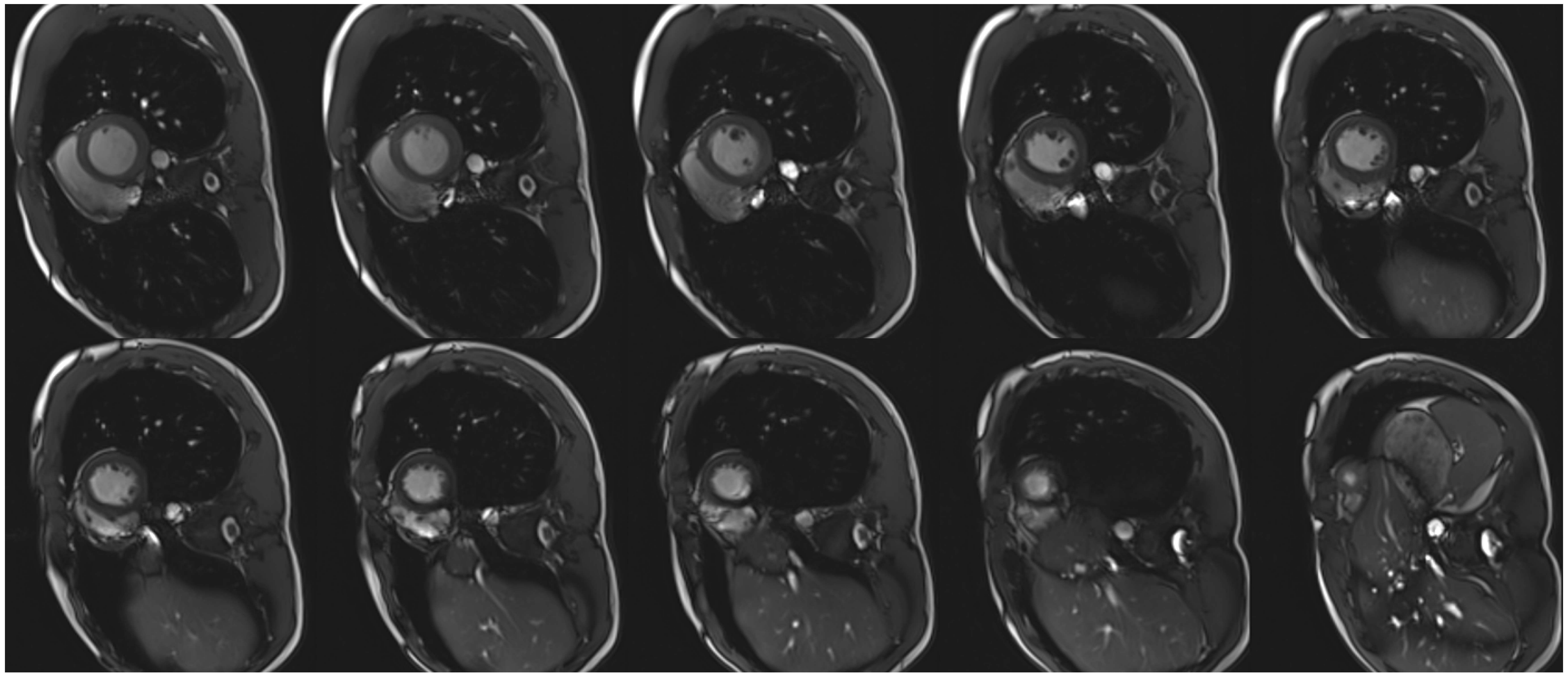

. (i)

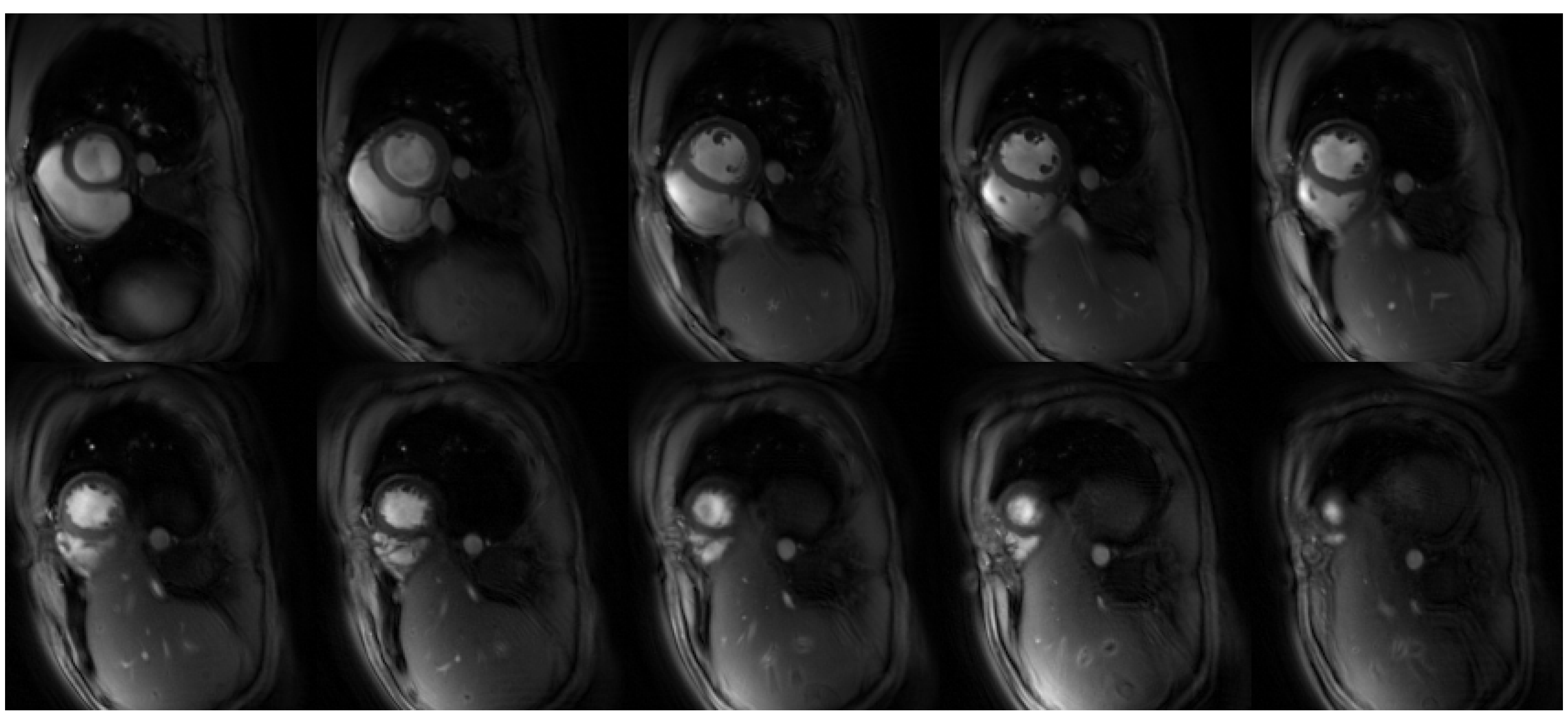

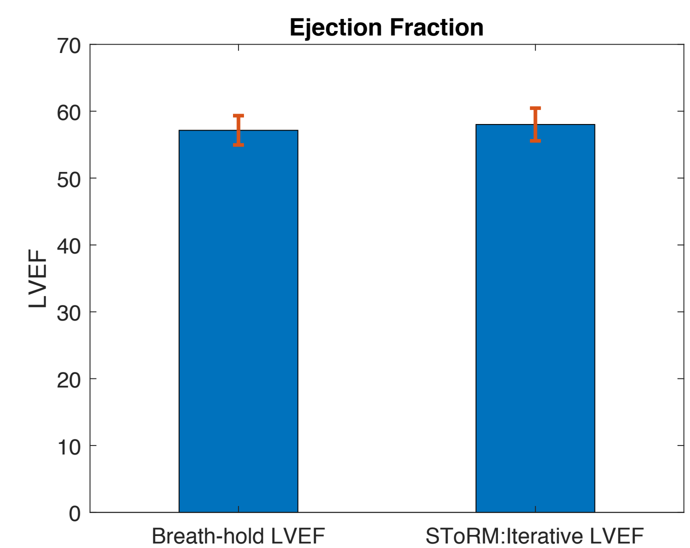

Comparison with Low-Rank (PSF)

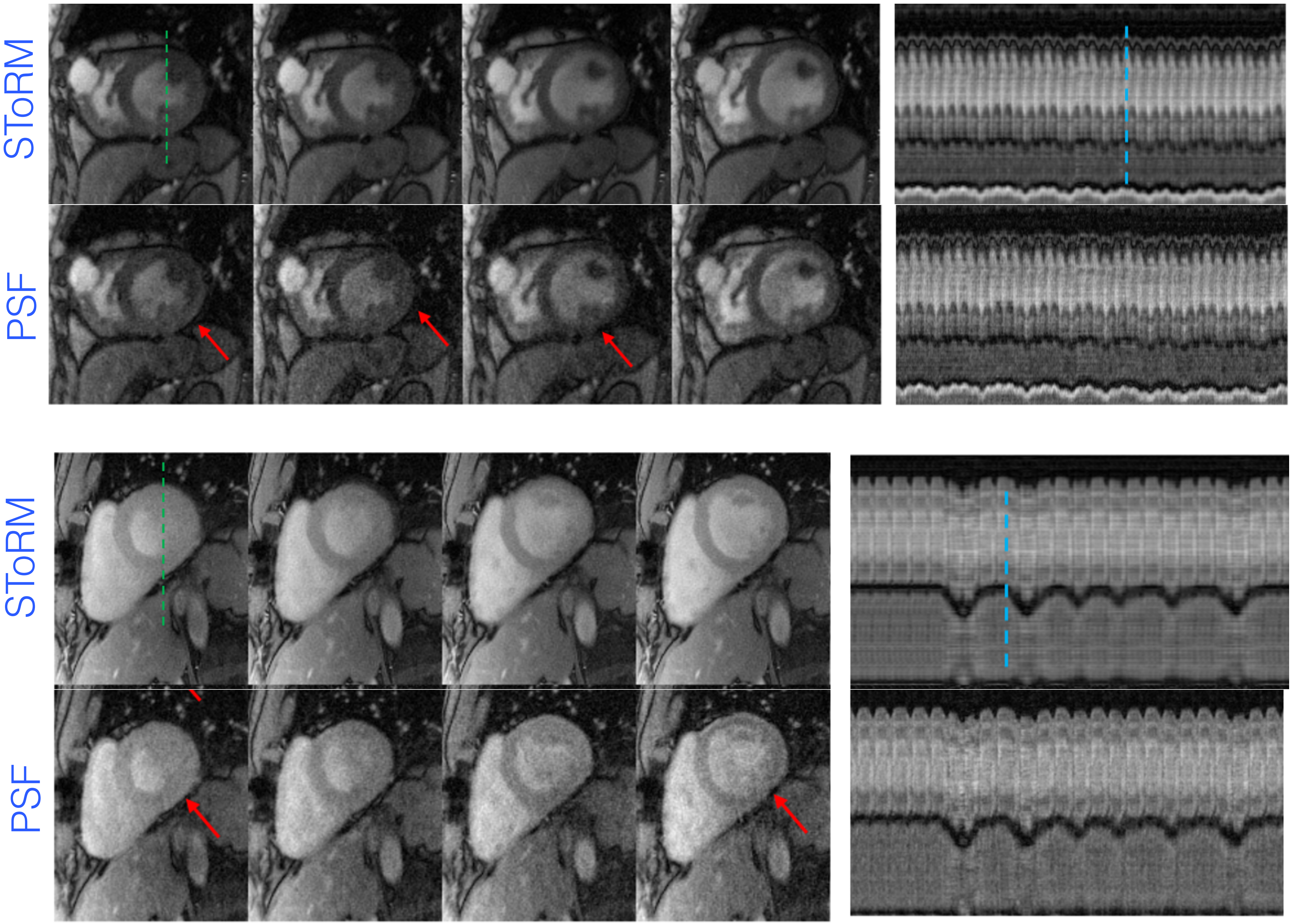

Lift to a high-dimensional space where solution is simple !!

Linear lifting operations

- Continuous domain compressed sensing
- Recovery of exponential signals: EPI correction & parameter mapping
- Auto-calibration: account for inconsistencies in acquisition

Non-linear lifting

- Recovery of data in high dimensional spaces
- Learning functions in high dimensional spaces: links to deep learning

Model based deep learning

- Using learning based models in imaging

Learning functions on Union of Surfaces

Machine learning: learn functions in high dimensions

- Patch surfaces: denoising

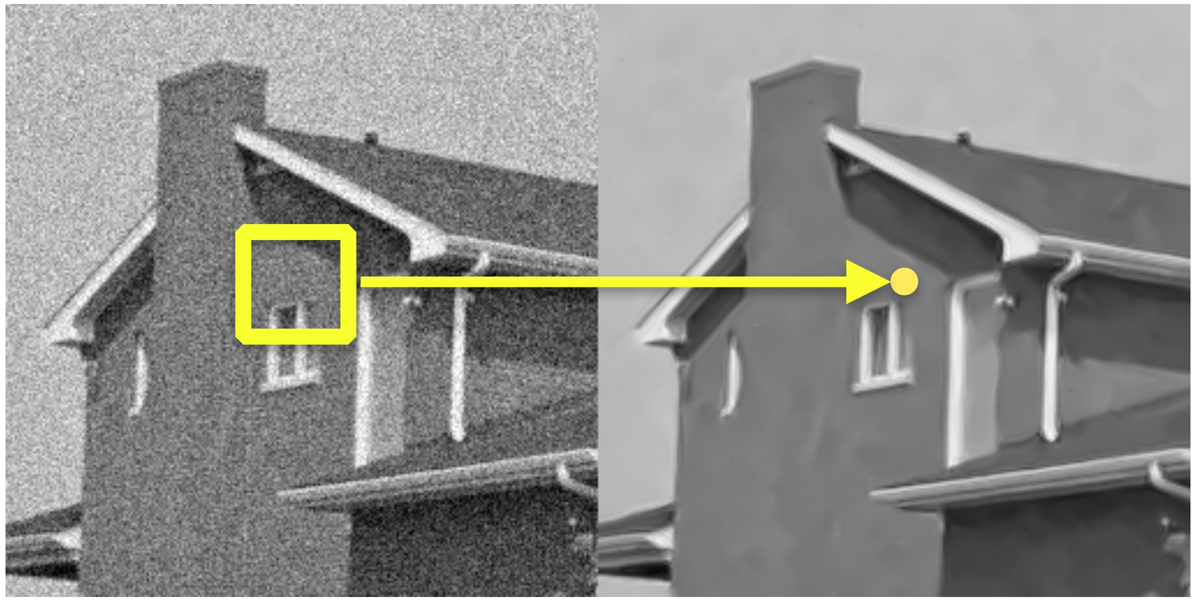

Challenges in learning complex multidimensional functions

- Curse of dimensionality: functions with too many parameters
- Difficult to learn from limited data

Feature vectors lie in a low-rank subspace

Overestimated Fourier support

$$\text{rank}\left(\boldsymbol{\Phi}(\mathbf{X})\right) = |\boldsymbol{\Gamma}| - |\boldsymbol{\Gamma} : \boldsymbol{\Lambda}|$$

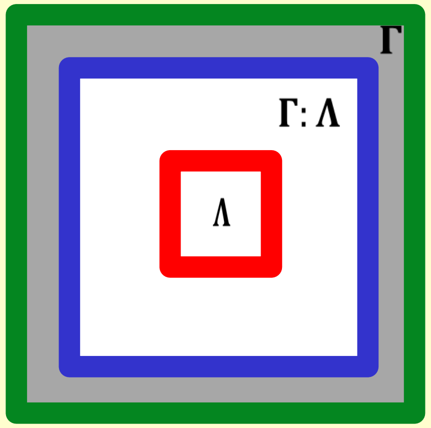

Compuationally efficient evaluation of functions

$$\mathbf{a}^T \Phi(\mathbf{x}) = c_1(\mathbf{x})\ \Phi(\mathbf{x}_1) + \ldots + c_r(\mathbf{x})\ \Phi(\mathbf{x}_r)$$

Linear combination of features of anchor points

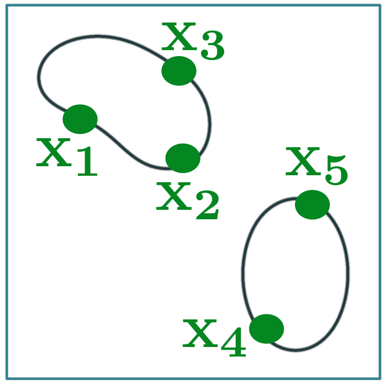

$$\{\mathbf{r} \in \mathbf{R}^n | \psi(\mathbf{r}) = \mathbf{0}\}$$

Example in 2D

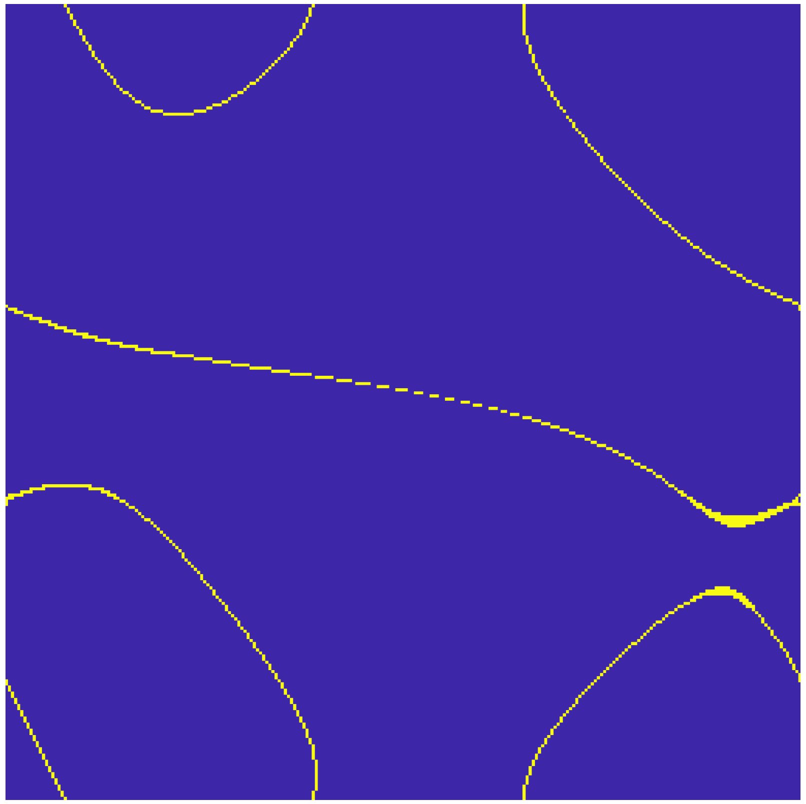

Curve

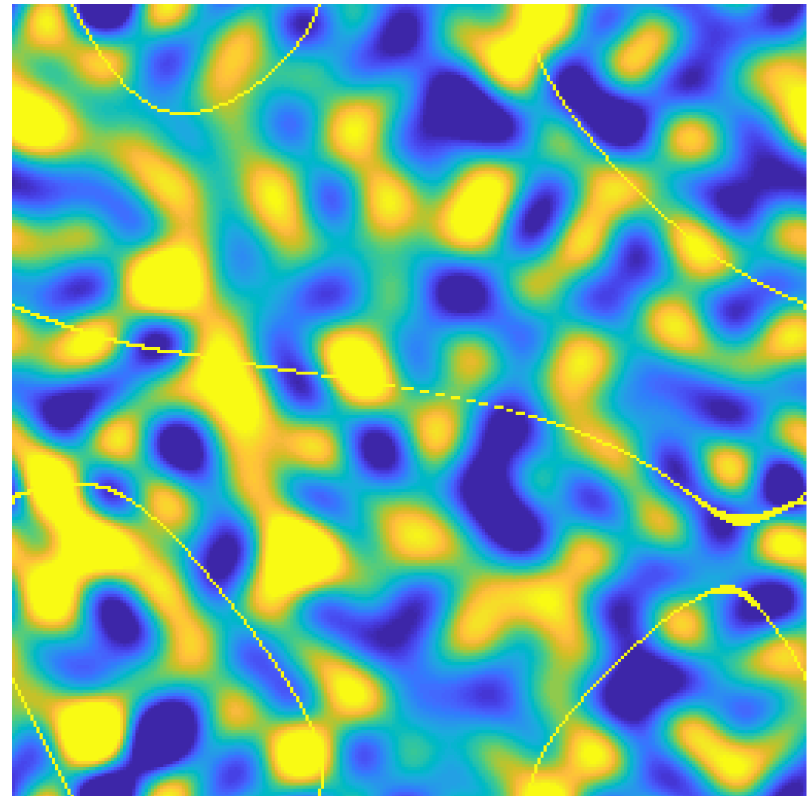

Function: 169 parameters

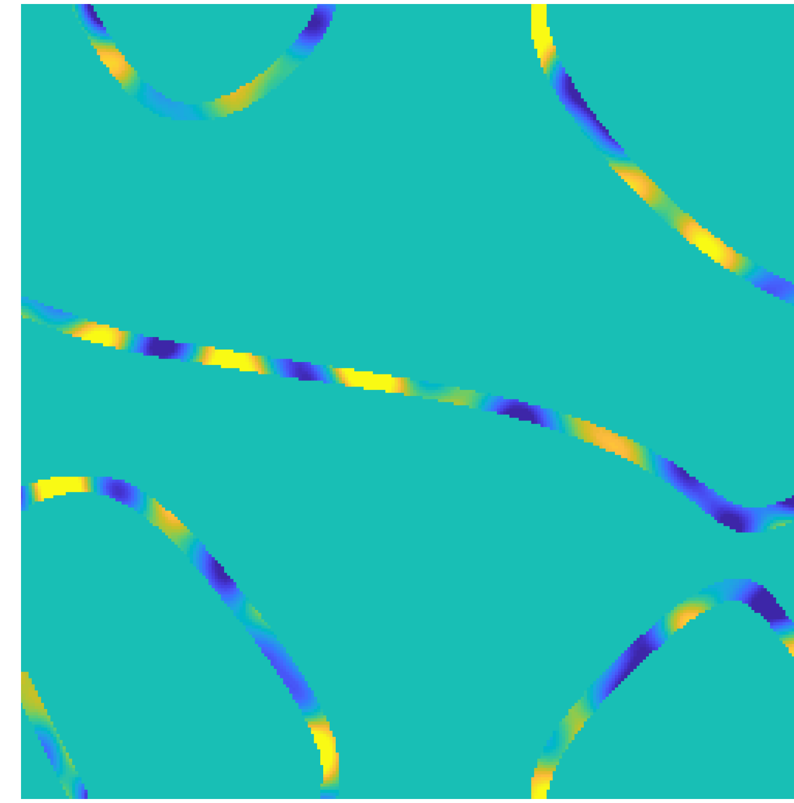

Function around curve

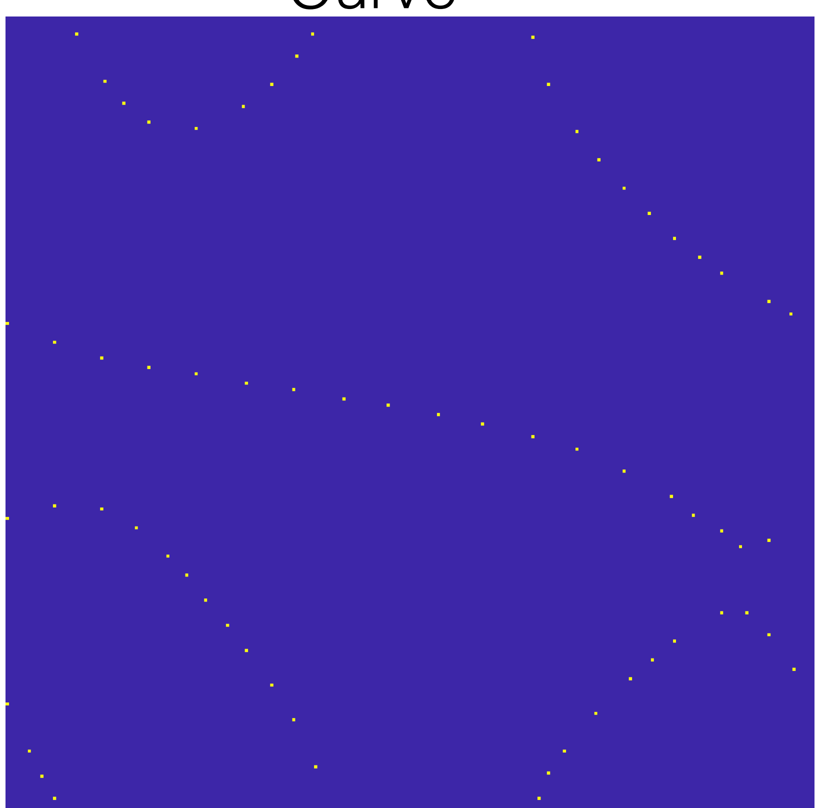

Anchor points

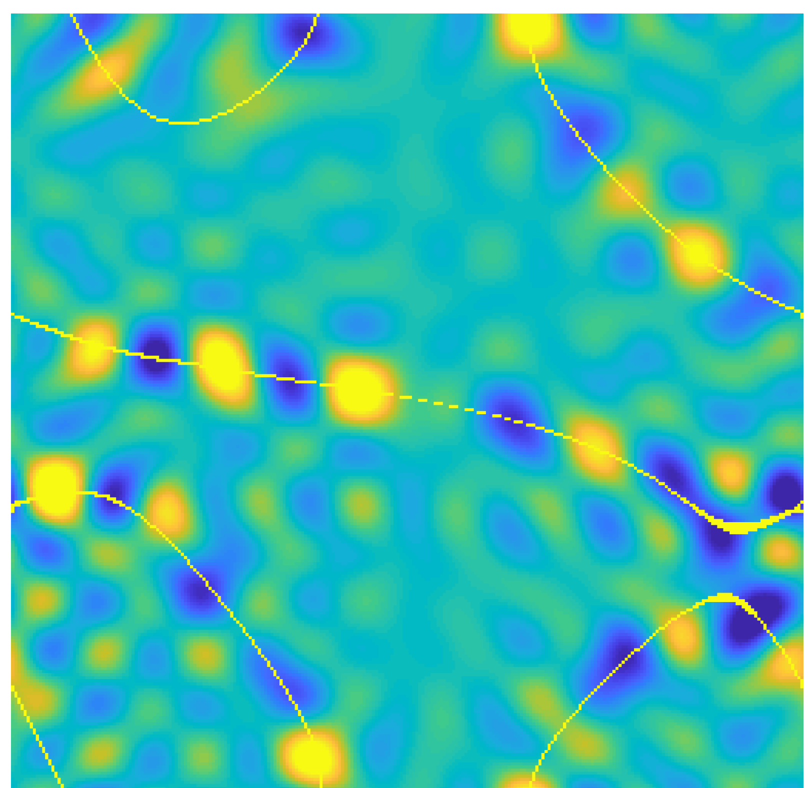

Global function: 48 params

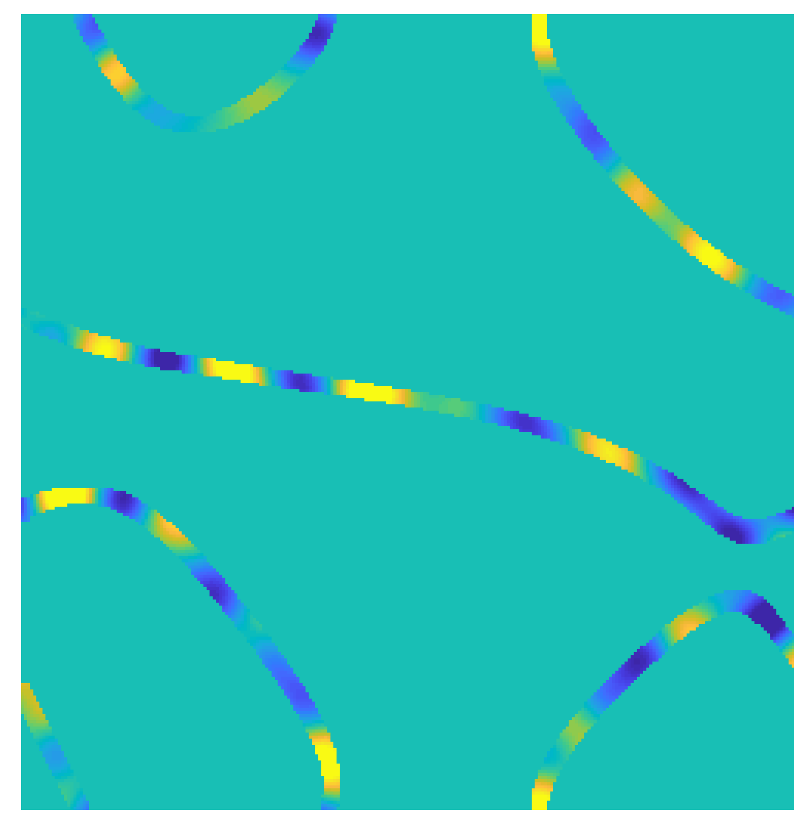

Local representation: 48 params

Local function representation

Single layer neural network

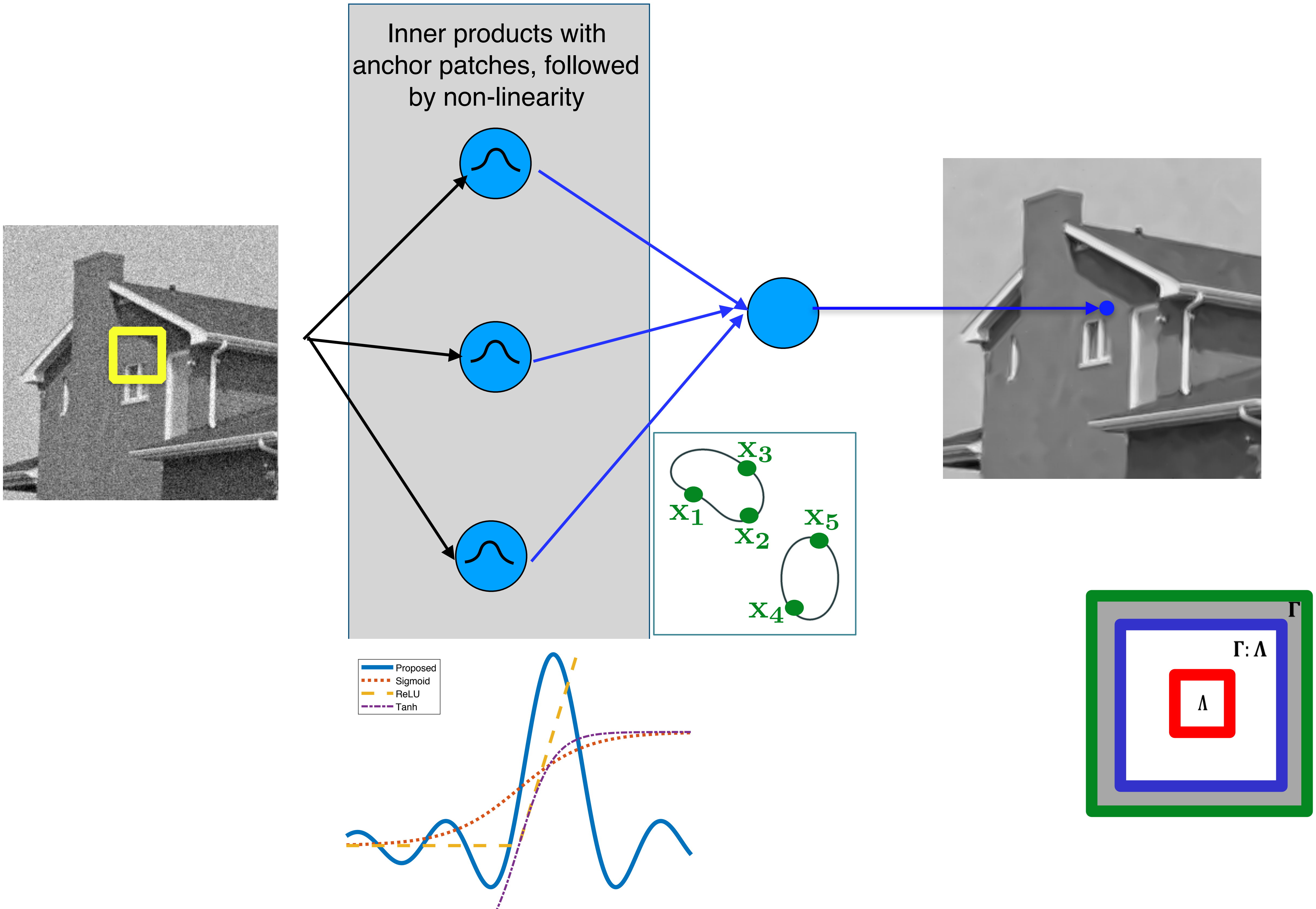

Single layer Dirichlet network: denoising

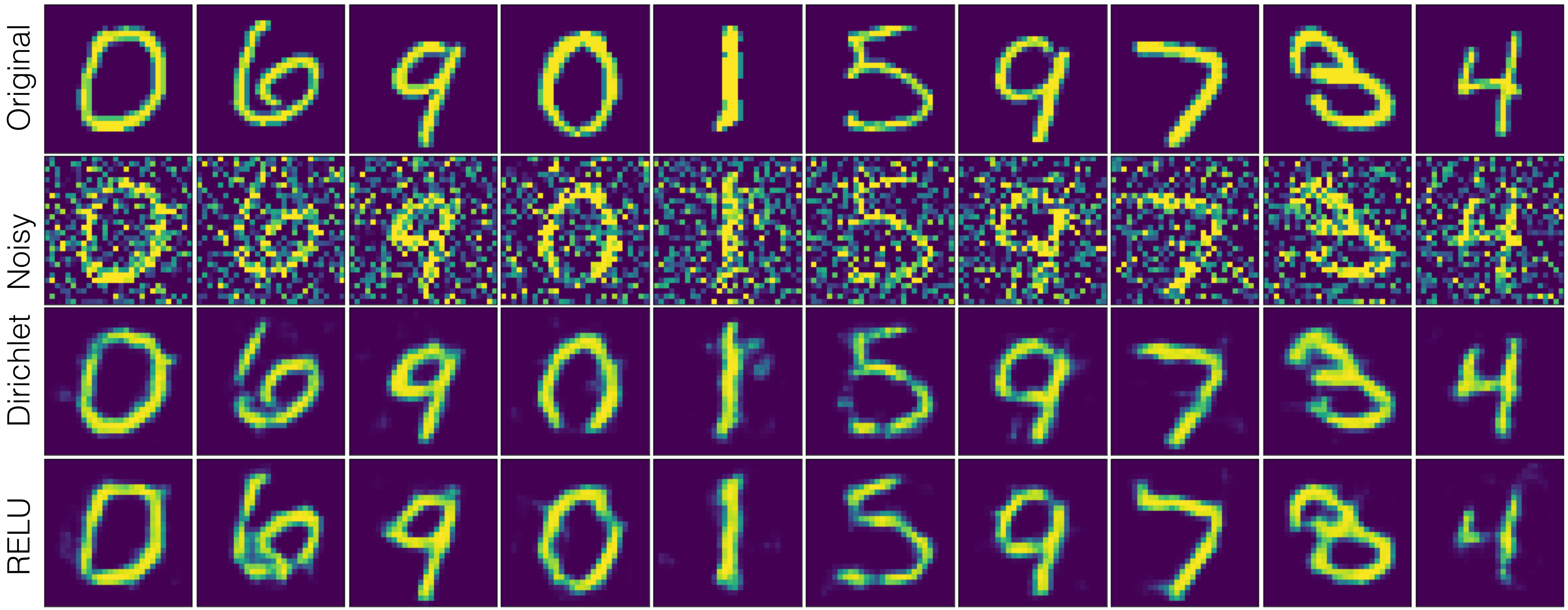

Multiply low-bandwidth functions: increase bandwidth

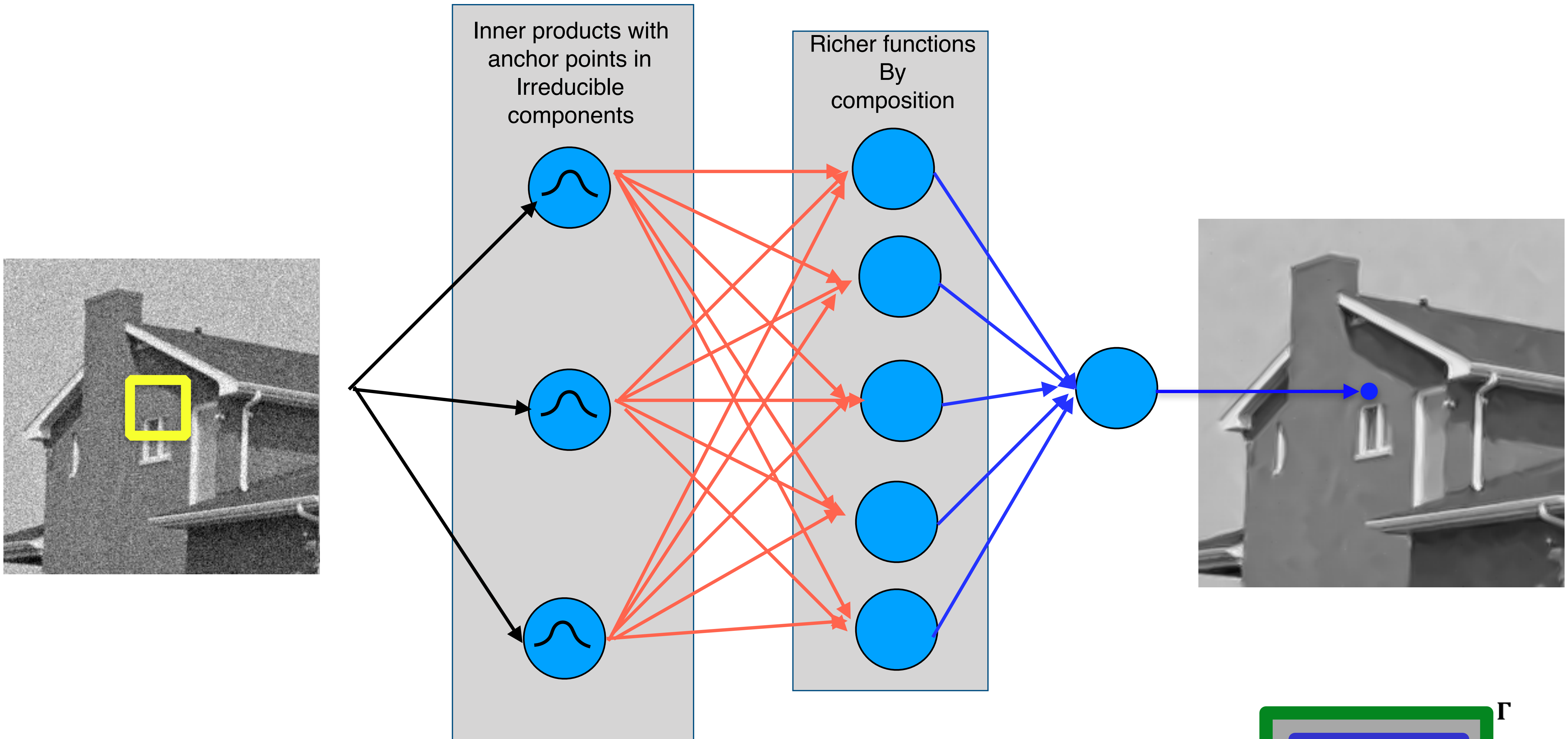

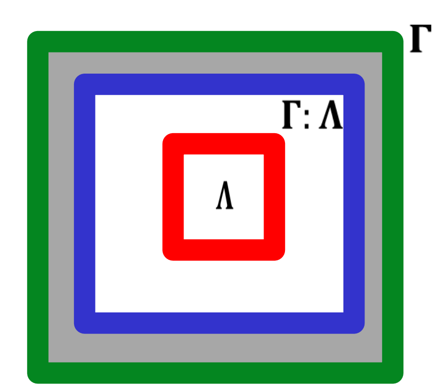

Deep network: efficiency from composition

Output: band-limited function of input

Lift to a high-dimensional space where solution is simple !!

Linear lifting operations

- Continuous domain compressed sensing
- Auto-calibration: account for inconsistencies in acquisition

Non-linear lifting

- Recovery of data in high dimensional spaces
- Learning functions in high dimensional spaces: links to deep learning

Model based deep learning

- Using learning based models in imaging

Using deep networks for computational MRI: MoDL

Noise/alias estimator

Model-Based Problem Formulation

$$\mathbf{x} = \arg\min_{\mathbf{x}} \underbrace{\|\mathbf{A}\,\mathbf{x} - \mathbf{b}\|_2^2}_{\text{data consistency}} + \lambda \underbrace{\|\mathcal{N}_{\mathbf{w}}(\mathbf{x})\|^2}_{\text{regularization}}$$

Denoiser

$$\mathcal{D}_{\mathbf{w}}(\mathbf{x}) = (\mathcal{I} - \mathcal{N}_{\mathrm{w}})\,(\mathbf{x}) = \mathbf{x} - \mathcal{N}_{\mathbf{w}}(\mathbf{x}).$$

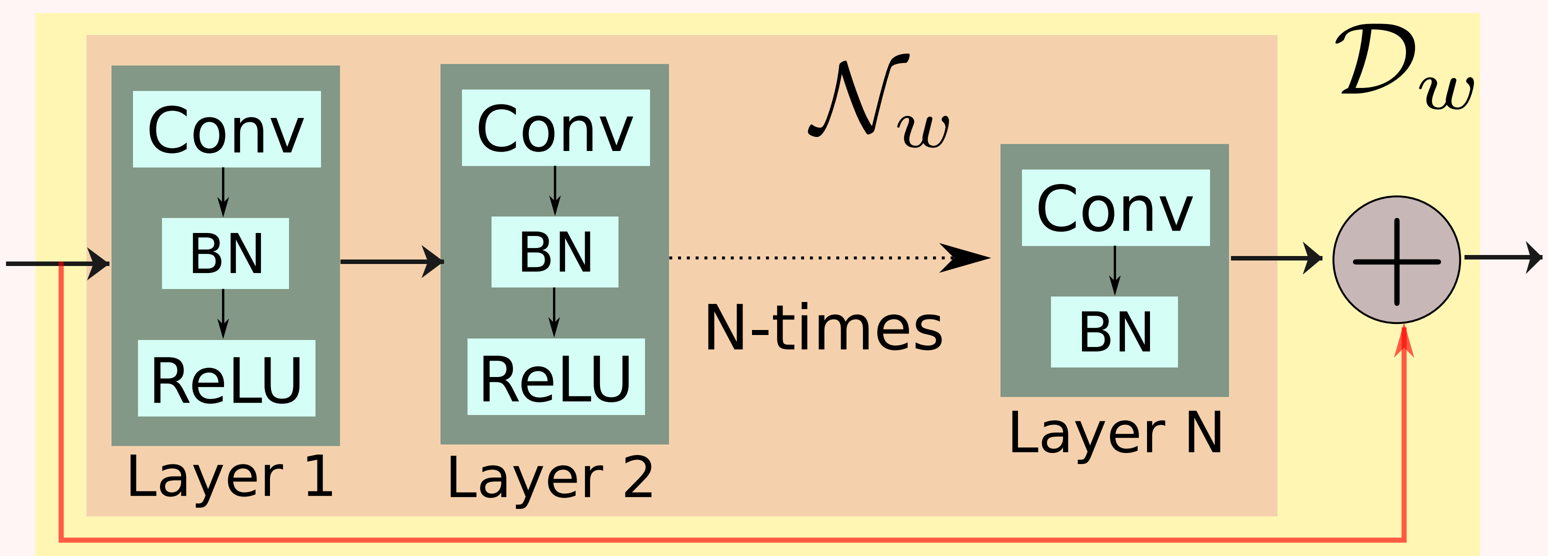

Aggarwal and Jacob, ISBI 2017,TMI 2019

Learned plug and play prior

Alternating minimization

Problem Formulation

$$\mathbf{x} = \arg\min_{\mathbf{x}} \|\mathbf{A}\,\mathbf{x} - \mathbf{b}\|_2^2 \; + \lambda \; \|\mathbf{x} - \mathcal{D}_{\mathbf{w}}(\mathbf{x})\|_2^2$$

Algorithm

$$\begin{aligned} \mathbf{z}_k &= \mathcal{D}_{\mathbf{w}}\left(\mathbf{x}_k\right) \\ \mathbf{x}_{k+1} &= \left(\mathbf{A}^H\mathbf{A} + \lambda\,\mathbf{I}\right)^{-1}\left(\mathbf{A}^H\mathbf{b} + \lambda\,\mathbf{z}_k\right) \end{aligned}$$

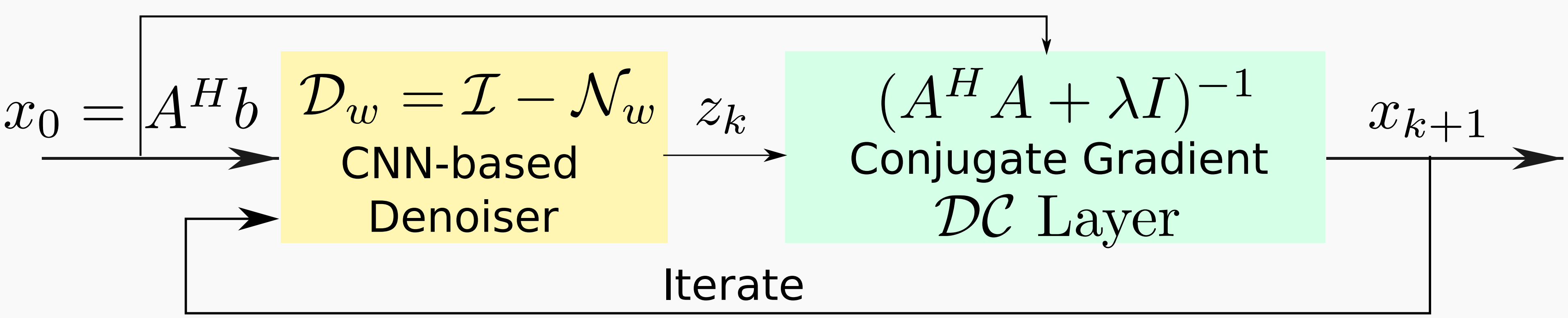

Recursive architecture: training using unrolled model

Recursive formulation

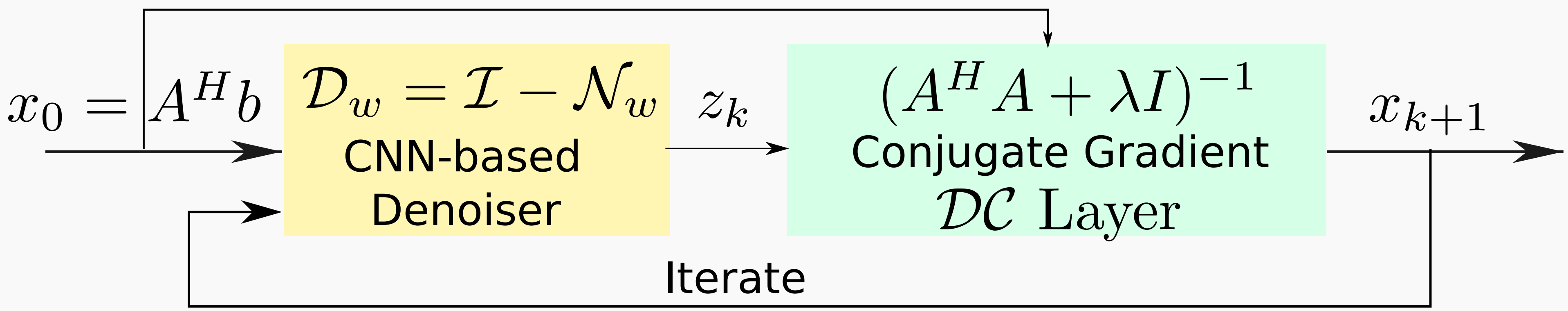

Unrolled architecture with end-to-end training

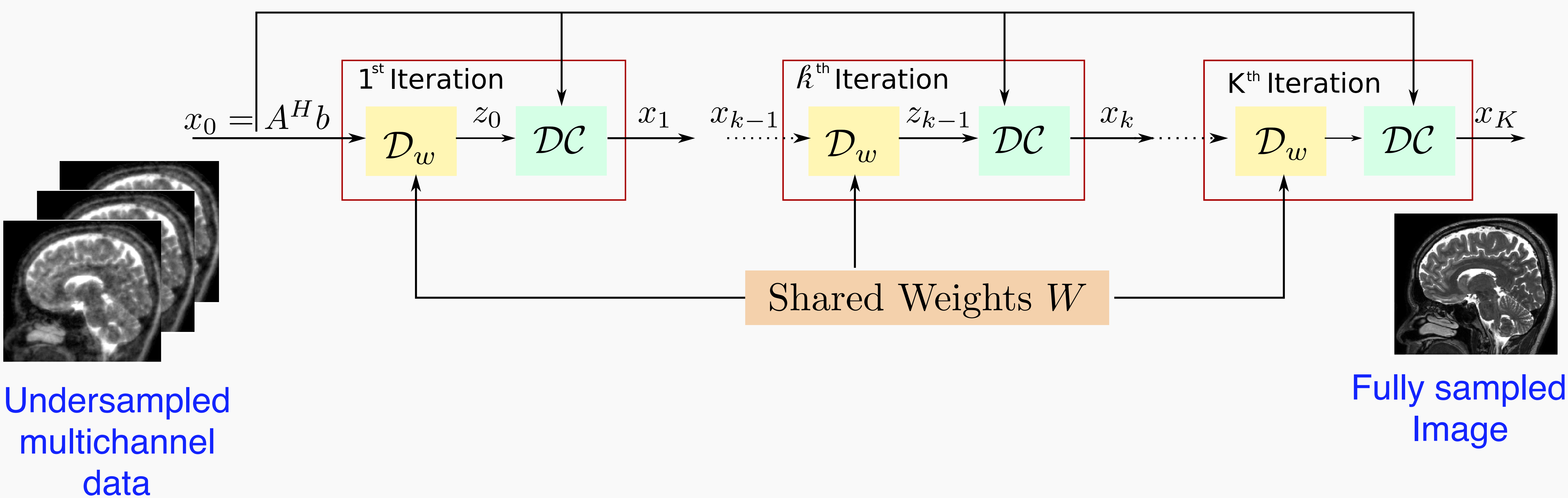

MoDL: benefits

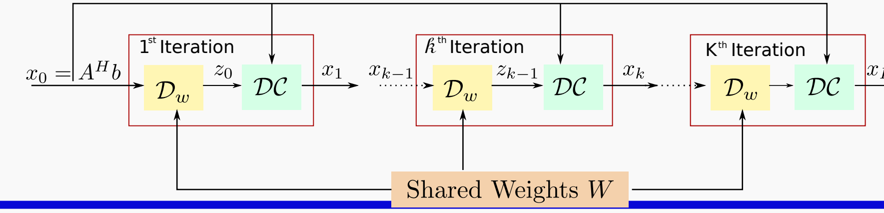

Weight sharing

- Need less training data

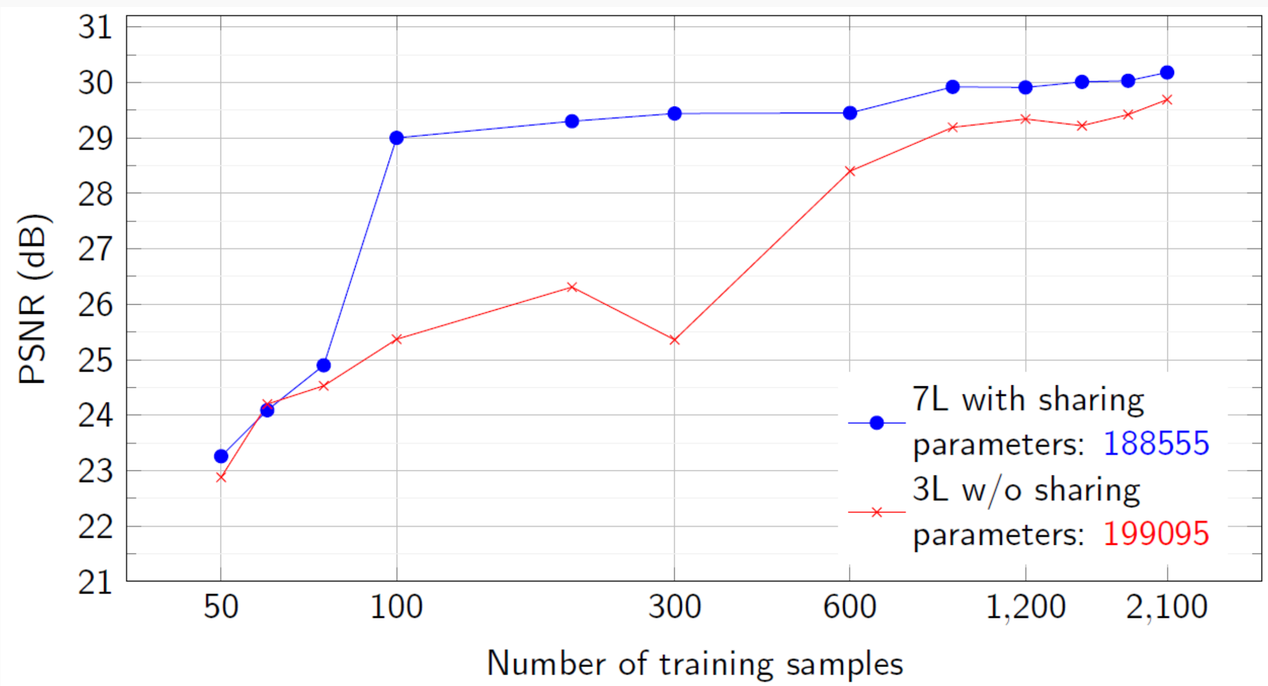

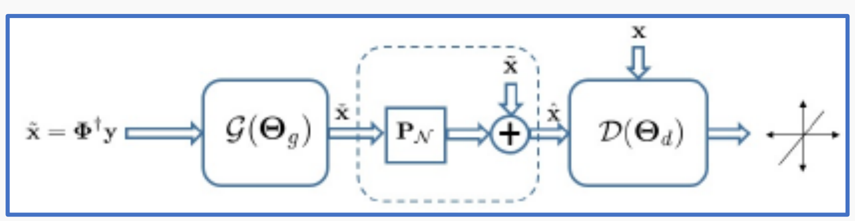

Generative adversarial networks, Mardani et al, 17

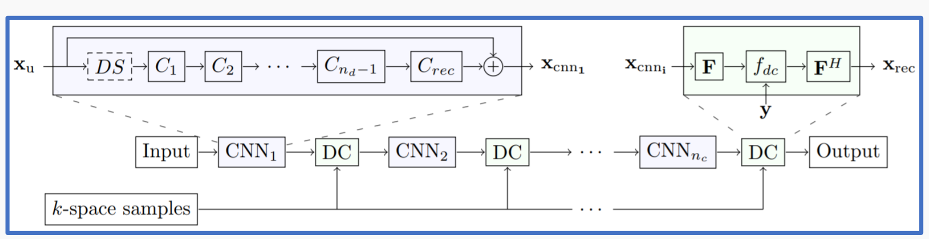

Cascade networks, Schlemper et al. 17

Data-consistency: CG within network

- SENSE forward model
- Faster convergence: better performance

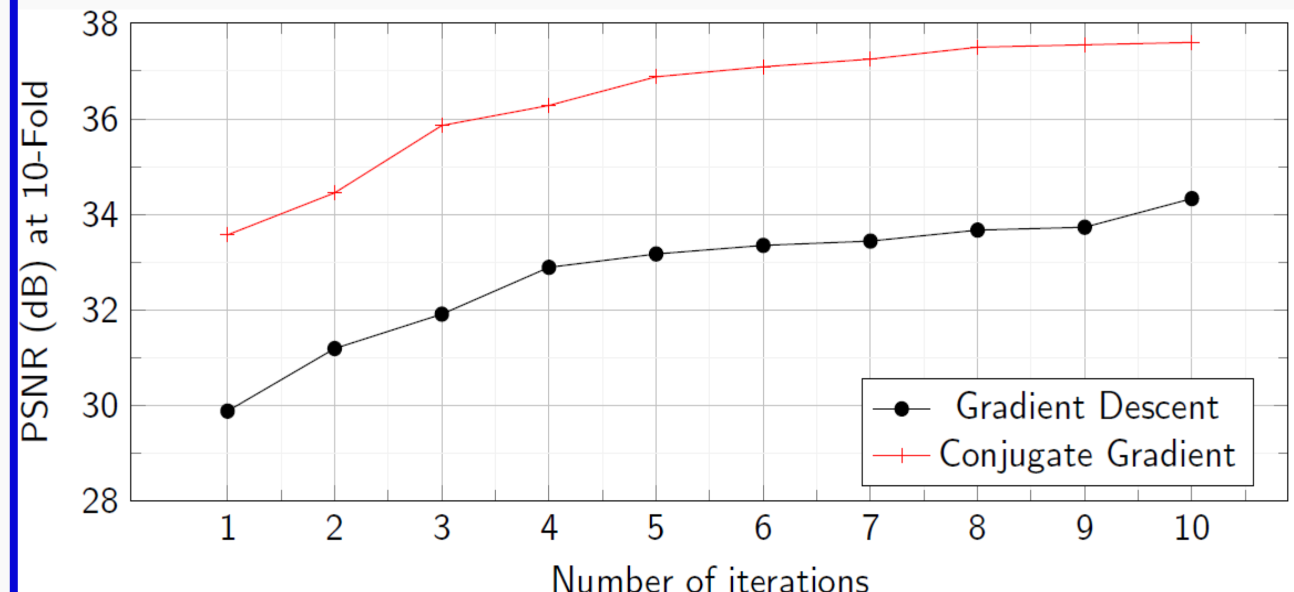

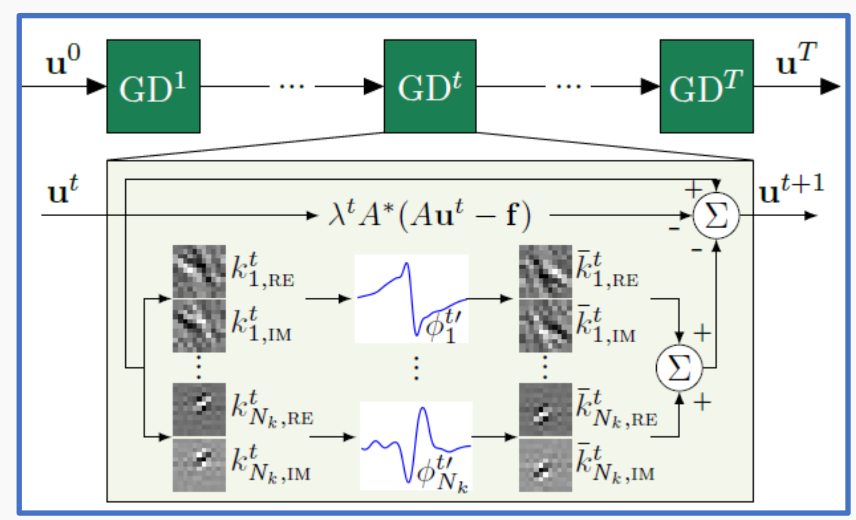

Steepest descent: Hammernick et al.

Code & data: https://github.com/hkaggarwal/modl

Backpropagation through CG layer

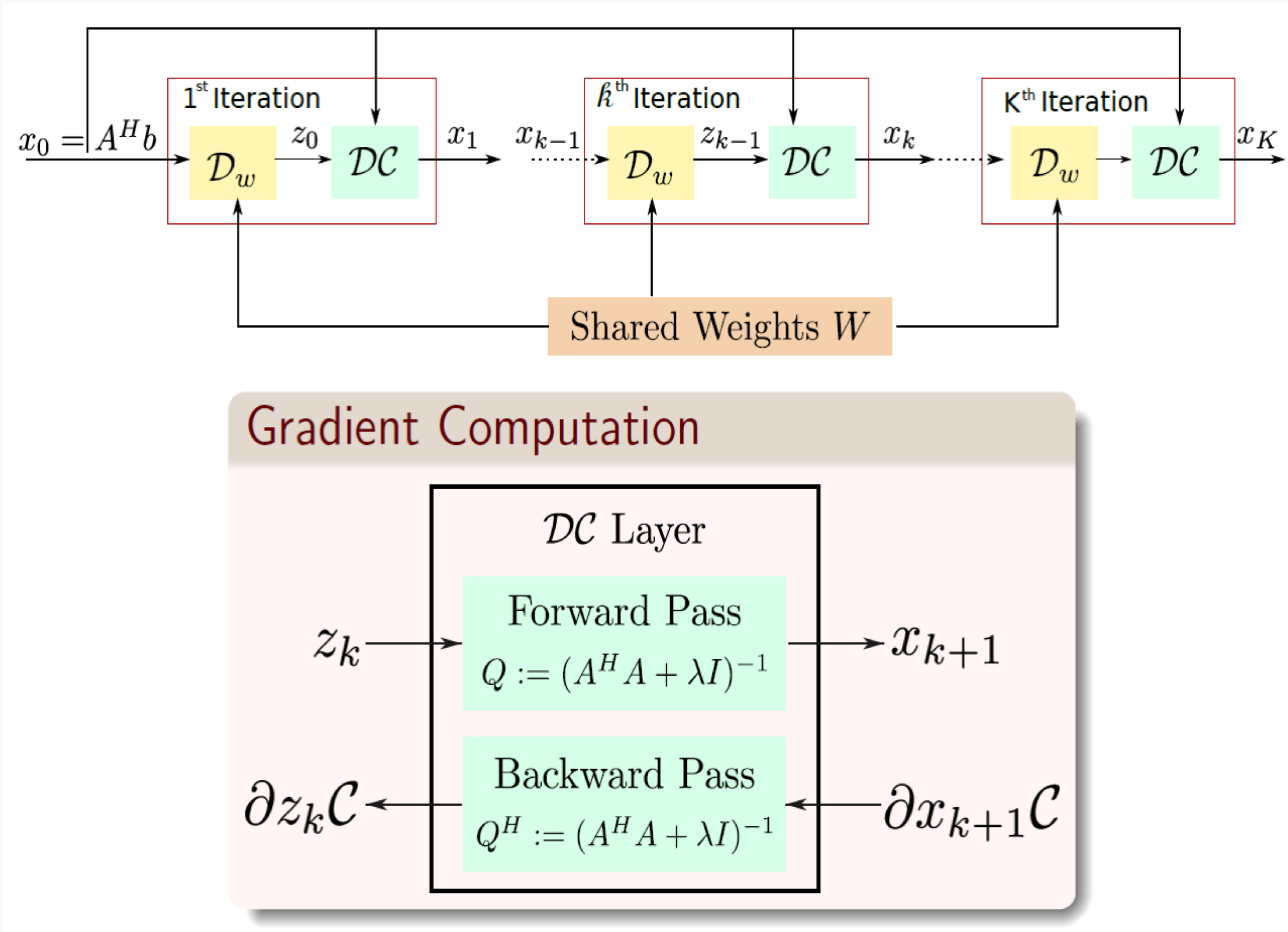

MoDL in action

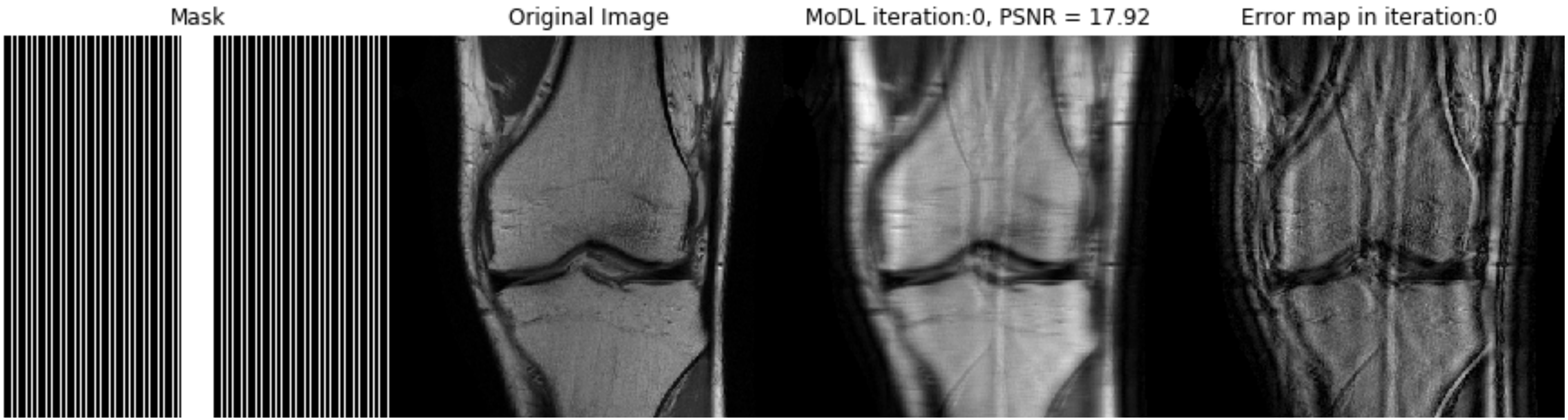

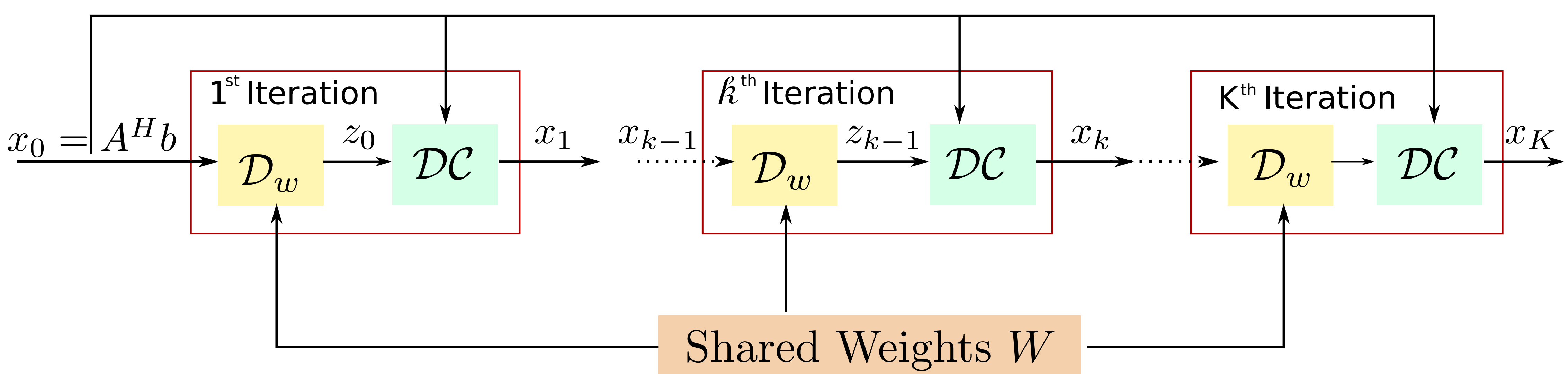

Aggarwal and Jacob, ISBI 2017,TMI 2019

Code & data: https://github.com/hkaggarwal/modl

SENSE with image domain MoDL (6x acceleration)

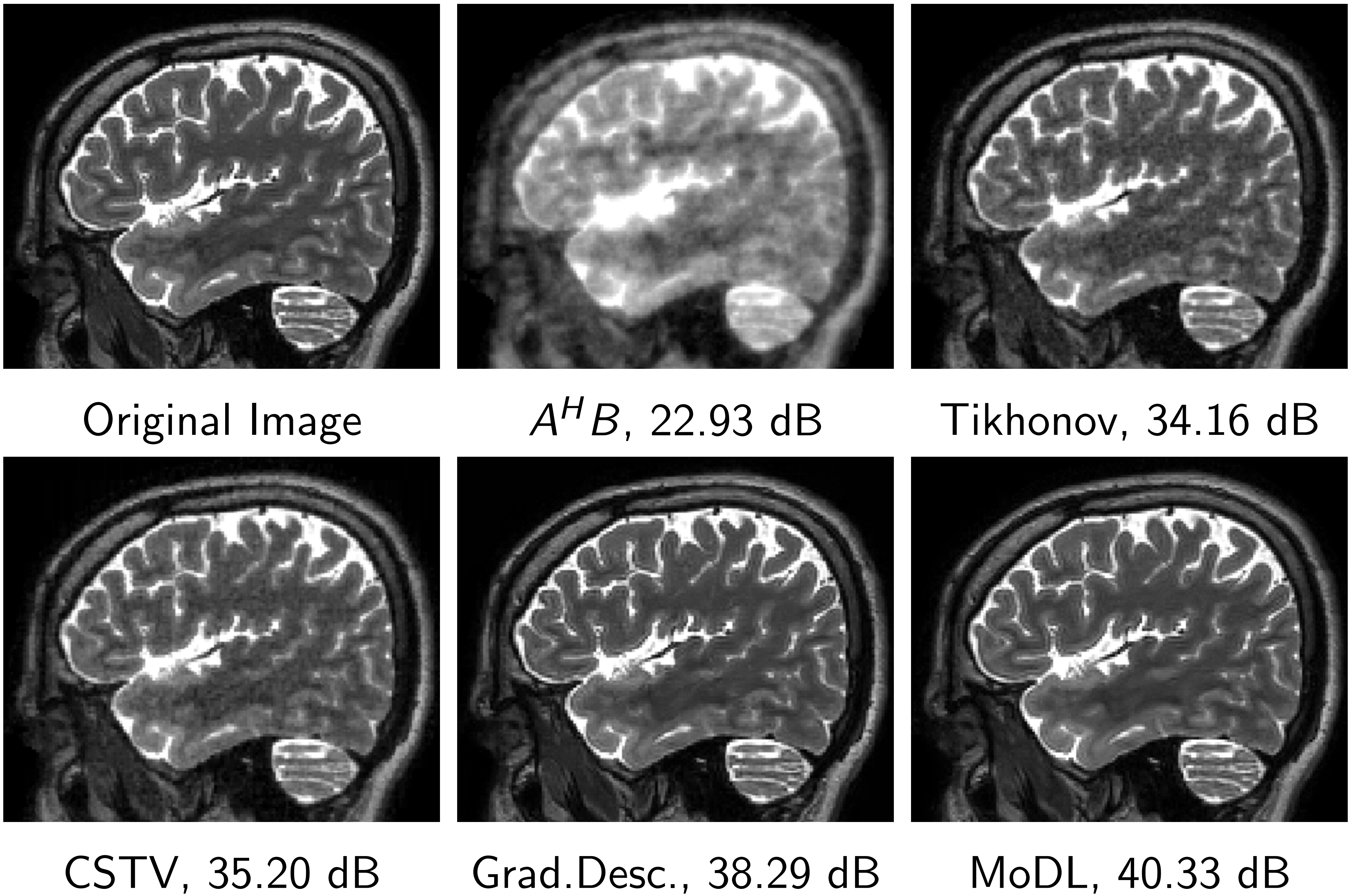

Aggarwal and Jacob, TMI, 2019

Code & data: https://github.com/hkaggarwal/modl

Comparison with competing methods (Courtesy F. Knoll)

Zero filled IFFT

TV-SENSE

TGV-SENSE


Original

Var. Net Hammernick & Knoll

MoDL

Exemplar learning of SLR priors: fast reconstruction

SLR algorithms: high computational complexity

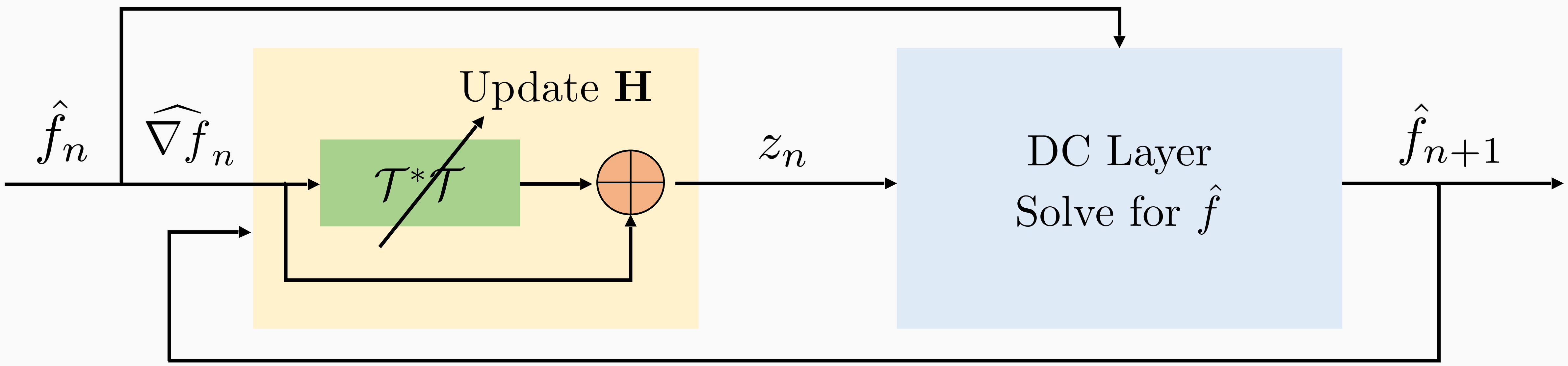

Deep learning in k-space

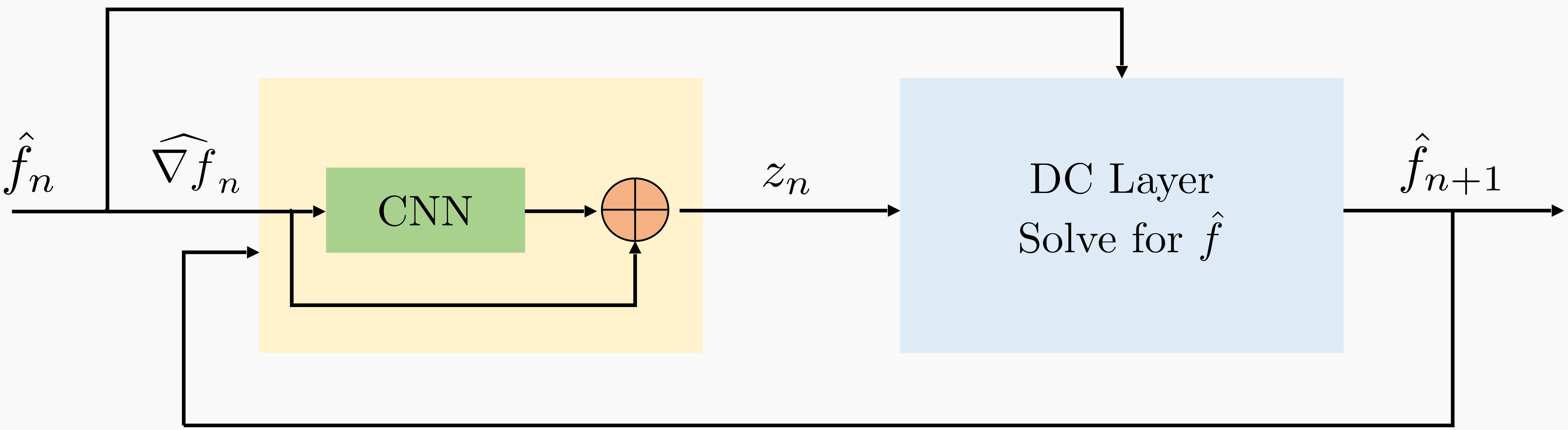

Pramanik, Aggarwal & Jacob, ISBI 2019

Uncalibrated parallel MRI & multishot DWI

Data acquisition using multiple coils: unknown sensitivities

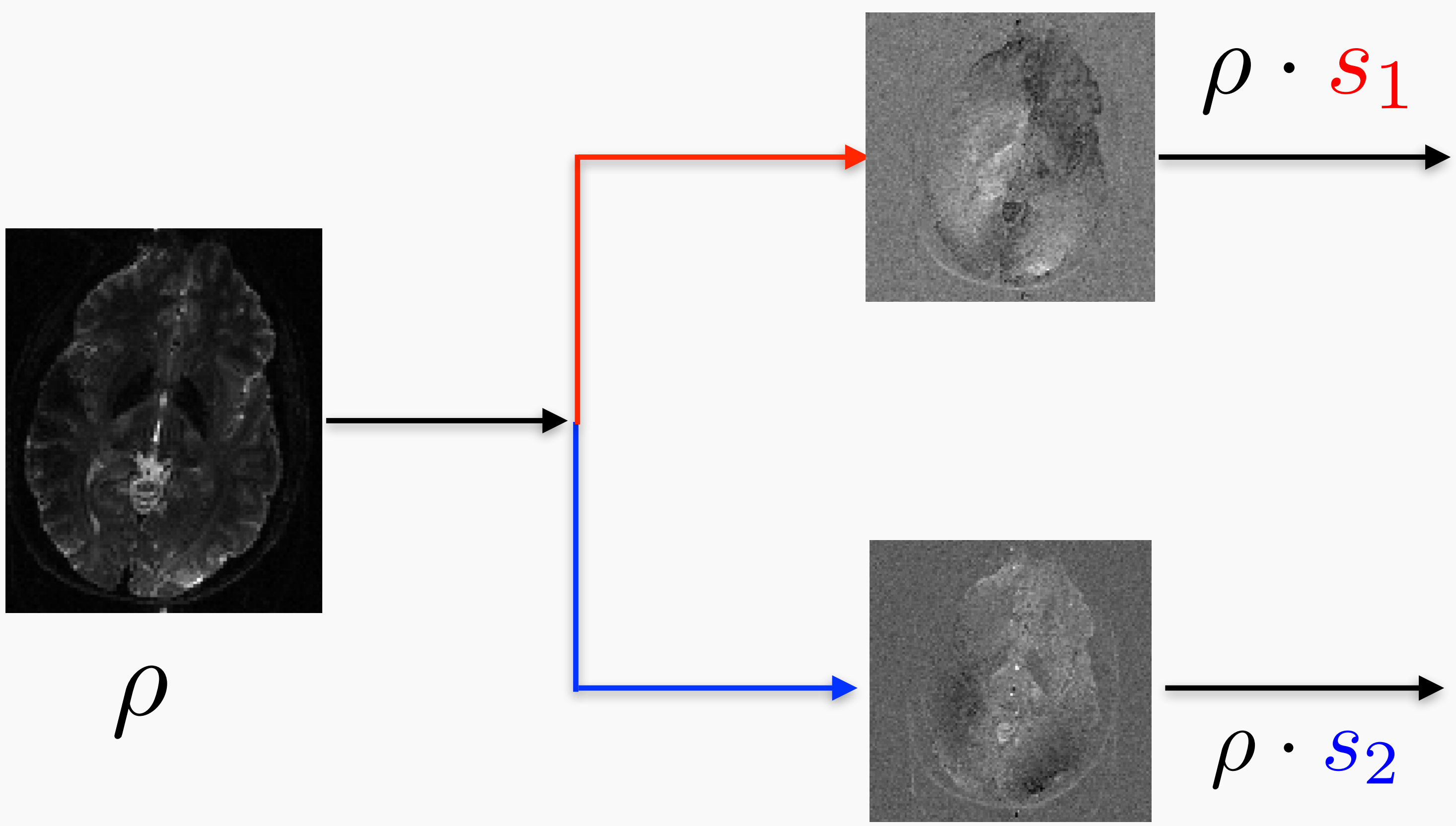

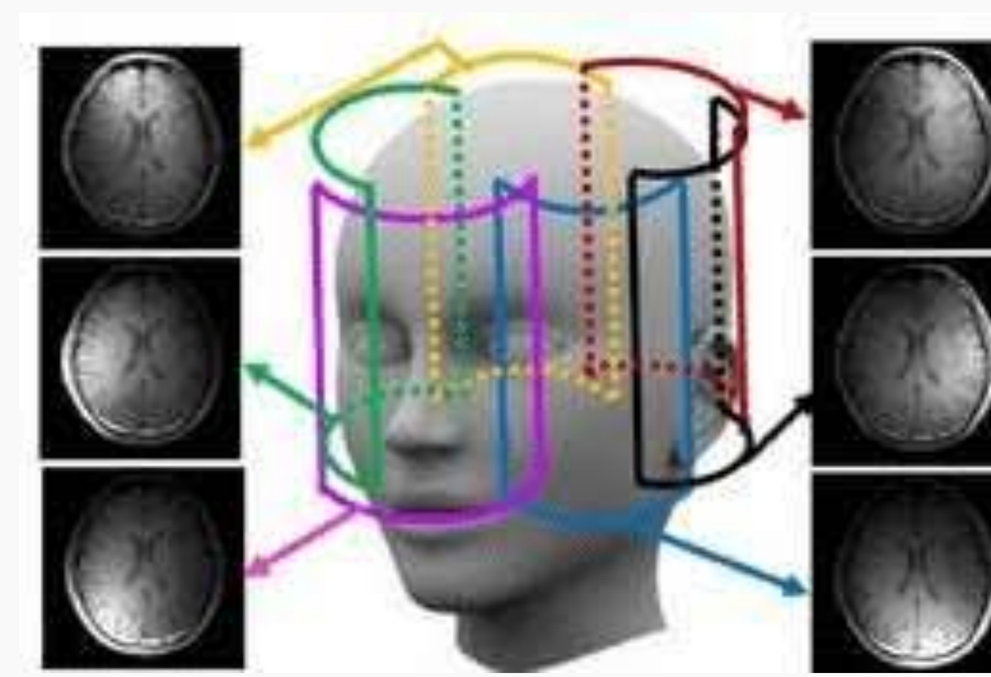

Calibration-free parallel MRI using multichannel MoDL

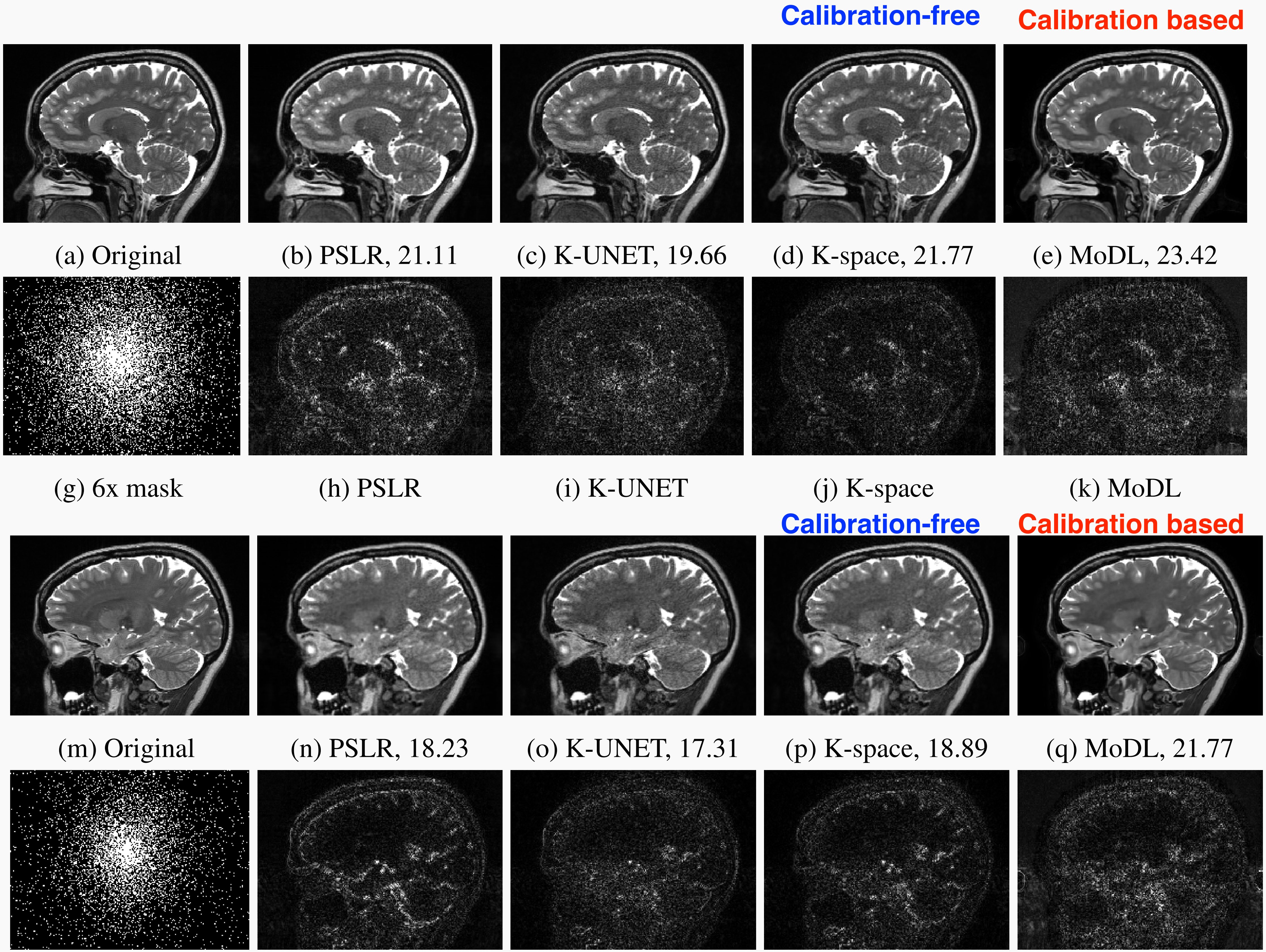

(a) Original (b) PSLR, 21.11 (c) K-UNET, 19.66 (d) K-space, 21.77 (e) MoDL, 23.42

(g) 6x mask (h) PSLR (i) K-UNET (j) K-space (k) MoDL

(m) Original (n) PSLR, 18.23 (o) K-UNET, 17.31 (p) K-space, 18.89 (q) MoDL, 21.77

(s) 10x mask (t) PSLR (u) K-UNET (v) K-space (w) MoDL

Add a image domain prior

Learned prior in k-space and image space

$$\mathbf{x} = \arg\min_{x} \|\mathbf{A}\mathbf{x} - \mathbf{b}\|^2 + \lambda_k \|\mathcal{N}_k(\widehat{\mathbf{x}})\|^2 + \lambda_I \|\mathcal{N}_I(\mathbf{x})\|^2$$

Structure of the network

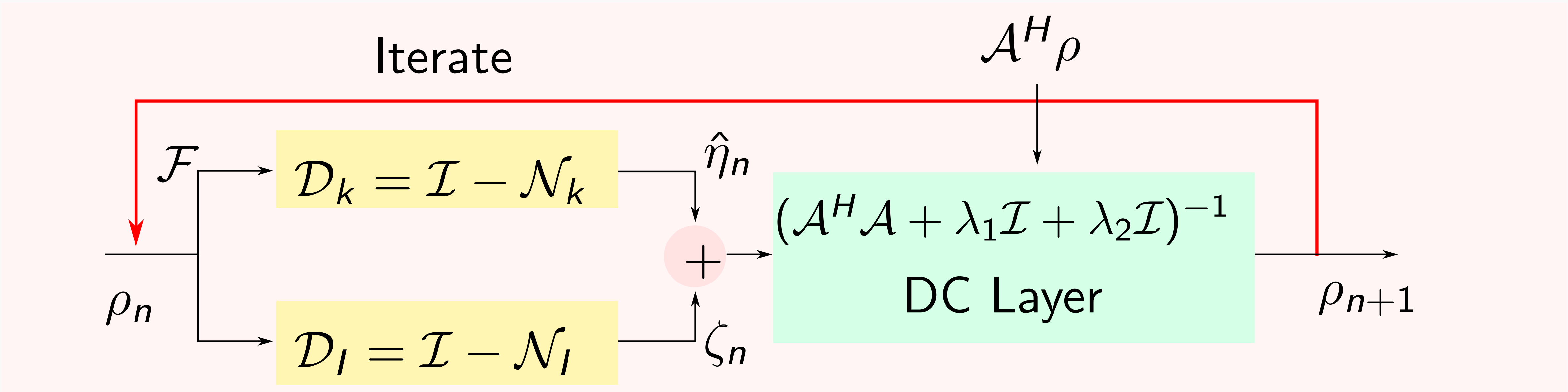

[MoDL-MUSSEL: Mani, Aggarwal & Jacob, MRM, in press]()

Calibration-free MRI using k-space & Image domain priors

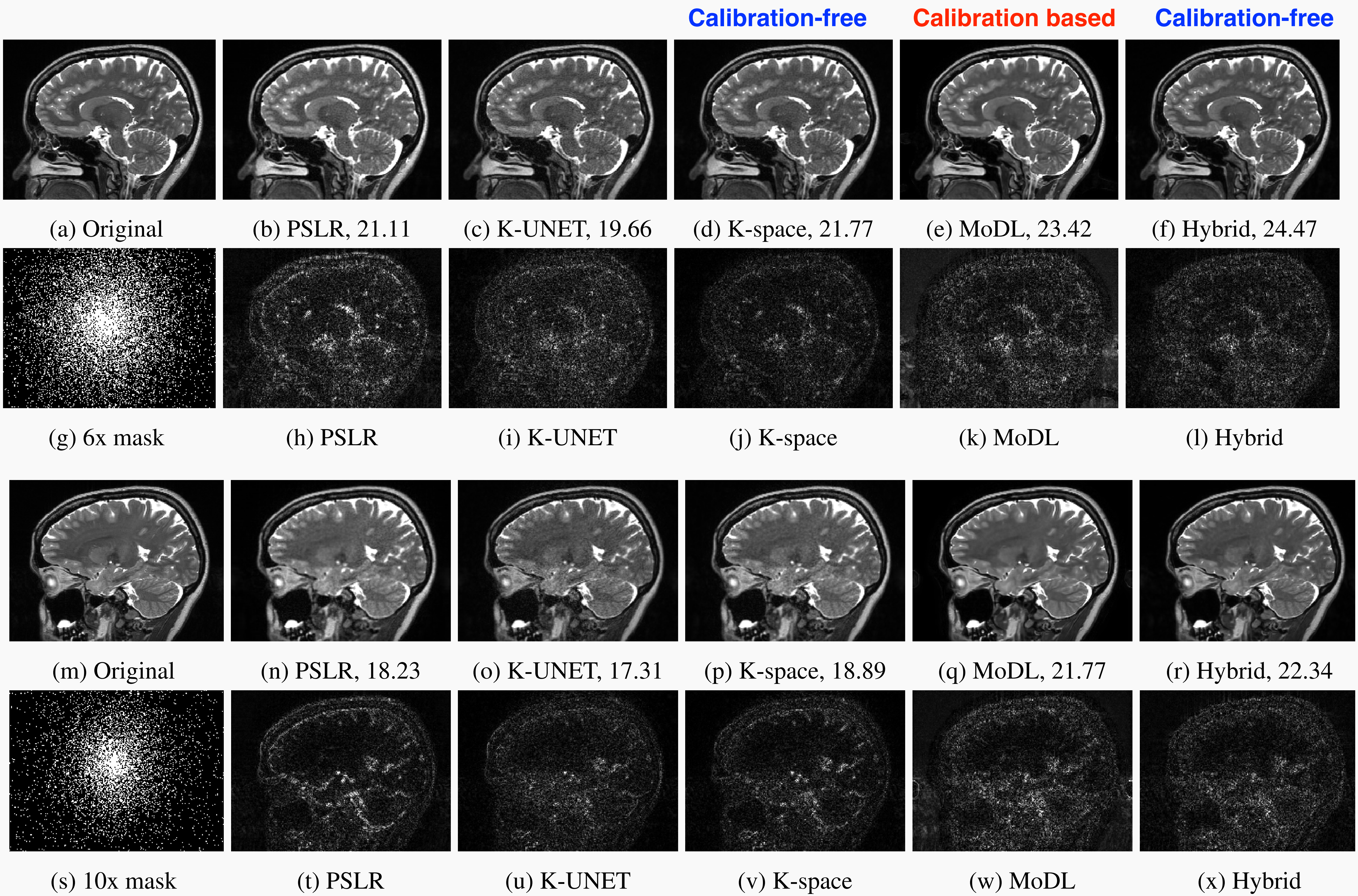

MoDL vs C-MoDL

Calibration based

Calibration-free

6x

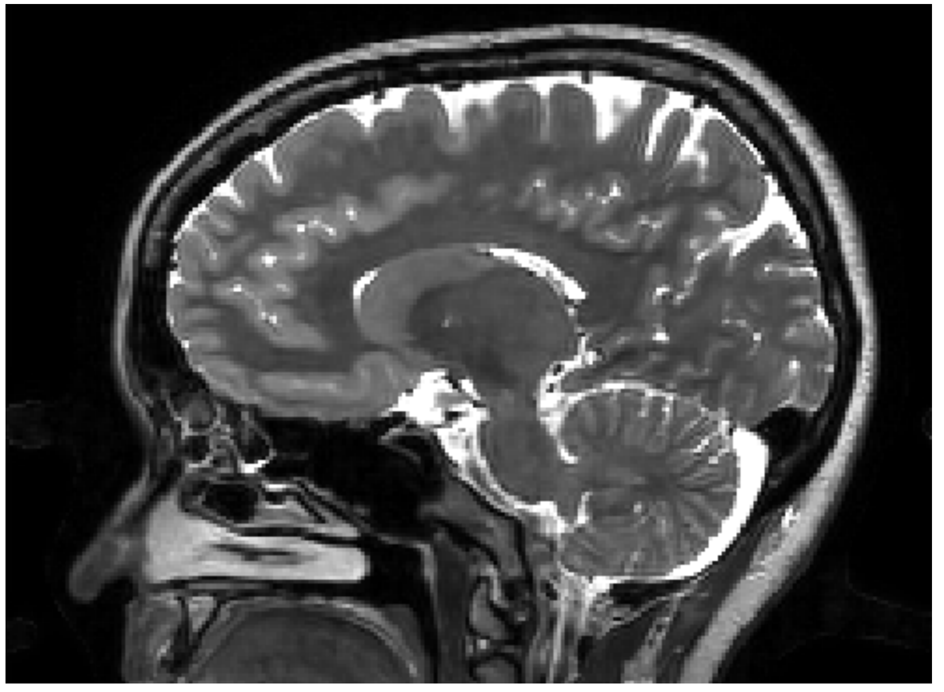

(e) MoDL, 23.42

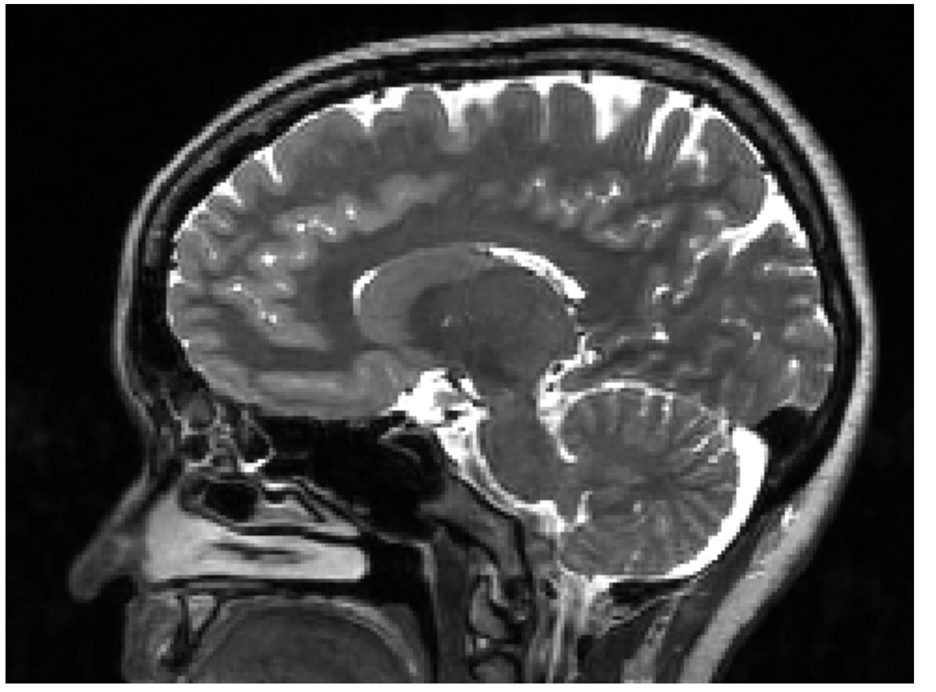

(f) Hybrid, 24.47

10x

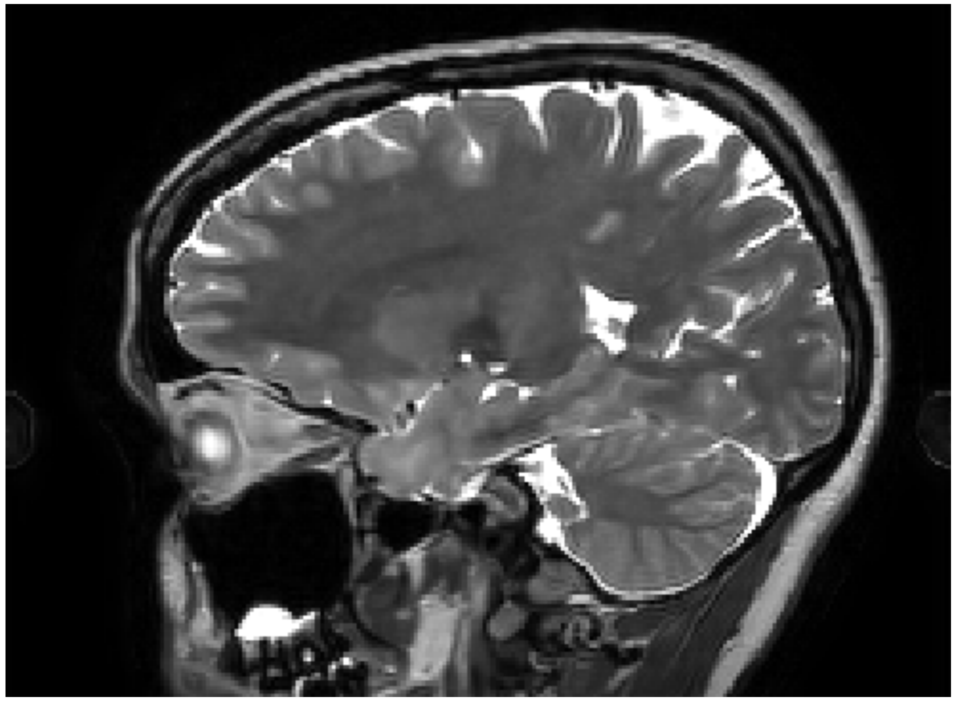

(q) MoDL, 21.77

(r) Hybrid, 22.34

Multishot diffusion MRI: phase compensation

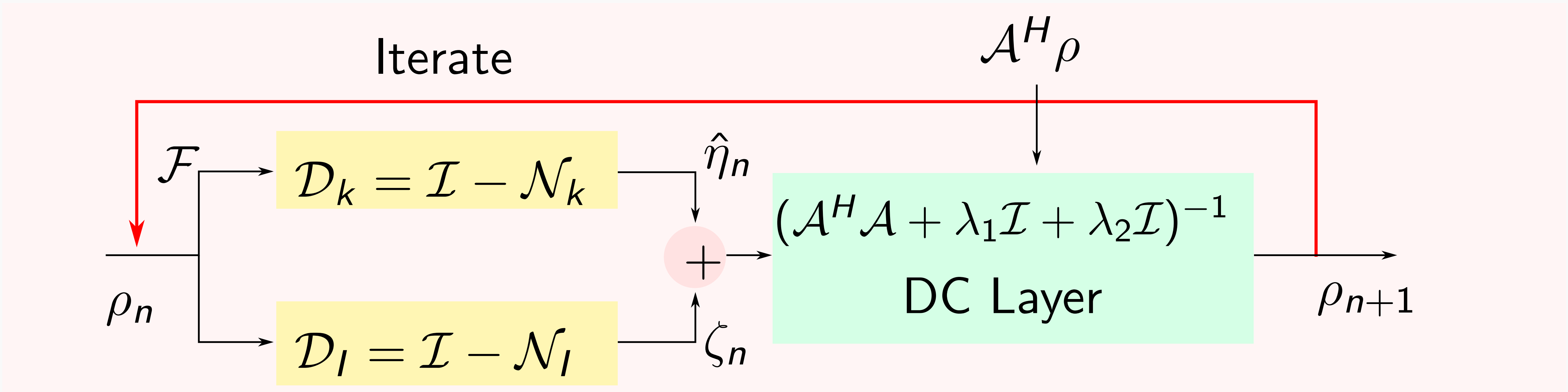

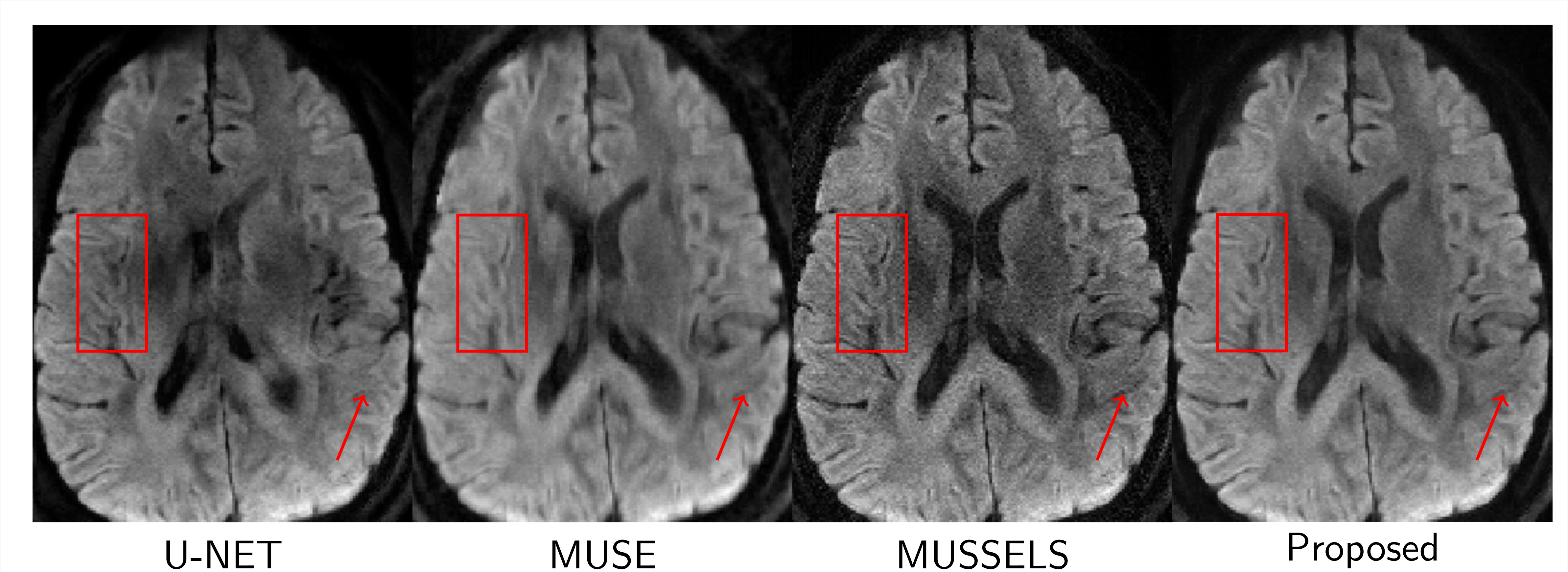

[MoDL-MUSSEL: Mani, Aggarwal & Jacob, MRM, in press]

MoDL-MUSSELS: real-time reconstructions

Demo of Diffusion Weighted Imaging

```
In [2]: _=interact(dwiRecon, Slice=Slice)
```

Slice 1

```
INFO:tensorflow:Restoring parameters from dwiModel/model-60
100%|██████████| 60/60 [00:09<00:00,  6.34it/s]
Now calculating the PSNR (dB) values
  Noisy  Recon
  20.82  34.91
```

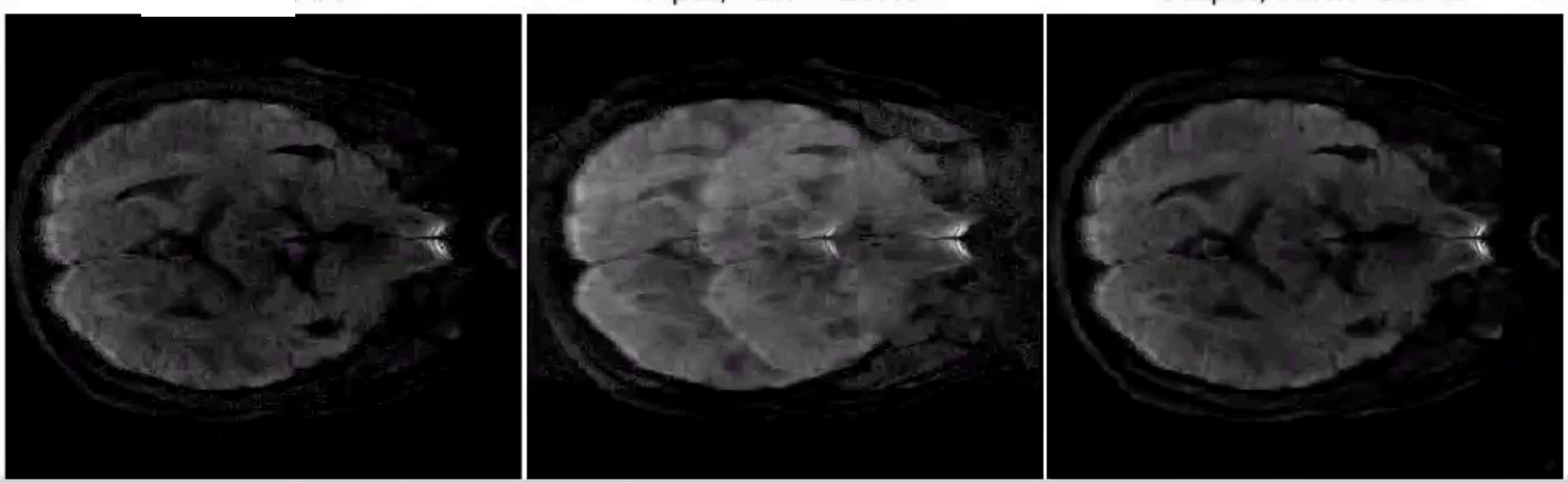

Synergistically combine priors: MoDL-SToRM

$$\mathcal{C}(\mathbf{X}) = \underbrace{\|\mathcal{A}(\mathbf{X}) - \mathbf{B}\|_2^2}_{\text{data consistency}} + \frac{\lambda_1}{2} \underbrace{\|\mathcal{N}_{\mathbf{w}}(\mathbf{X})\|^2}_{\text{CNN prior}} + \frac{\lambda_2}{2} \underbrace{\operatorname{tr}\left(\mathbf{X}^T\mathbf{L}\mathbf{X}\right)}_{\text{SToRM prior}}.$$

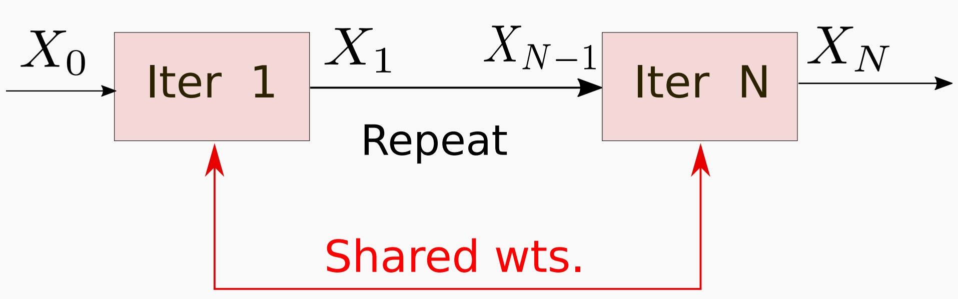

(a)

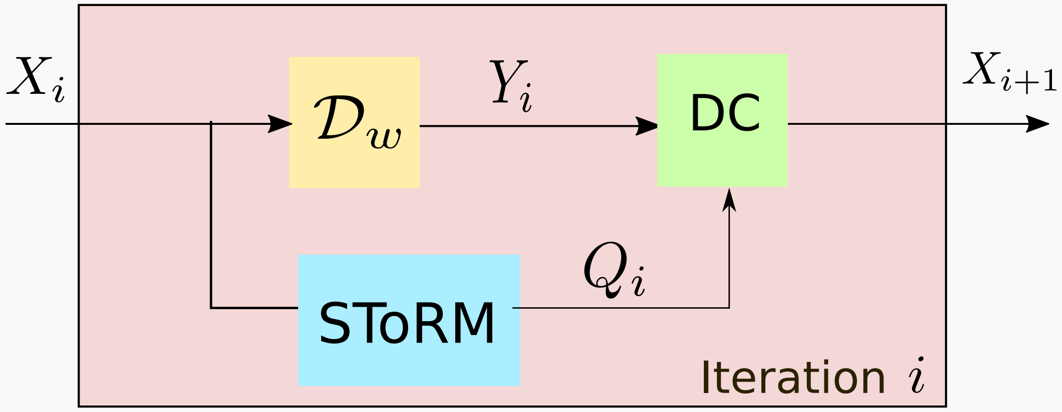

Biswas, Aggarwal and Jacob, MRM, in press

Combine deep learned and manifold priors

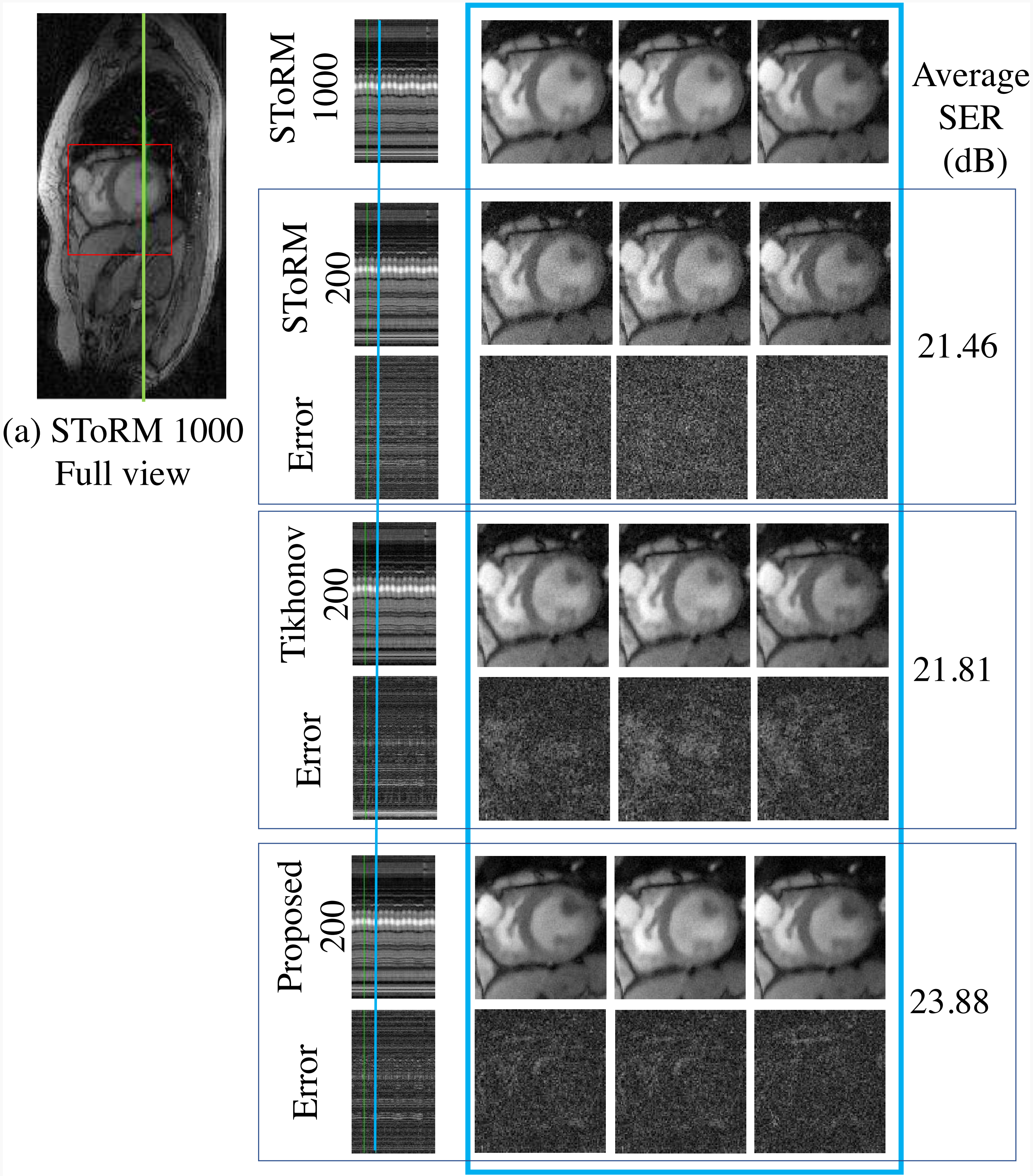

(a) SToRM 1000
Full view

Acquisition time = 40s

Acquisition time = 8s

Biswas, Aggarwal and Jacob, MRM, 2019

Self-learning of manifolds using denoising auto-encoder

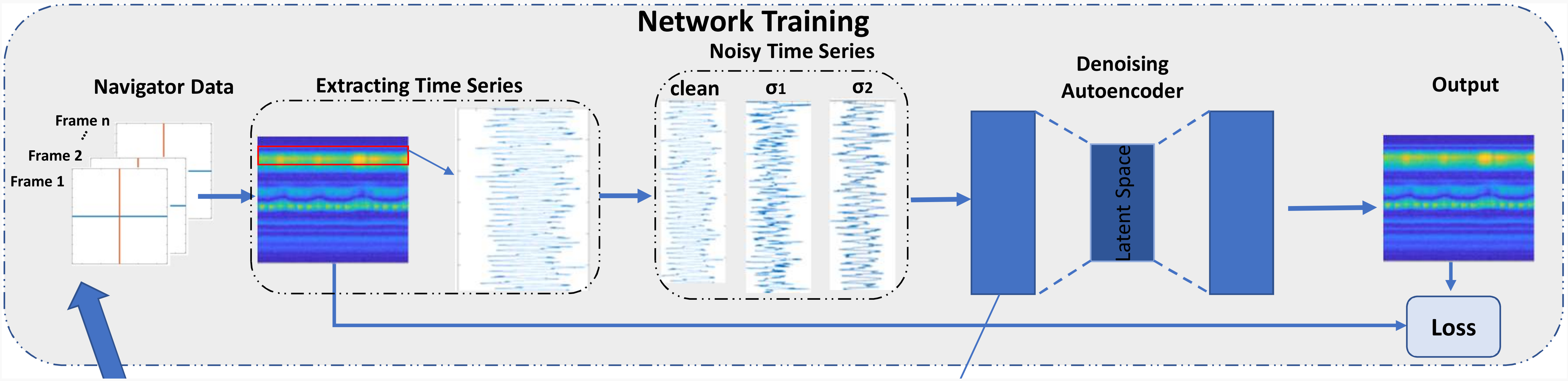

Self-learning of manifolds using denoising auto-encoder

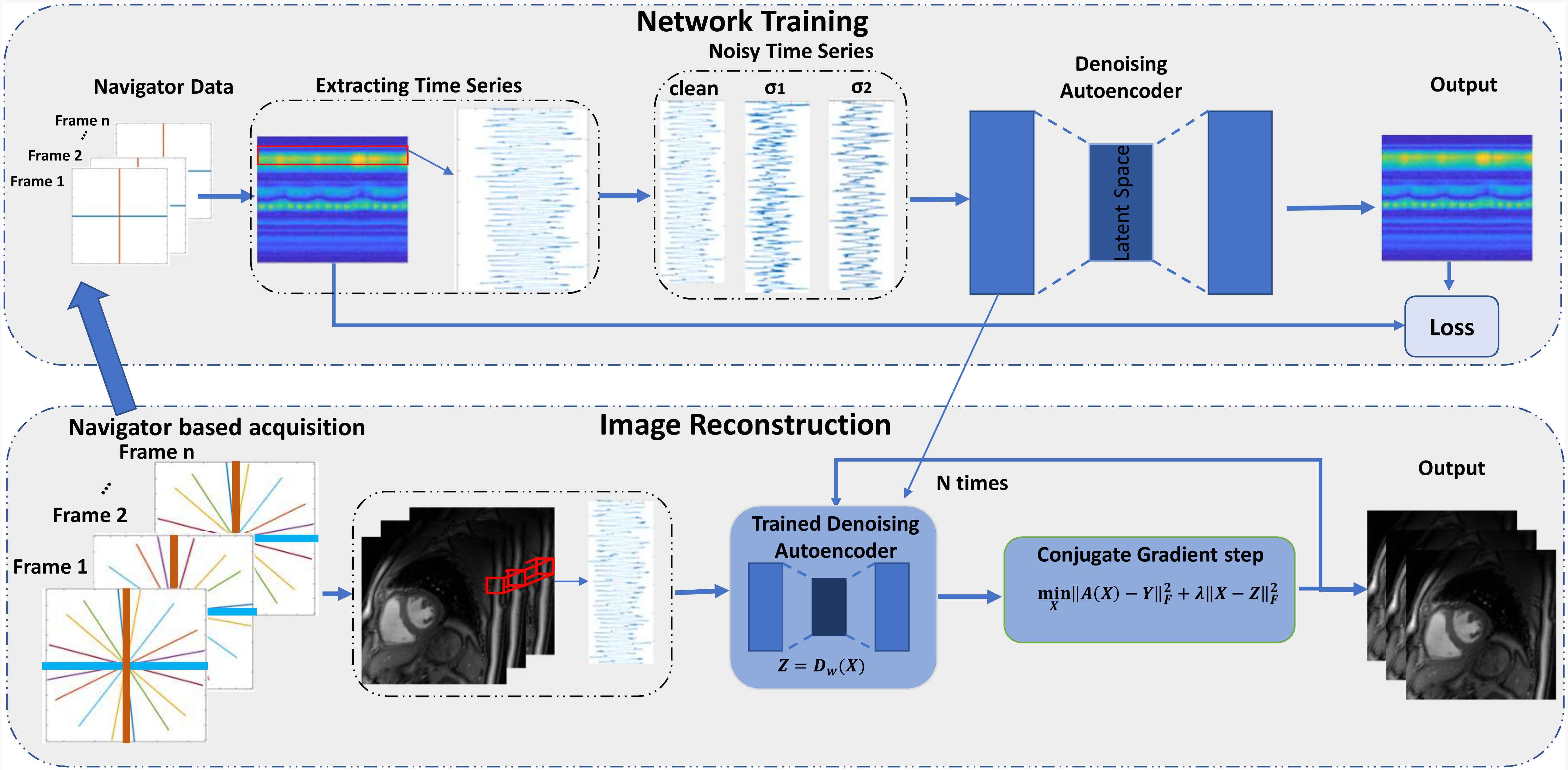

DAE: initial results

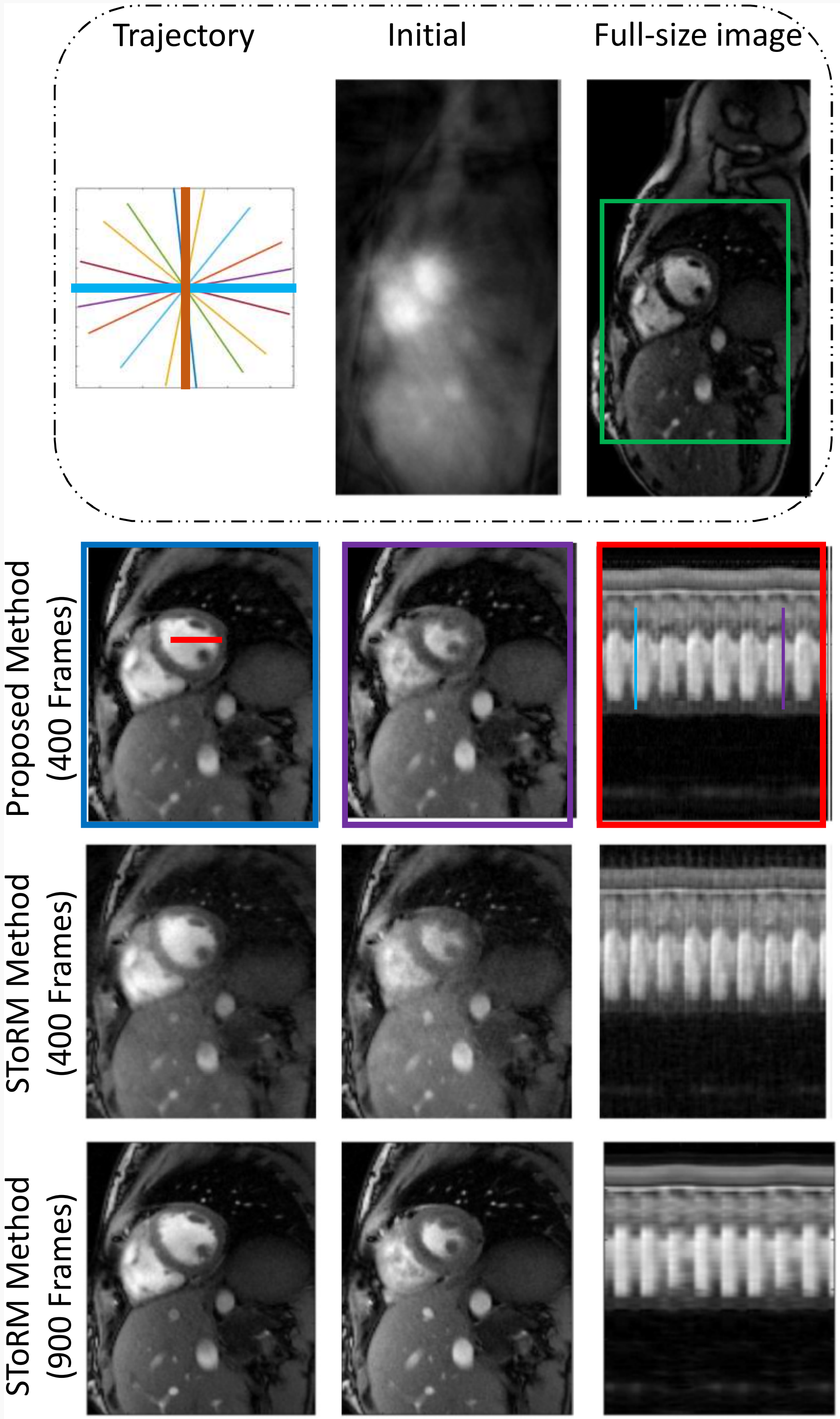

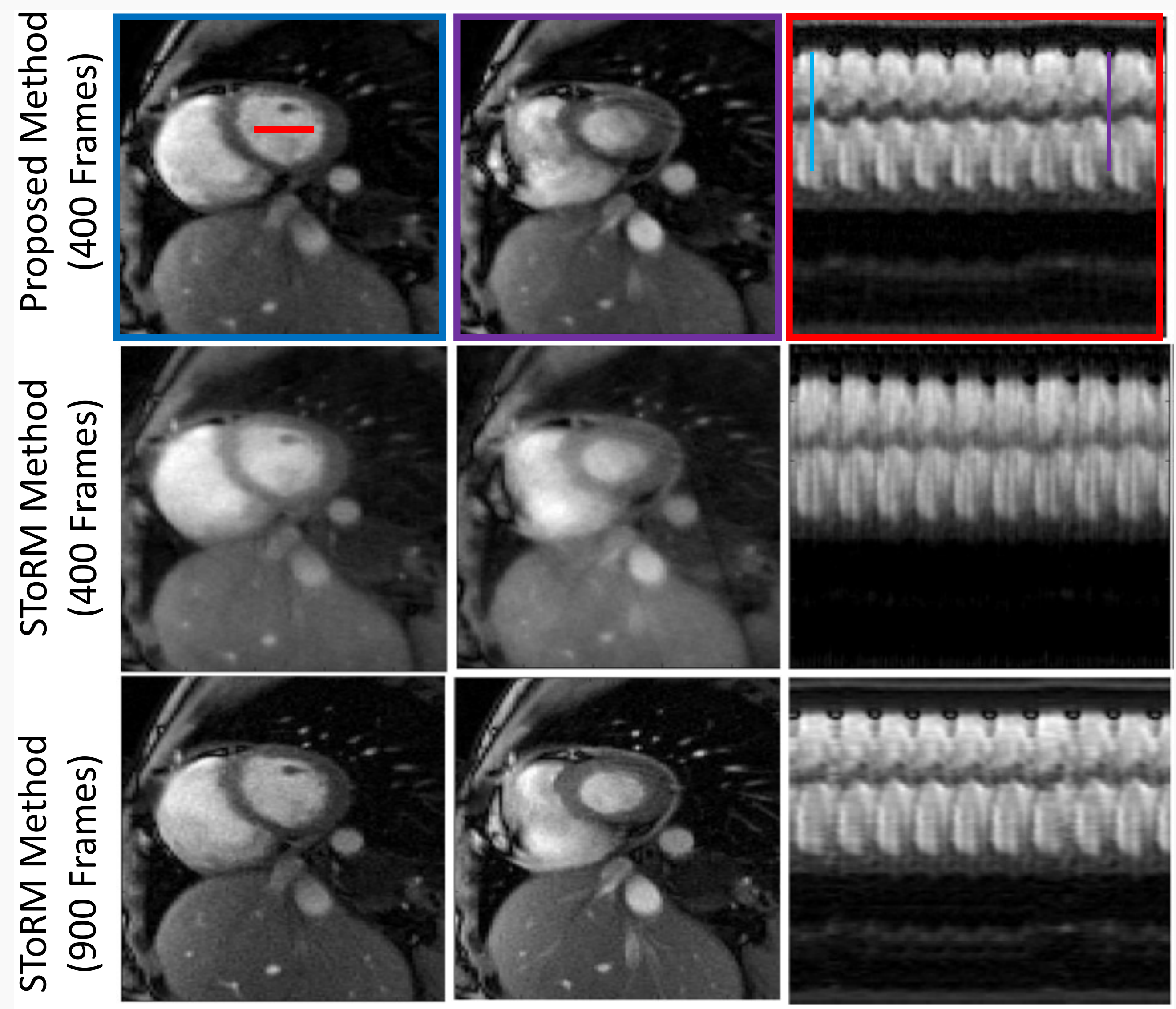

Summary: From SLR to MoDL

Structured low-rank algorithms

Lift data to higher dimensional matrix

Exploit subspace structure

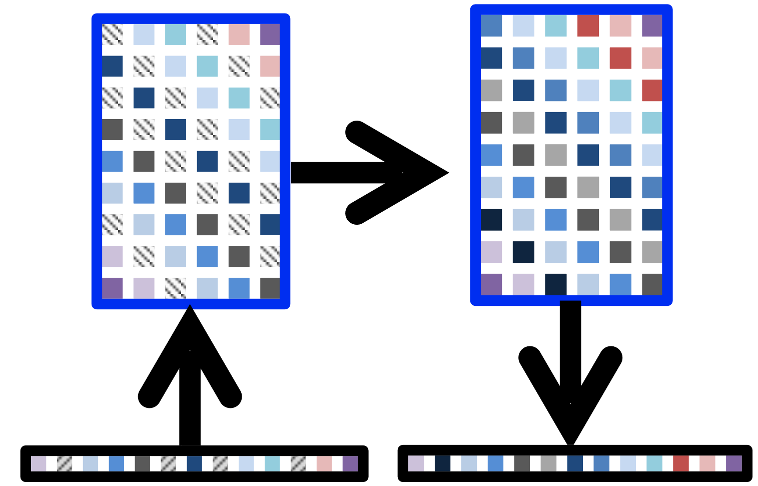

Union of surfaces model

Recovery of images on surfaces

Learning functions: link to DL

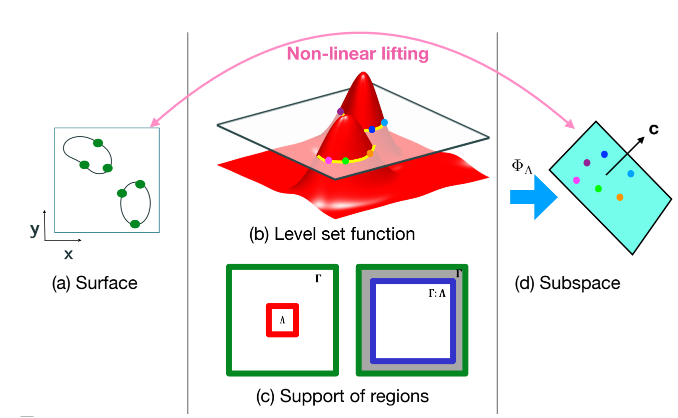

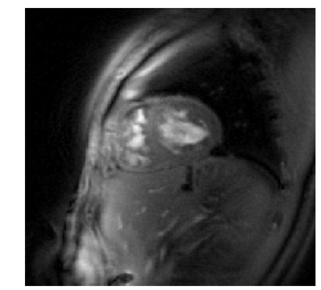

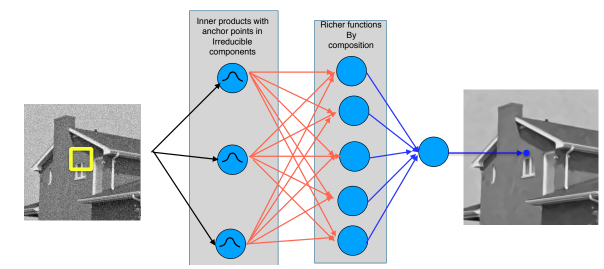

Using learned representations in CI: MoDL

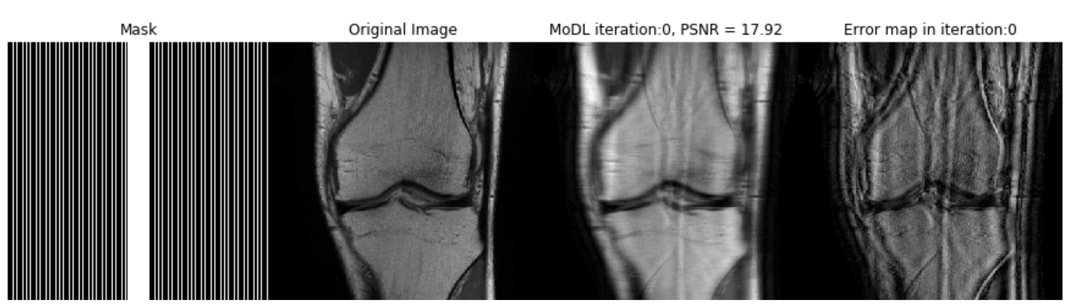

Unrolled SLR: Calibrationless PMRI

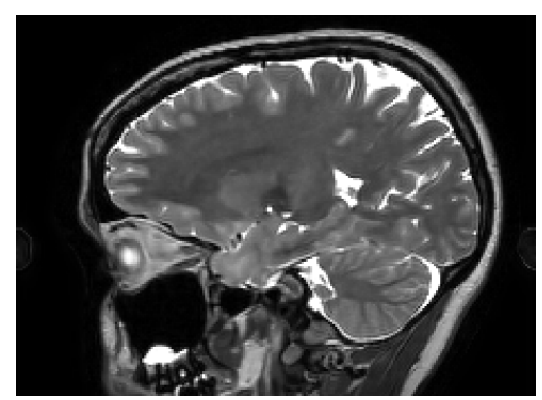

(q) MoDL, 21.77

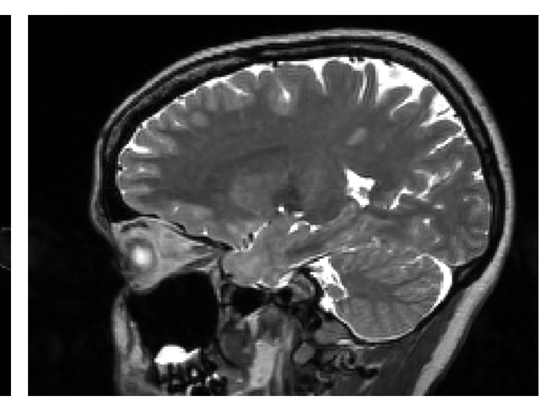

(r) Hybrid, 22.34

Acknowlegements
NIH 1R01EB019961

https://research.engineering.uiowa.edu/cbig